STUDY REPORT

SR 292 (2013)

B-RISK 2013 Software Benchmarking Examples

C.A. Wade

Preface

This report presents comparisons between B-RISK fire model predictions with experiments. The results contained therein were generated using B-RISK Version 2013.

Acknowledgments

Note

This report is intended for users of the B-RISK software.

B-RISK 2013 Software Benchmarking Examples

BRANZ Study Report SR 292

C.A. Wade

Reference

Abstract

This report comprises a series of comparisons between experimental data and model predictions using the B-RISK software. The report does not draw detailed conclusions about the acceptability or otherwise of the level of agreement reached and users are left to decide on the applicability of B-RISK to any specific application or scenario under consideration.

Contents

Figures   Page

Tables   **Page**

1. INTRODUCTION

This document is a compilation of some benchmarking examples for the B-RISK computer fire zone model (Wade, et al., 2013).

B-RISK is a computer program which simulates the spread of fire and smoke in single or multiple compartments connected to each other or to the outside with vent openings. The fire environment within each compartment is described in terms of a (hot) upper layer and a (cool) lower layer, with each layer assumed to contain homogenous volumes possessing a uniform temperature, density and species concentration at any given point in time. Conservation of mass and energy are applied along with numerous empirical correlations and analytical expressions for describing the magnitude of the compartment vent flows, entrainment of air by the fire plume and various other parameters. Depending on the type of scenario selected, the user is either required to provide a heat release rate (HRR) description of the fire (for zone model applications) or provide material bench-scale fire test data (for flame spread applications).

The benchmarking examples presented show comparisons between predictions made using the B-RISK program and experimental measurements obtained from the published literature for various parameters. Readers need to have an appreciation of the uncertainties associated with the input data used in the model, the accuracy and errors associated with the experiments and the assumptions associated with the various hard-coded and user-selected theories and calculation methods used in the implementation of the model, when drawing conclusions about the level of agreement between model and experiment.

It is generally not possible to completely "validate" a model for all possible uses and applications because of the large number of combinations and permutations possible from the wide range of input parameters. Therefore comparative data for a limited number of configurations, for which experimental data is available, is presented here that may provide an initial guide to the user. It is the aim of this document to summarise some of that data to help the user evaluate the suitability of the model for the intended application.

The report does not draw detailed conclusions about the acceptability or otherwise of the level of agreement reached between experiments and model predictions, and in general, users are left to decide on the applicability of B-RISK to the specific scenario or application for which they wish to use the model.

2. SINGLE ROOM WITH A SINGLE VENT

2.1 CASE 2-1

2.1.1 References

Steckler, K. D., Baum, H. & Quintiere, J. G., 1983. Fire Induced Flows Through Room Openings – Flow Coefficients. NBSIR 83-2801, Gaithersburg, USA: National Bureau of Standards.

Steckler, K. D., Quintiere, J. G. & Rinkinen, W. J., 1982. Flow induced by fire in a compartment. NBSIR 82-2520, Gaithersburg, USA: National Bureau of Standards.

http://fire.nist.gov/bfrlpubs/fire82/PDF/f82001.pdf

2.1.2 Description

A series of steady-state experiments using a methane gas burner (dimensions 0.42 x 0.48 x 0.02 m above floor level) located at the centre of a room 2.8 x 2.8 x 2.18 m high were conducted (Steckler, et al., 1983). The room was lined with a ceramic fibre insulation board. The room had a single vent opening, the size of which was able to be varied. The output from the methane burner was steady at 61.9 kW (Tests 1-10), 31.6 kW (Test 11), 105.3 kW (Test 12) and 158 kW (Test 13).

2.1.3 Model Parameters

B-RISK 2013.09 is used.

The vent opening size, burner output and ambient temperature are shown in Table 1.

The following fuel properties for the methane burner are used: heat of combustion 49.6 kJ/g; radiant loss fraction 0.14; and heat release rate per unit area (HRRPUA) 312 kW/m^2.

2.1.4 Comparison

Figure 1 and Table 1 compare the predicted and experimental data for the layer interface height, upper and lower layer temperatures, and mass flow leaving the vent. The predictions and experimental data are compared at 30 minutes. A typical SmokeView visualisation of a simulation is shown in Figure 2.

Statistics illustrating the difference between the predicted and measured values (assessed at 30 minutes) and based on a sample of 13 tests are:

	Mean difference	Min	Max	Standard deviation
Layer height (m)	+21%	+10.7%	+51.5%	17.9%
Upper layer temperature (°C)	+6%	+0.6%	+16.3%	6.4%
Lower layer temperature (°C)	-11%	0%	-29.6%	17.2%
Vent flow out (kg/s)	-16%	-1.7%	-27.2%	7.8%
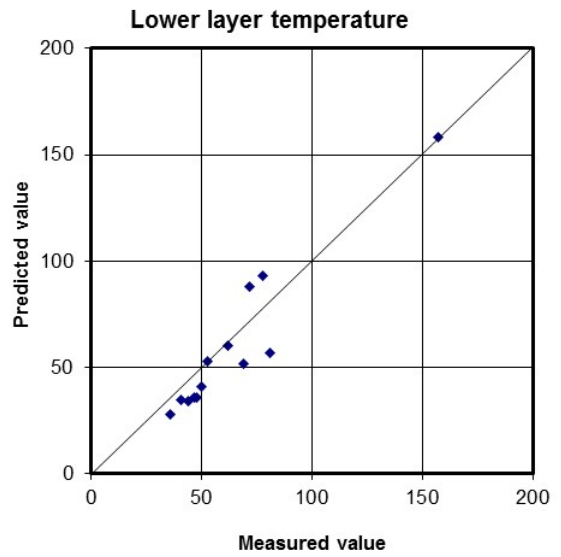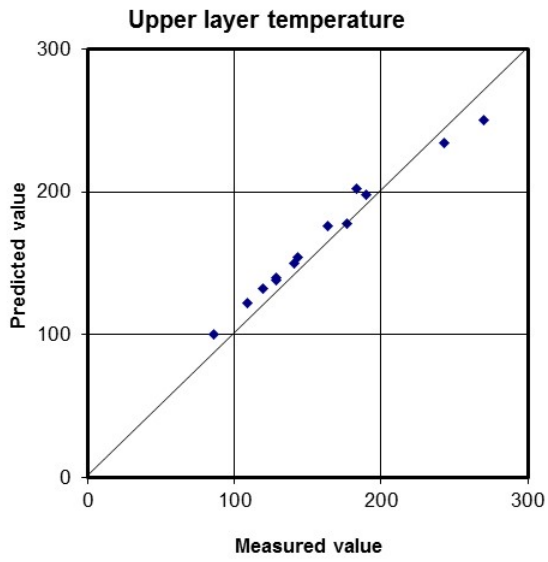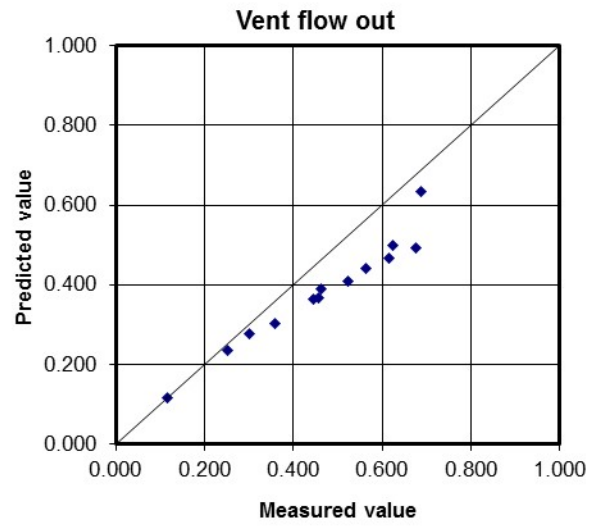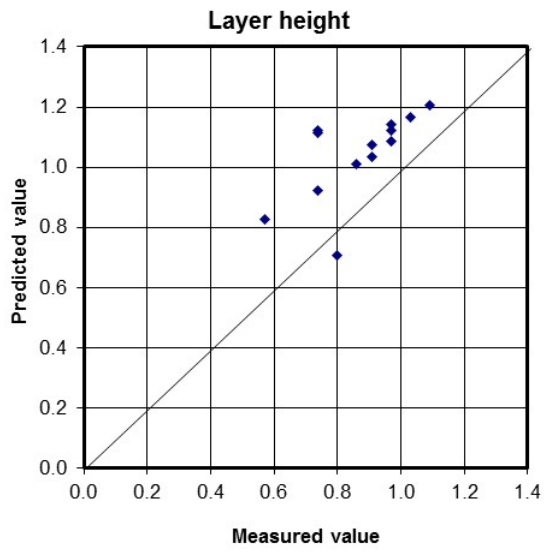
Figure 1. Comparison of steady-state measured and predicted values
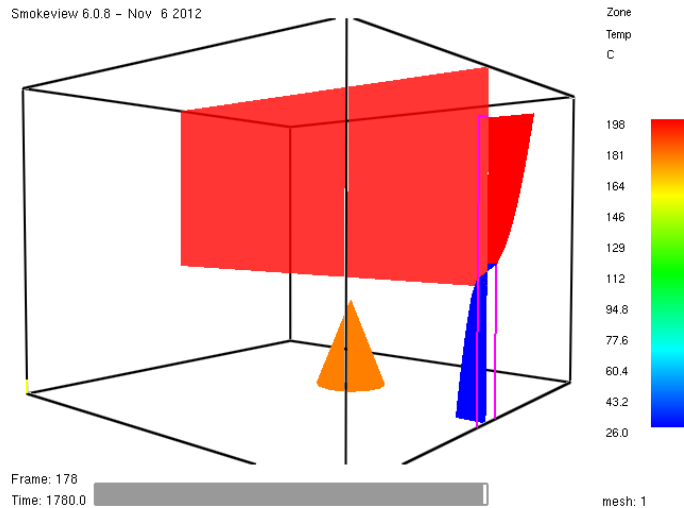
Figure 2. SmokeView visualisation (Test 1)

Table 1. Comparison of results for steady-state conditions

	Experiment	B-RISK prediction
Test 1: Fire size = 62.9 kW, vent 0.24 m wide x 1.83 m high with sill at 0 m, ambient temperature = 26ºC		
Interface height (m)	0.57 ± 0.28	**0.826**
Upper temp (ºC)	190	**198**
Lower temp (ºC)	72	**88**
Vent flow (kg/s)	0.251	**0.235**
Test 2: Fire size = 62.9 kW, vent 0.36 m wide x 1.83 m high with sill at 0 m, ambient temperature = 28ºC		
Interface height (m)	0.74 ± 0.23	**0.923**
Upper temp (ºC)	164	**176**
Lower temp (ºC)	62	**60**
Vent flow (kg/s)	0.358	**0.304**
Test 3: Fire size = 62.9 kW, vent 0.49 m wide x 1.83 m high with sill at 0 m, ambient temperature = 22ºC		
Interface height (m)	0.86 ± 0.28	**1.012**
Upper temp (ºC)	141	**150**
Lower temp (ºC)	50	**41**
Vent flow (kg/s)	0.457	**0.366**
Test 4: Fire size = 62.9 kW, vent 0.62 m wide x 1.83 m high with sill at 0 m, ambient temperature = 23ºC		
Interface height (m)	0.91 ± 0.17	**1.076**
Upper temp (ºC)	129	**140**
Lower temp (ºC)	47	**36**
Vent flow (kg/s)	0.523	**0.409**
Test 5: Fire size = 62.9 kW, vent 0.74 m wide x 1.83 m high with sill at 0 m, ambient temperature = 29ºC		
Interface height (m)	0.97 ± 0.23	**1.123**
Upper temp (ºC)	129	**138**
Lower temp (ºC)	48	**36**
Vent flow (kg/s)	0.563	**0.44**

Test 6: Fire size = 62.9 kW, vent 0.86 m wide x 1.83 m high with sill at 0 m, ambient temperature = 26ºC

Interface height (m)	1.03 ± 0.17	**1.165**
Upper temp (ºC)	120	**132**
Lower temp (ºC)	44	**34**
Vent flow (kg/s)	0.616	**0.466**

Test 7: Fire size = 62.9 kW, vent 0.99 m wide x 1.83 m high with sill at 0 m, ambient temperature = 22ºC

Interface height (m)	1.09 ± 0.23	**1.207**
Upper temp (ºC)	109	**122**
Lower temp (ºC)	36	**28**
Vent flow (kg/s)	0.677	**0.493**

Test 8: Fire size = 62.9 kW, vent 0.74 m wide x 1.38 m high with sill at 0.45 m, ambient temperature = 30ºC

Interface height (m)	0.74 ± 0.34	**1.121**
Upper temp (ºC)	143	**154**
Lower temp (ºC)	53	**53**
Vent flow (kg/s)	0.464	**0.39**

Test 9: Fire size = 62.9 kW, vent 0.74 m wide x 0.92 m high with sill at 0.91 m, ambient temperature = 26ºC

Interface height (m)	0.74 ± 0.34	**1.115**
Upper temp (ºC)	177	**178**
Lower temp (ºC)	78	**93**
Vent flow (kg/s)	0.302	**0.278**

Test 10: Fire size = 62.9 kW, vent 0.74 m wide x 0.46 m high with sill at 1.37 m, ambient temperature = 16ºC

Interface height (m)	0.80 ± 0.17	**0.706**
Upper temp (ºC)	270	**250**
Lower temp (ºC)	157	**158**
Vent flow (kg/s)	0.117	**0.115**

Test 11: Fire size = 31.6 kW, vent 0.74 m wide x 1.83 m high with sill at 0 m, ambient temperature = 29ºC

Interface height (m)	0.97 ± 0.11	**1.141**
Upper temp (ºC)	86	**100**
Lower temp (ºC)	41	**35**
Vent flow (kg/s)	0.446	**0.365**

Test 12: Fire size = 105.3 kW, vent 0.74 m wide x 1.83 m high with sill at 0 m, ambient temperature = 35ºC

Interface height (m)	0.97 ± 0.11	**1.085**
Upper temp (ºC)	183	**202**
Lower temp (ºC)	69	**52**
Vent flow (kg/s)	0.624	**0.498**

Test 13: Fire size = 158 kW, vent 0.86 m wide x 1.83 m high with sill at 0 m, ambient temperature = 36ºC

Interface height (m)	0.91 ± 0.17	**1.035**
Upper temp (ºC)	243	**234**
Lower temp (ºC)	81	**57**
Vent flow (kg/s)	0.688	**0.635**

3. MULTI-ROOM SCENARIO

3.1 CASE 3-1

3.1.1 Reference

Peacock, R. D., Davis, S. & Lee, B. T., 1988. An Experimental Data Set for the Accuracy Assessment of Room Fire Models. NBSIR-3752, Gaithersburg, USA: National Bureau of Standards.

http://fire.nist.gov/bfrlpubs/fire88/PDF/f88002.pdf

3.1.2 Description

The experiments were conducted in a three-compartment configuration, with two smaller rooms opening off a corridor 12.4 m long. Details of room dimensions and construction materials may be found in Table 2 and Table 3. A plan view of the experimental layout is shown in Figure 3.

Table 2 Room and doorway dimensions [extracted from (Peacock, et al., 1988)]

Location	Dimensions (m)
First room (R1)	2.34 W x 2.34 L x 2.16 H
First room stub corridor (R2)	1.02 W x 1.03 L x 2.00 H
First room doorway	0.81 W x 1.60 H
Second room corridor (R3)	2.44 W x 12.19 L x 2.44 H
Second room exit doorway	0.76 W x 2.03 H
Third room (R5)	2.24 W x 2.22 L x 2.43 H
Third room stub corridor (R4)	0.79 W x 0.94 L x 2.04 H
Third room doorway	0.79 W x 2.04 H
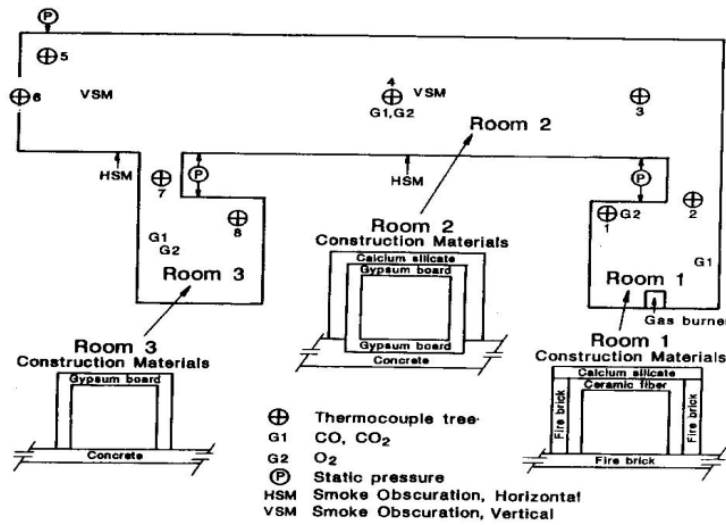
Figure 3. Experimental layout and instrumentation configuration for gas burner tests (extracted from Peacock, et al., 1988)

Table 3. Construction materials (extracted from Peacock, et al., 1988)

Location	Material	Thickness (mm)	Density (kg/m³)	Heat Capacity (kJ/kg · K)	Thermal Conductivity (W/m · K)	Emissivity
First Room						
Wall substrate	Fire Brick	113	750	1.04	0.36 at 200°C 0.38 at 300°C 0.45 at 600°C	0.80
Ceiling substrate	Calcium Silicate		Same as second room walls			
Walls and ceiling[a]	Ceramic Fiber	50	128	1.04	0.09 at 300°C 0.17 at 600°C 0.25 at 900°C	0.97
Floor[a]	Fire Brick		Same as wall substrate			
Second Room						
Ceiling and wall substrate	Gypsum Board	12.7	930	1.09	0.17	–
Ceiling and walls[a]	Calcium Silicate	12.7	720	1.25 at 200°C 1.33 at 300°C 1.55 at 600°C	0.12 at 200°C 0.11 at 300°C 0.12 at 600°C	0.83
Floor substrate	Concrete	102	2280	1.04	1.8	–
Floor[a]	Gypsum Board	12.7	930	1.09	0.17	–
Third Room						
Walls and ceiling[a]	Gypsum Board[b]	12.7	930	1.09	0.17	–
Floor[a]	Concrete	102	2280	1.04	1.8	–

Notes to Table 2

a -- Interior finish
b -- Gypsum board over studs

The structure was instrumented to provide data on temperatures as well as mass and heat flows in a simple multi-room configuration. There were a total of eight thermocouple trees strategically positioned within the three rooms (Figure 3).

3.1.3 Model Parameters

B-RISK 2013.09 is used.

B-RISK predictions use the nominal steady HRR from the experiments and assumed the gas fuel was a mixture of methane and acetylene as indicated in the report. The radiant loss fraction was taken as 0.23, the net heat of combustion as 46.6 kJ/g, the HRRPUA as 865 kW/m^2, the soot yield as 0.049 g/g and the CO_2 yield as 2.67 g/g. The burner was assumed to be in contact with the rear wall and elevated 0.5 m above the floor.

The experiments were modelled as five connected compartments, with the two sub-passageways connecting the rooms to the corridor represented as separate rooms in the model as shown in Figure 4.
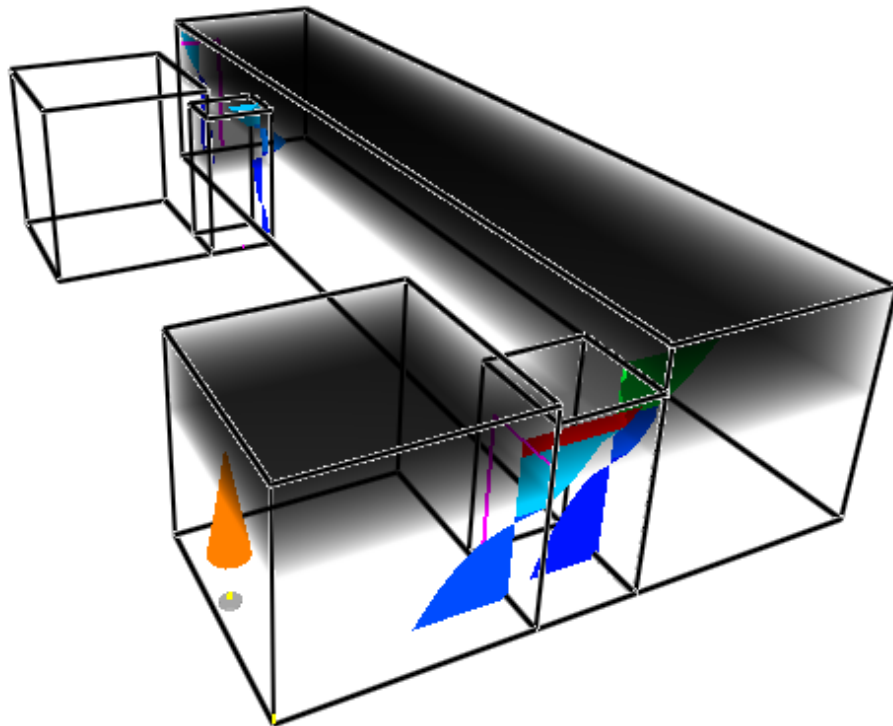
Figure 4. SmokeView visualisation – Set 1 – 100J

3.1.4 Comparison

A summary of the experiments presented is shown in Table 4.

Table 4. Summary of experiments

Test ID	Nominal fire size	Corridor exit	Door to Room 3
Set 1 – 100J (Figure 5)	100 kW	Open	Closed
Set 6 – 300D (Figure 6)	300 kW	Closed	Open
Set 8 – 500A (Figure 7)	500 kW	Open	Closed

Figure 5**. Test 100J comparison of predicted and measured parameters in the burn room and corridor for Set 1 – 100J (100 kW, corridor exit door open and third room closed)**
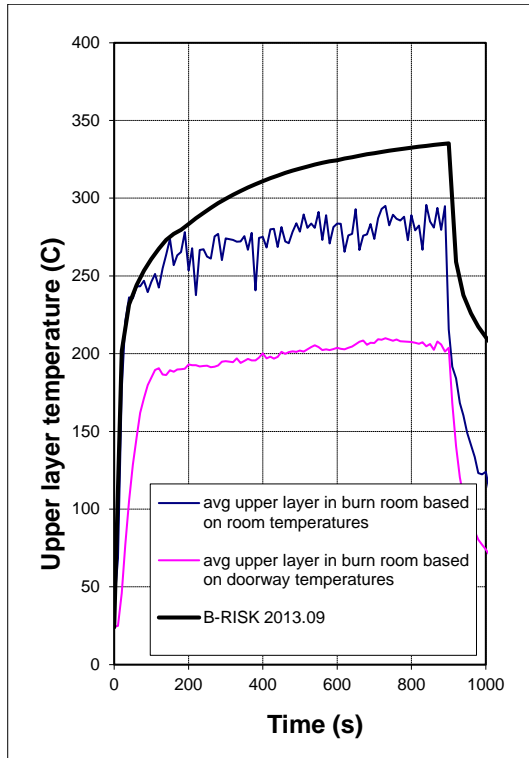
(a)
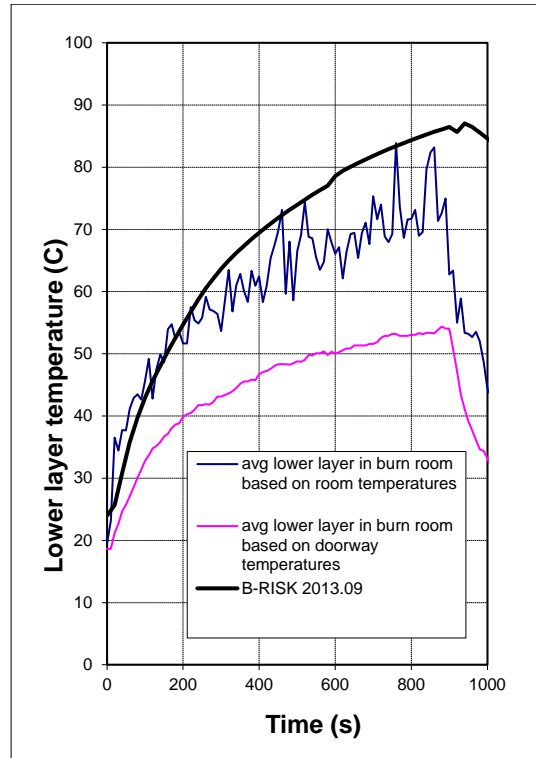
(b)
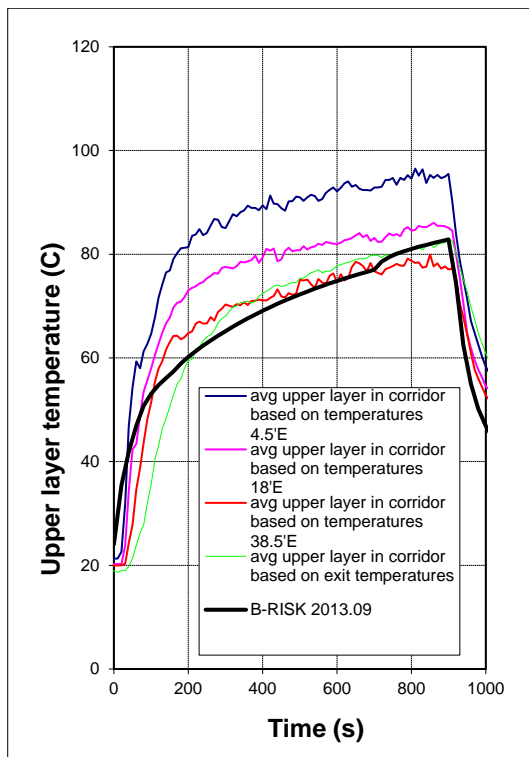
(c)
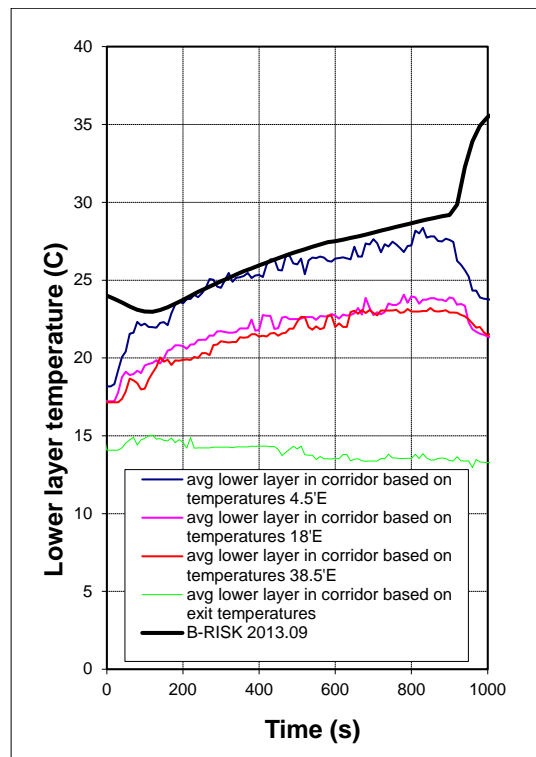
(d)
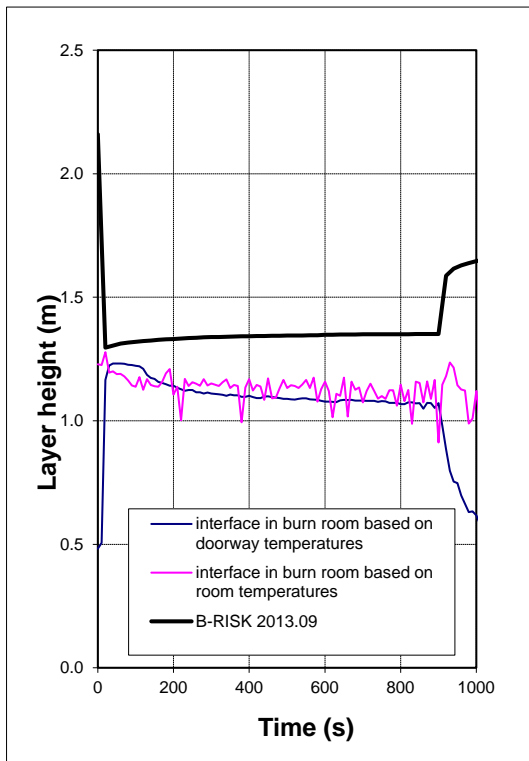
(e)
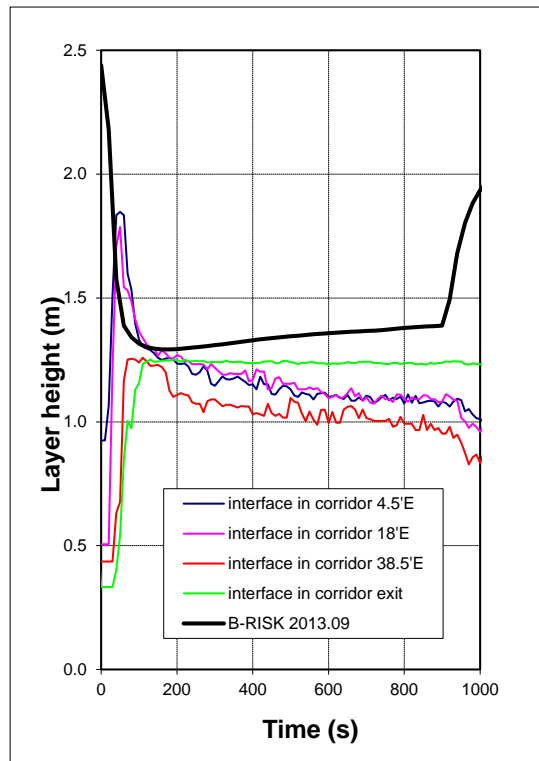
(f)
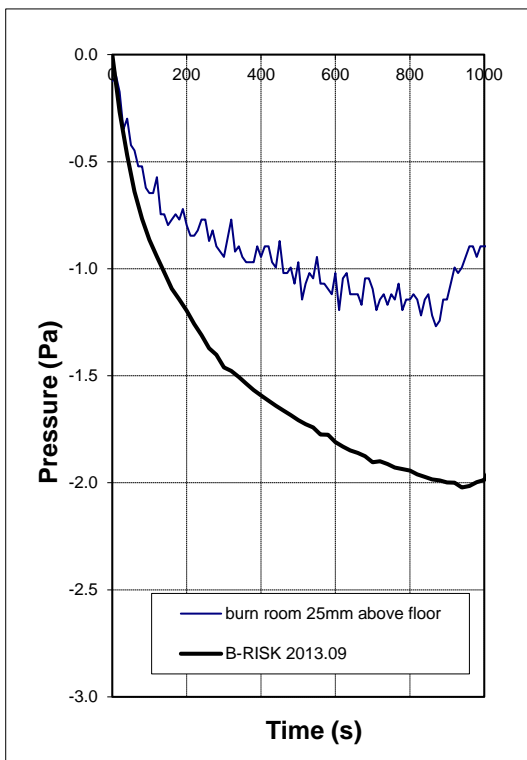
(g)
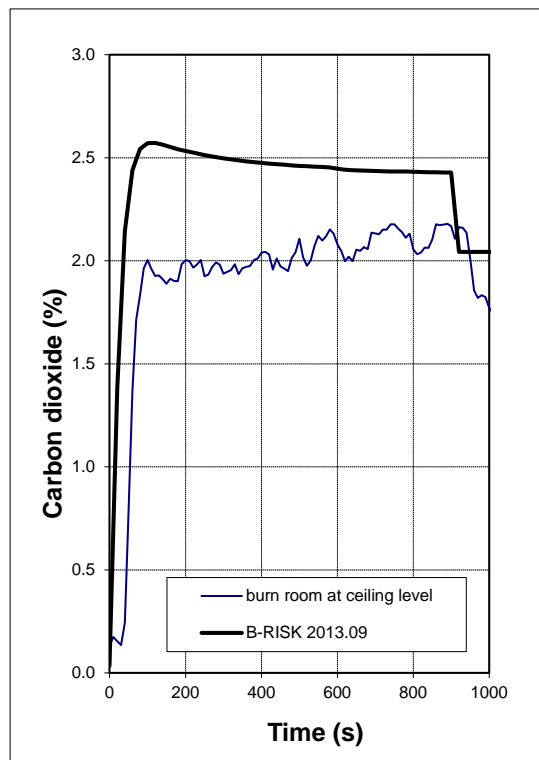
(h)

Figure 6. **Test 300D comparison of predicted and measured parameters in the burn room and corridor for Set 6 – 300D (300 kW, corridor exit door closed and third room open)**

(a)

(b)

(c)

(d)

(e)

(f)

(g)

(h)

13
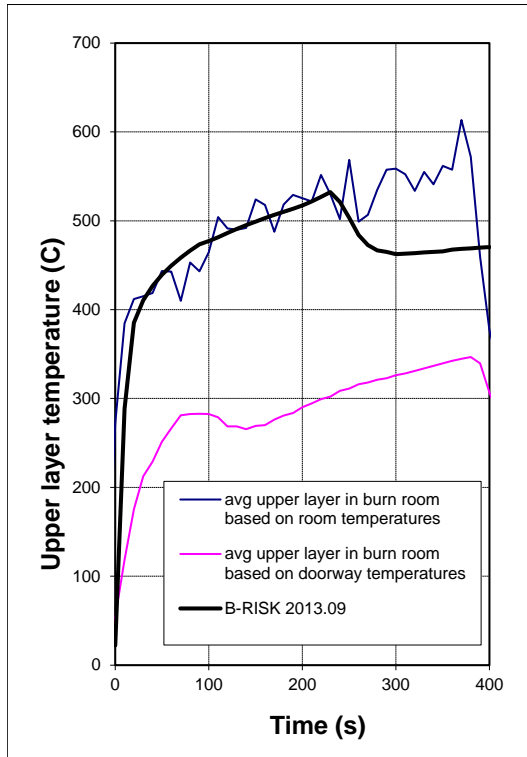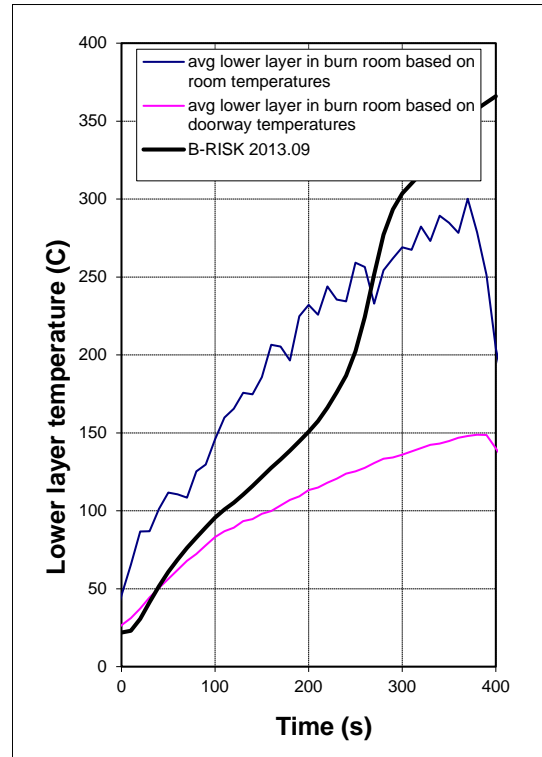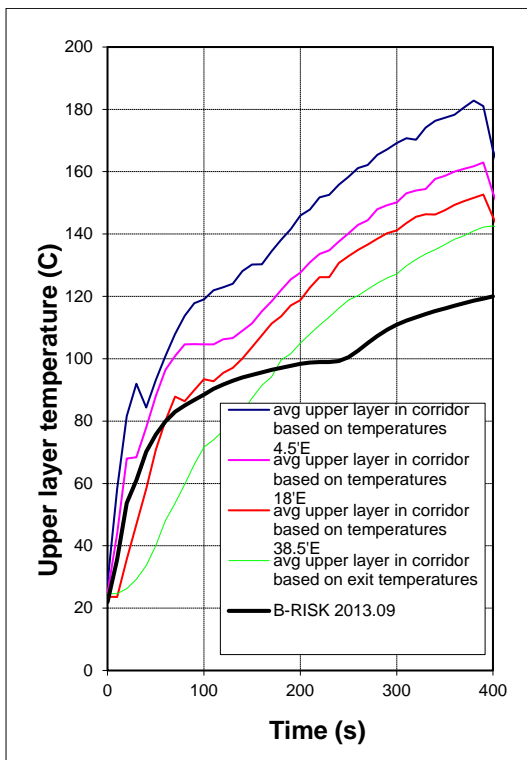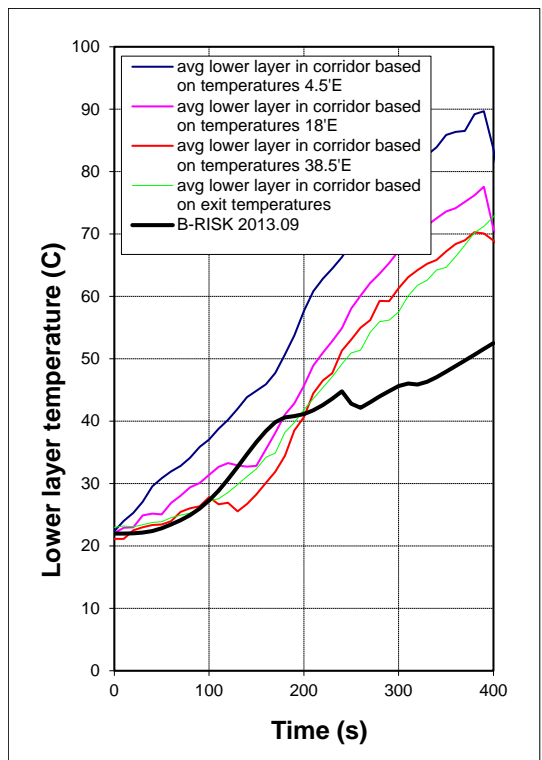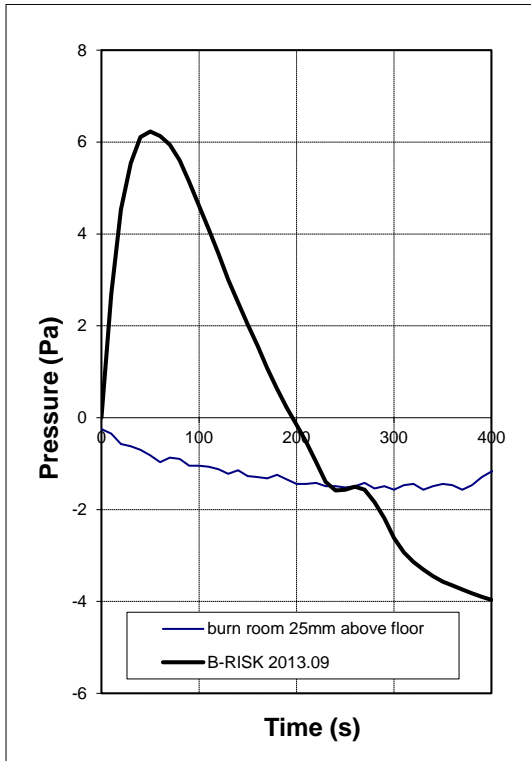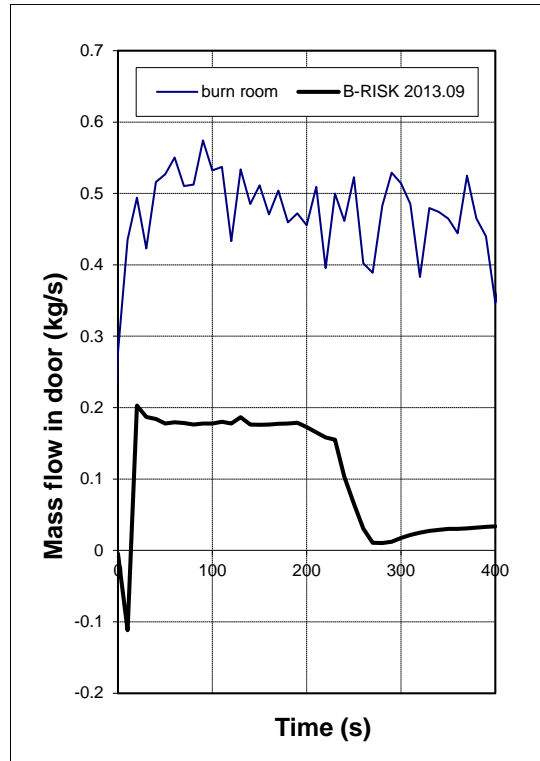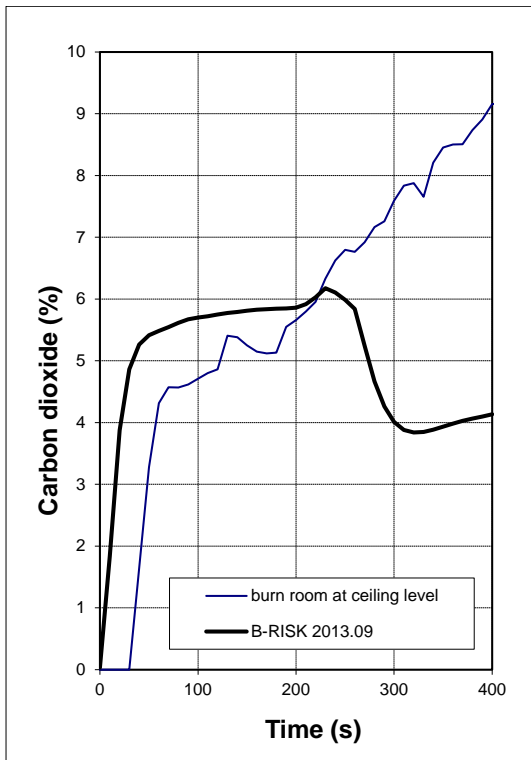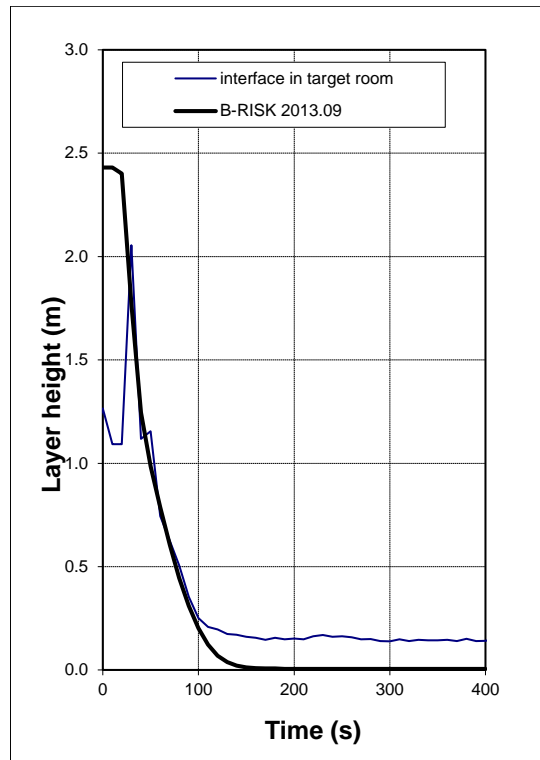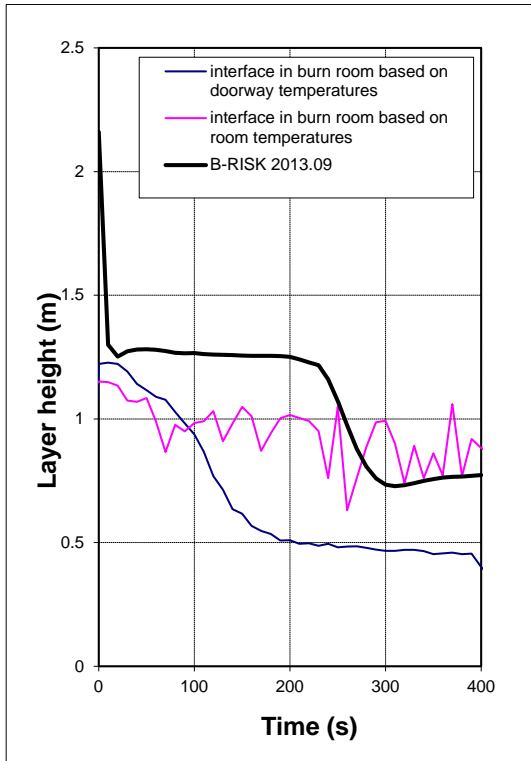
(i)
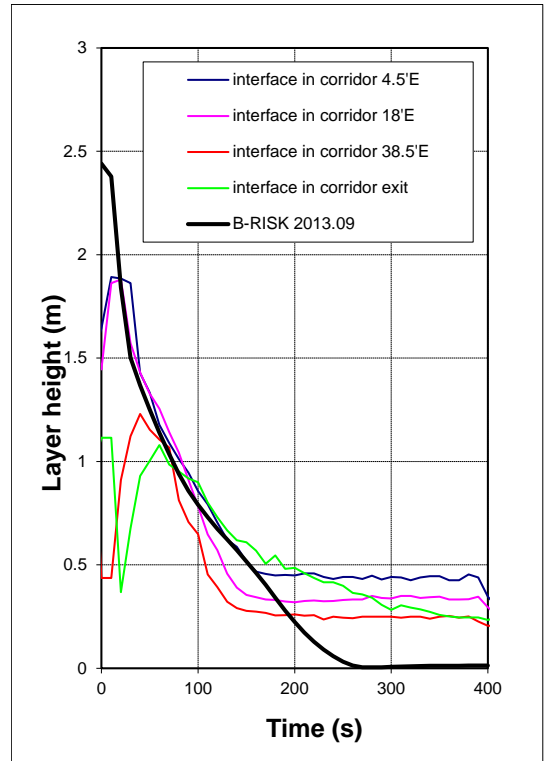
(j)
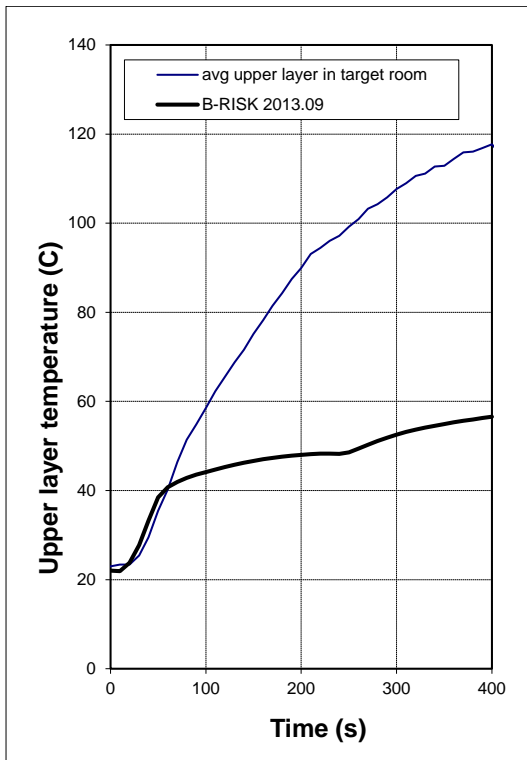
(k)
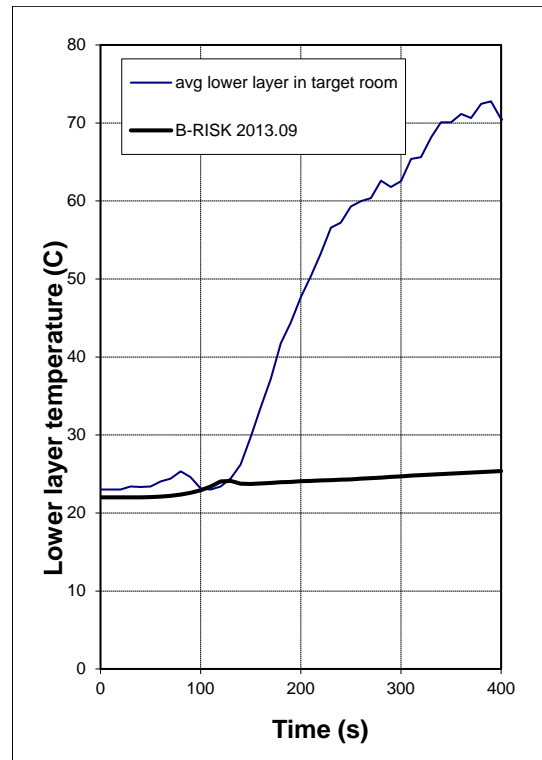
(l)

Figure 7. Test 500A comparison of predicted and measured parameters in the burn room and corridor for Set 8 – 500A (500 kW, corridor exit door open and third room closed)

(a)

(b)

(c)

(d)

(e)

(f)

(g)

(h)

16

(i)

(j)

17
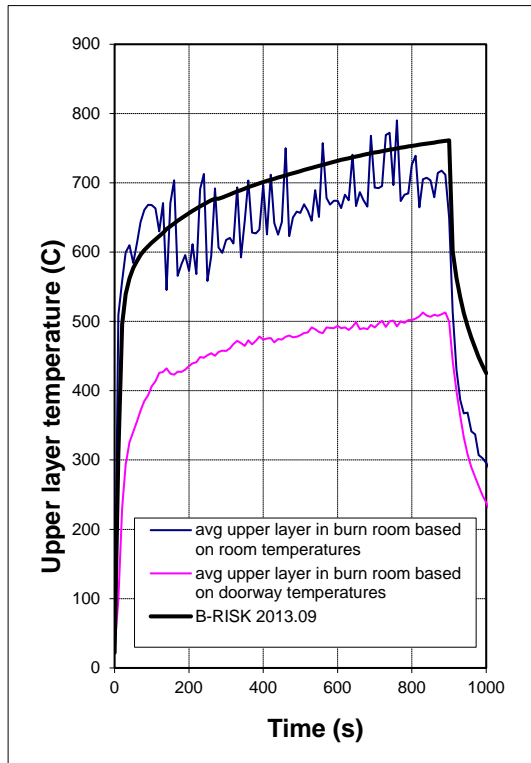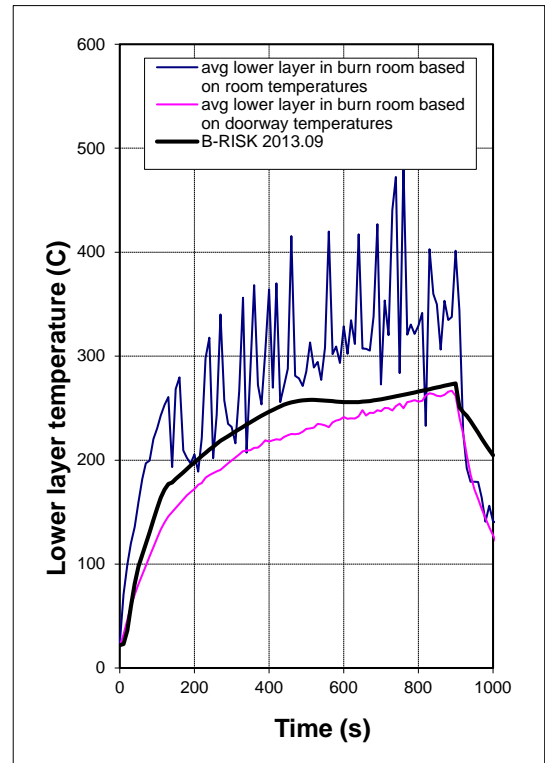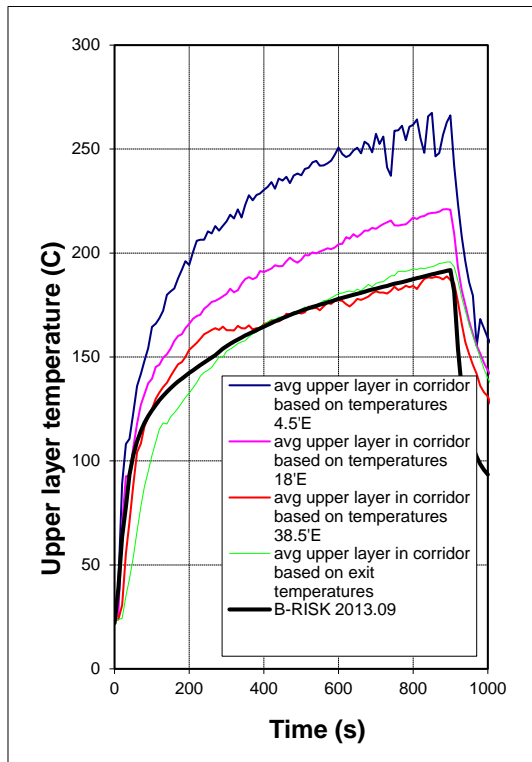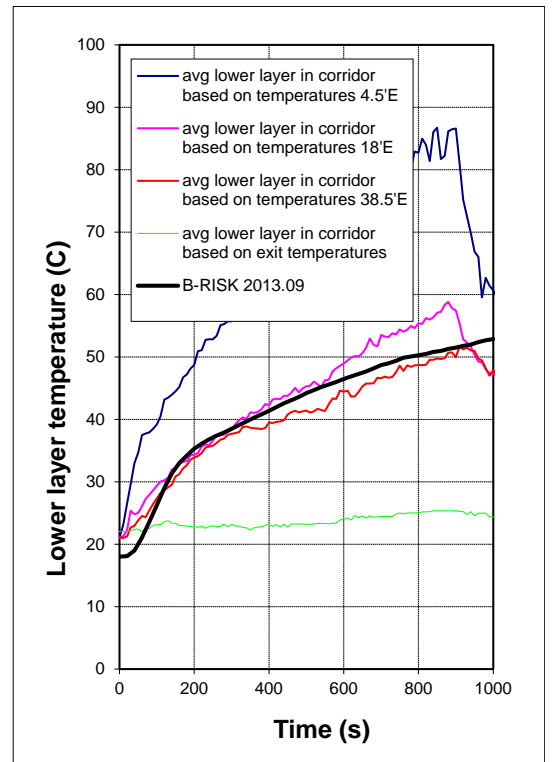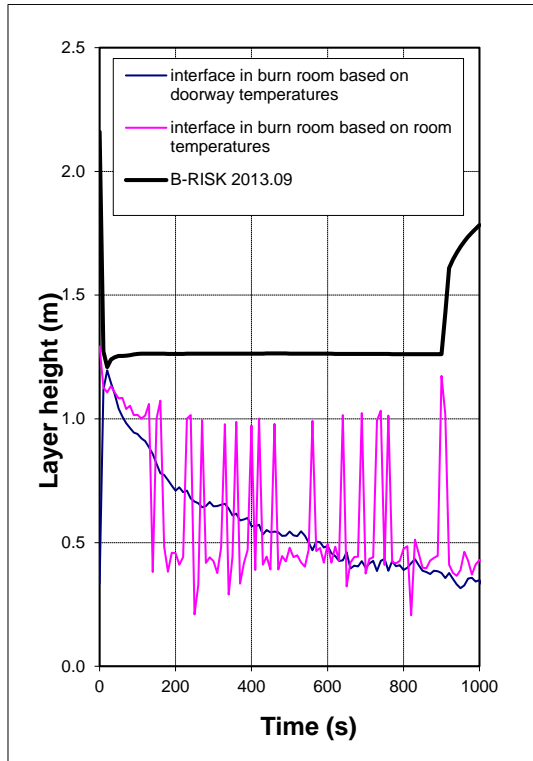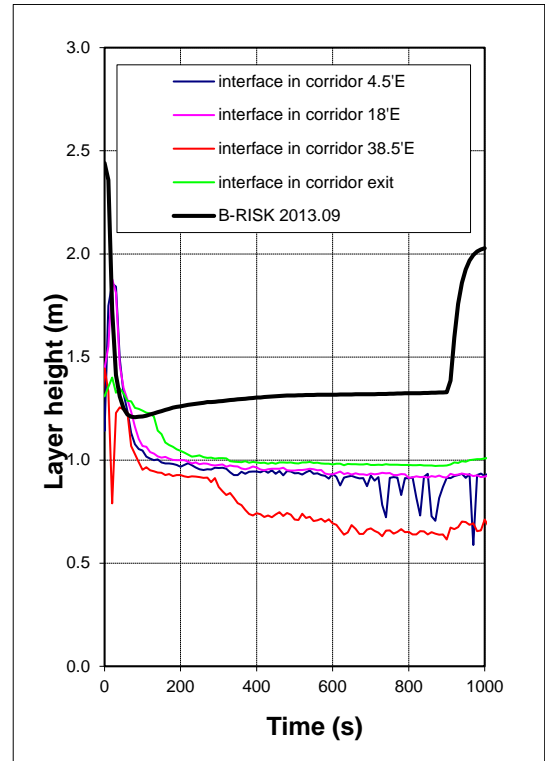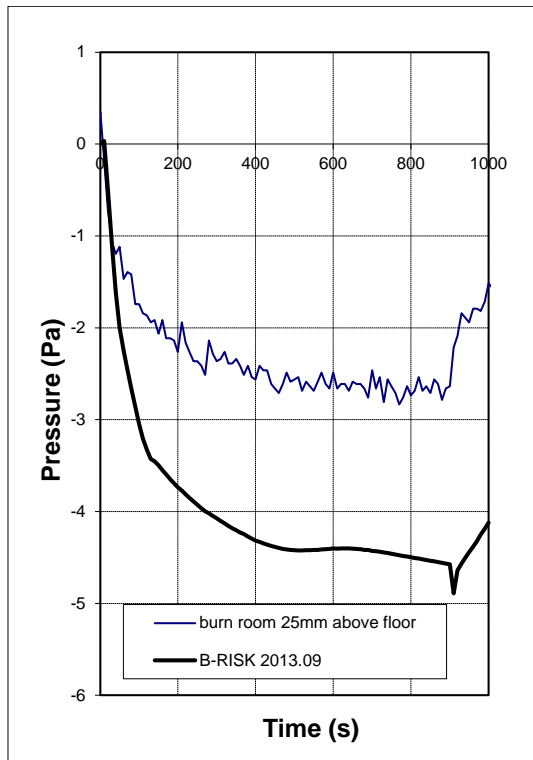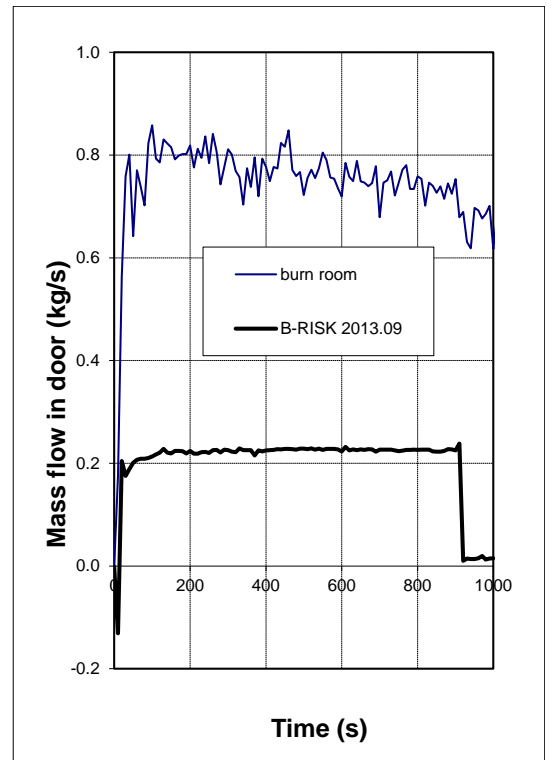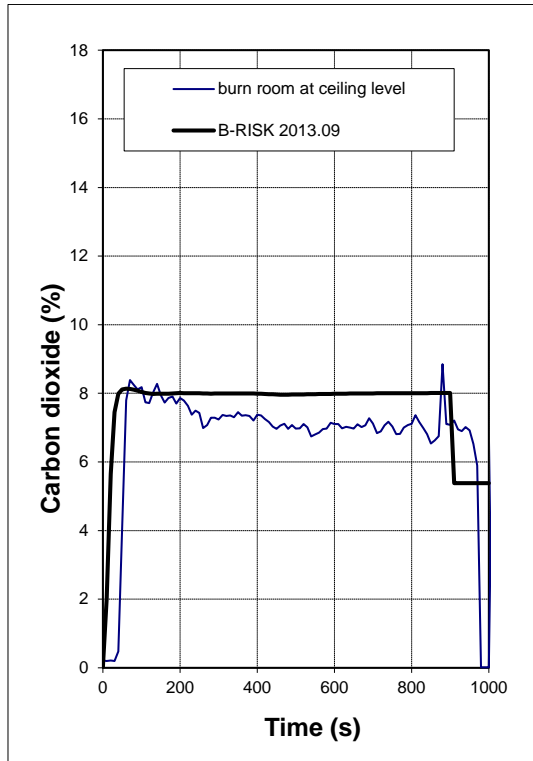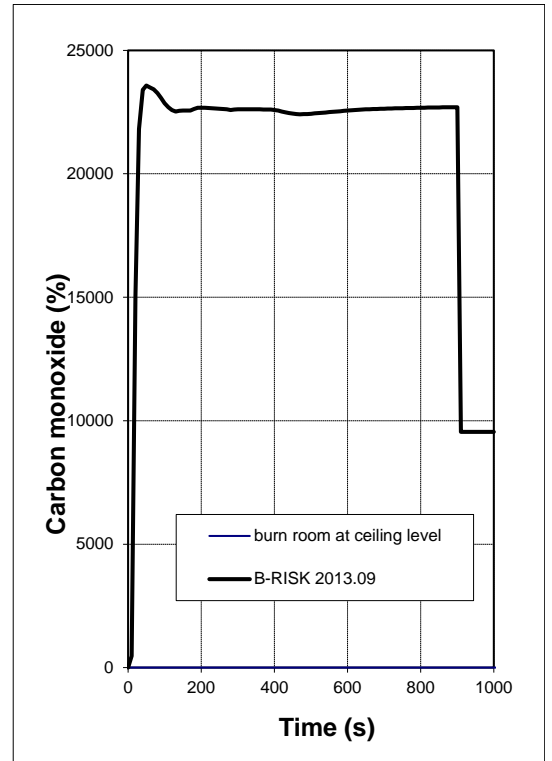
4. ISO 9705 – FIRE GROWTH ON SURFACE LININGS

4.1 CASE 4-1

4.1.1 Reference

Interscience Communications Ltd (ICL), 1991. *EUREFIC European Reaction to Fire Classification.* Copenhagen, Denmark, Interscience Communications Ltd.

4.1.2 Description

The EUREFIC research programme (Interscience Communications Ltd (ICL), 1991) included experiments on 11 different surface lining products using the ISO 9705 full-scale room test apparatus and ISO 5660 cone calorimeter. B-RISK modelling relies on use of the cone calorimeter test data for input to the model.

The ISO 9705 test procedure requires that a square gas burner be placed in the corner of a room (3.6 m long x 2.4 m wide x 2.4 m high). The room had a single opening 2 m high by 0.8 m wide in the wall located opposite the burner. The burner dimensions were 170 mm square. Three walls and the ceiling were lined with the surface lining material. The burner output was controlled to be 100 kW for ten minutes followed by 300 kW for a further ten minutes. The total HRR was determined using oxygen consumption calorimetry techniques after measuring the oxygen concentration of the exhaust gases. A fire size of 1 MW in the ISO 9705 room is generally considered to be indicative of "flashover" and if reached, the test is terminated.

4.1.3 Model Parameters

B-RISK 2013.09 is used.

Simulations use the "flame spread model" option.

B-RISK predictions use the nominal steady HRR from the experiments (100 kW for ten minutes followed by 300 kW for a further ten minutes) and assumed the gas fuel was propane. The radiant loss fraction was taken as 0.3, the net heat of combustion as 43.7 kJ/g, the HRRPUA as 3460 kW/m^2, the soot yield as 0.024 g/g and the CO_2 yield as 2.34 g/g. The burner was assumed to be in contact with two rear walls (in corner) and elevated 0.3 m above the floor.

4.1.4 Comparison

Nine of the 11 materials are shown here in a comparison of the HRR measured in the ISO 9705 test compared to the predicted values over the 20-minute period of the test. The available small-scale test data for the two materials omitted were considered to be inadequate and they are therefore not included in the comparison.

The available cone calorimeter data for each material comprised experiments carried out at three different external heat fluxes, typically 25, 35 and 50 kW/m². The B-RISK model used all available data and the FTP method of correlating the ignition times.

Figure 8 to Figure 16 show the measured and predicted HRR for each material.

Eurefic Material #1
Painted gypsum paper-faced plasterboard (12 mm thick)
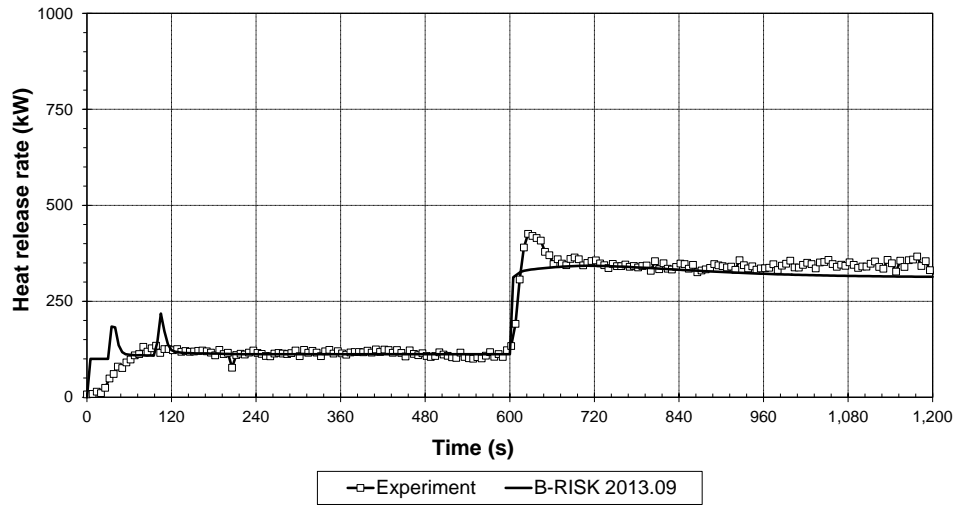
Figure 8. Painted gypsum paper-faced plasterboard

Eurefic Material #2
Ordinary birch plywood (12 mm thick)
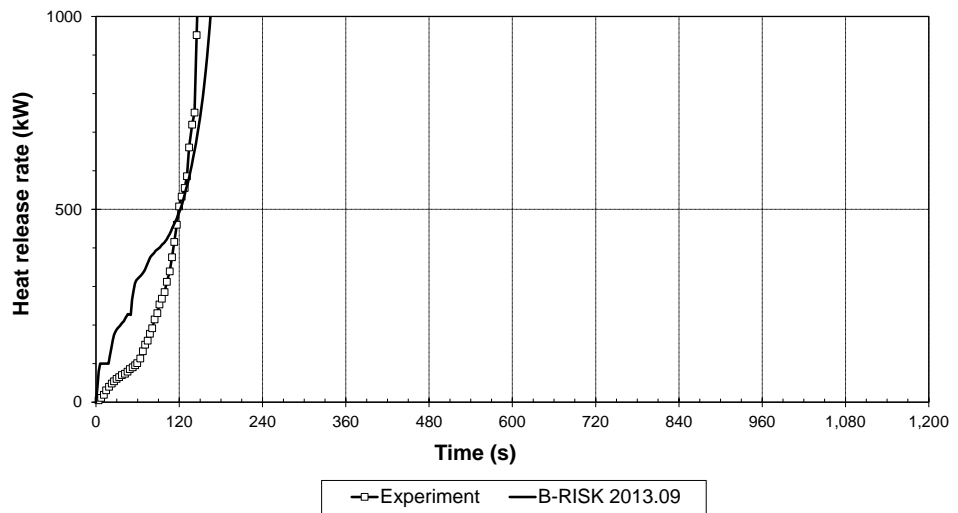
Figure 9. Ordinary birch plywood

Eurefic Material #3
Textile wallcovering on gypsum paper-faced plasterboard (12 mm thick)
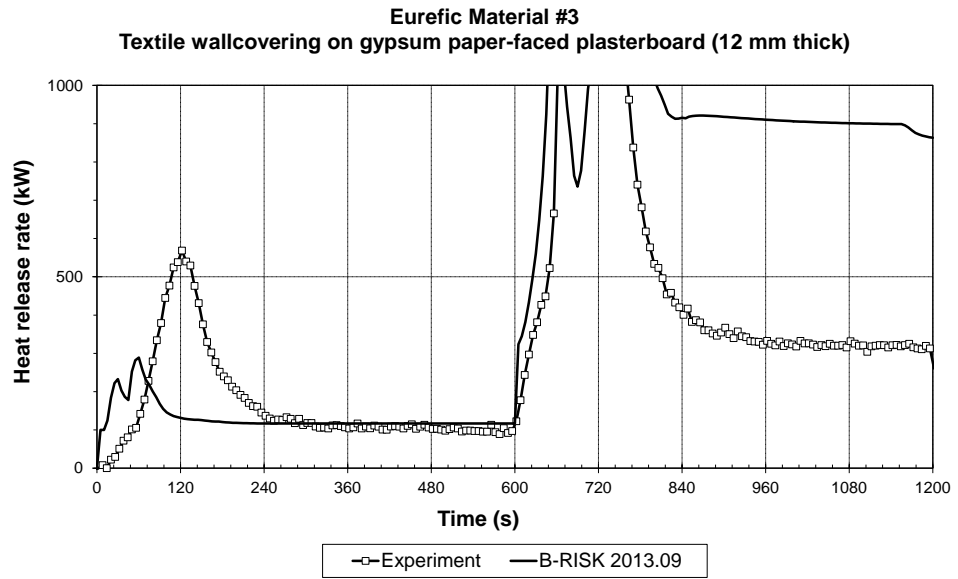
Figure 10. Textile wall covering on gypsum paper-faced plasterboard

Eurefic Material #4
Melamine-faced high density non-combustible board (12.5 mm thick)
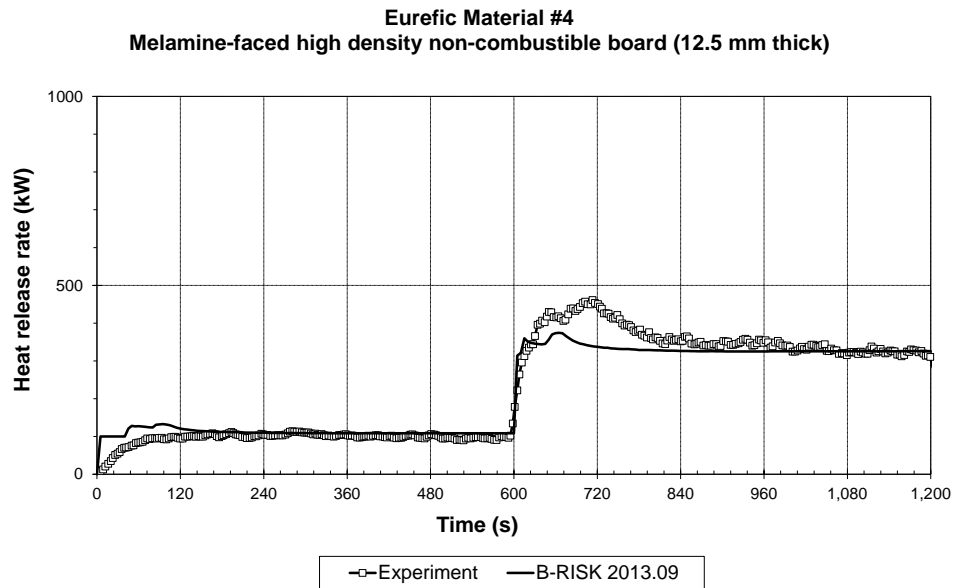
Figure 11. Melamine-faced high density non-combustible board

Eurefic Material #5
Plastic-faced steel sheet on mineral wool (23 mm thick)
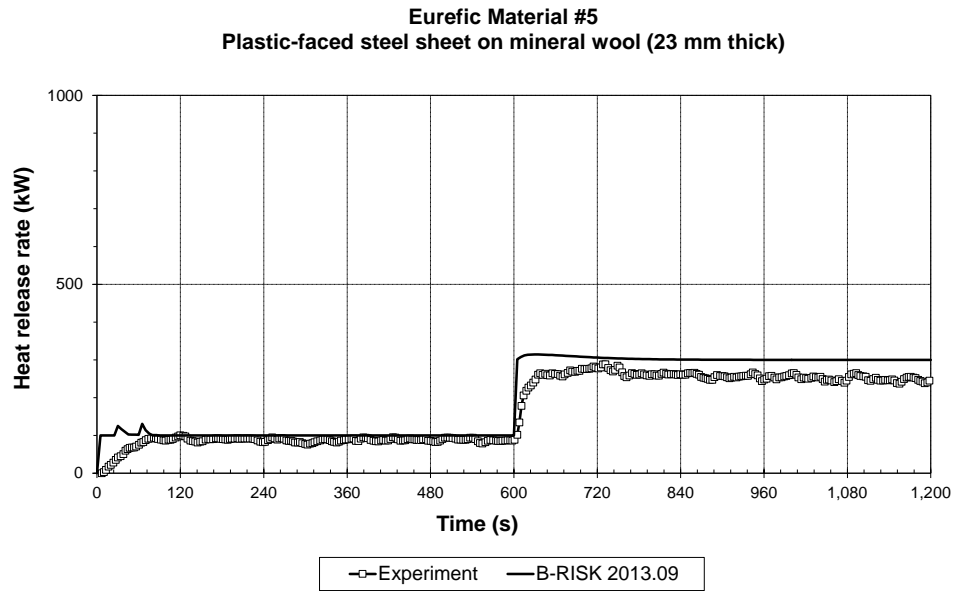
Figure 12. Plastic-faced steel sheet on mineral wool

Eurefic Material #6
FR particleboard type B1 (16 mm thick)
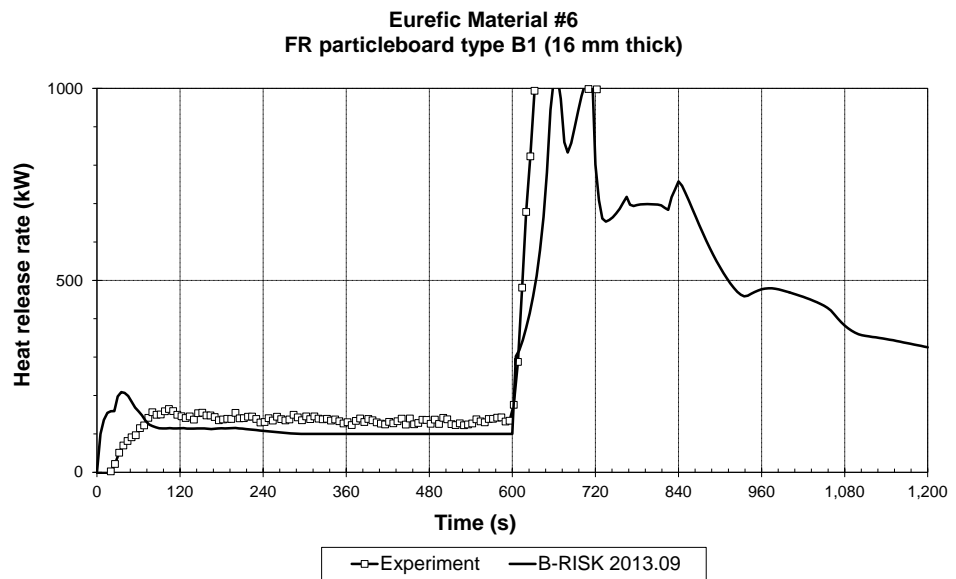
Figure 13. FR particleboard Type B1

Eurefic Material #9
Polyurethane foam covered with steel sheets (80 mm thick)
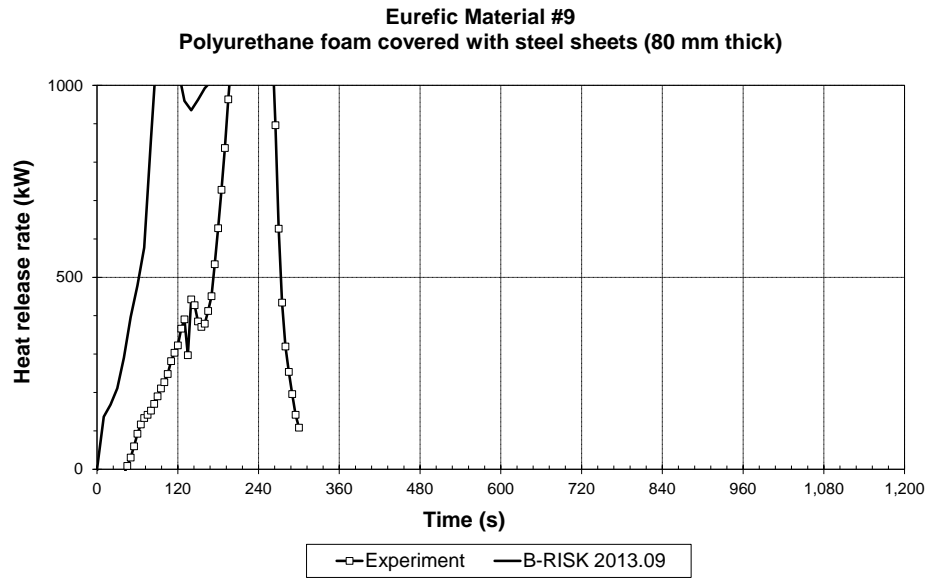
Figure 14. Polyurethane foam covered with steel sheets

Eurefic Material #10
PVC wallcarpet on gypsum paper-faced plasterboard (12 mm thick)
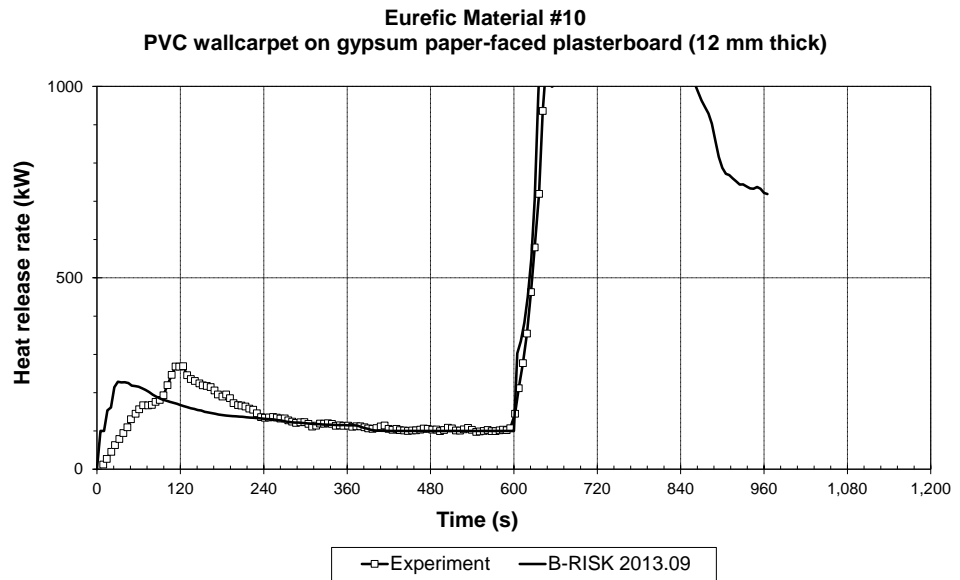
Figure 15. PVC wallcarpet on gypsum paper-faced plasterboard

Eurefic Material #11
FR polystyrene foam (25 mm thick)
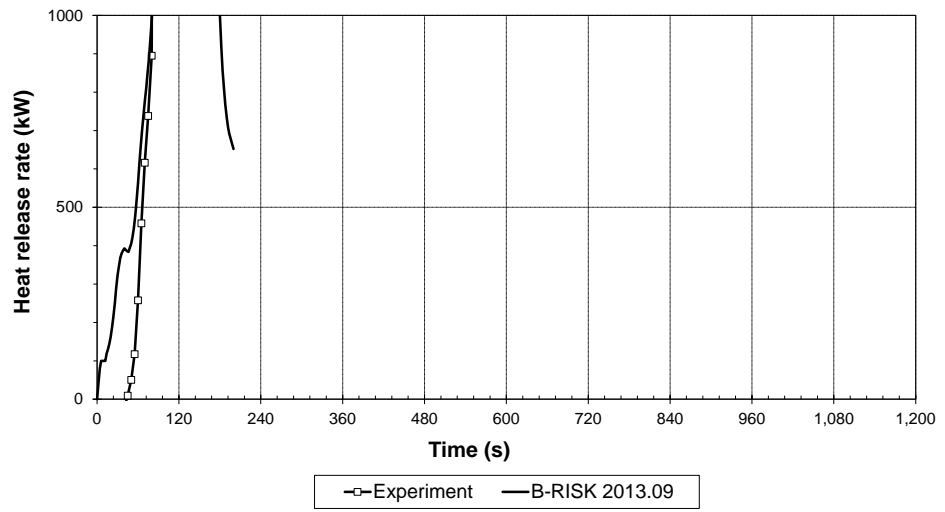
Figure 16. FR polystyrene foam

4.2 CASE 4-2

4.2.1 Reference

Dowling V, McArthur NA, Webb AK, Leonard JE and Blackmore J. 1999. *Large Scale Fire Tests on Three Building Materials.* Proceedings Third International Conference on Fire Research and Engineering, 4-8 October 1999, Chicago, USA. p217-227.

4.2.2 Description

Experiments were conducted (Dowling, et al., 1999) on three surface lining materials (16 mm plasterboard, 4 mm fire retardant treated plywood and 4 mm non-fire retardant plywood) using the ISO 9705 full-scale room test apparatus and bench-scale cone calorimeter. The set-up and test procedure were similar to that described in Section 4.1, except that the burner dimensions were 300 mm square.

In the case of the fire retardant and non-fire retardant plywoods, additional tests were carried out with the plywood fixed to the wall only and the ceiling only.

4.2.3 Model Parameters

B-RISK 2013.09 is used.

Simulations use the "flame spread model" option.

B-RISK predictions use the nominal steady HRR from the experiments (100 kW for ten minutes followed by 300 kW for a further ten minutes) and assume the gas fuel is propane. The radiant loss fraction is taken as 0.3, the net heat of combustion as 43.7 kJ/g, the HRRPUA as 1111 kW/m^2, the soot yield as 0.024 g/g and the CO_2 yield as 2.34 g/g. The burner is assumed to be in contact with two rear walls (in corner) and elevated 0.3 m above the floor.

4.2.4 Comparison

A comparison of the HRR measured in the experiments with the B-RISK predicted values over the 20-minute period of the test is shown in Figure 17 to Figure 23.

CSIRO Material 115
16 mm Gypsum plasterboard, walls and ceiling
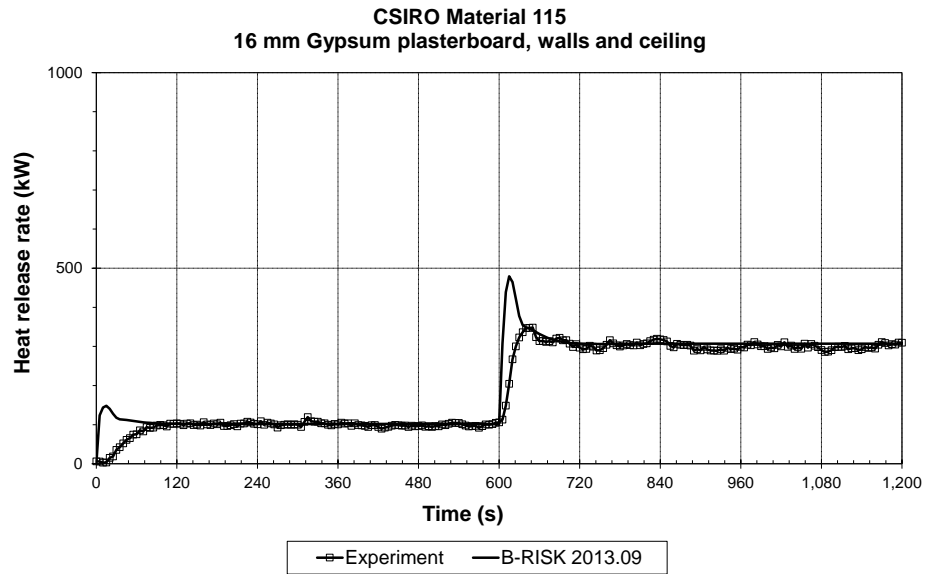
Figure 17. Gypsum plasterboard, wall and ceiling

CSIRO Material 104
Plywood (4 mm thick) on 16 mm gypsum plasterboard, walls only
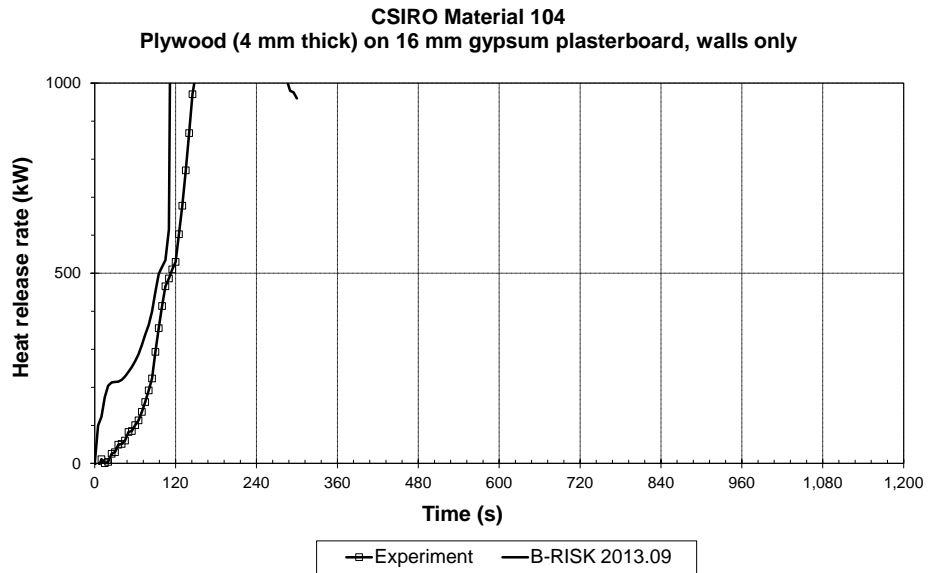
Figure 18. Plywood, walls only

CSIRO Material 104
Plywood (4 mm thick) on 16 mm Gypsum Plasterboard, Ceiling Only
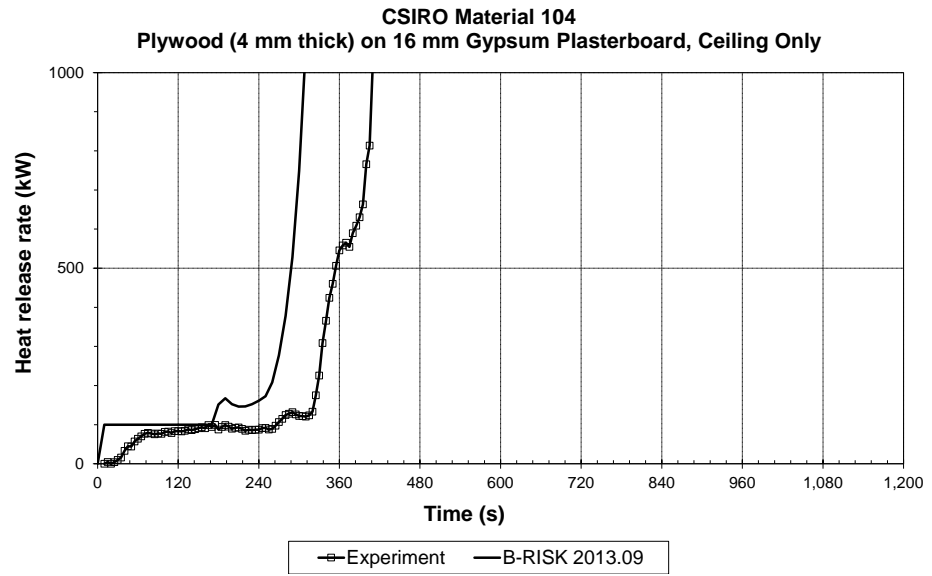
Figure 19. Plywood, ceiling only

CSIRO Material 104
Plywood (4 mm thick) on 16 mm gypsum plasterboard, walls and ceiling
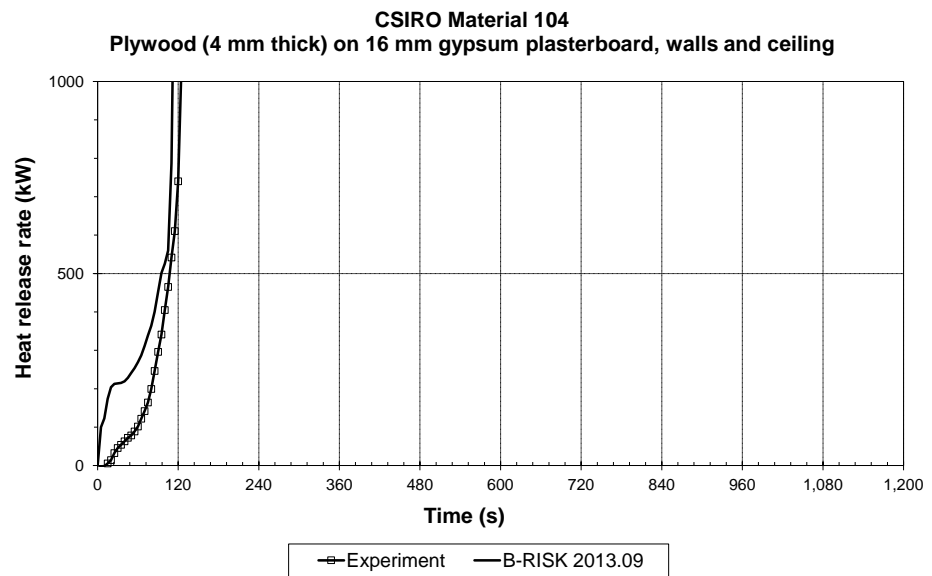
Figure 20. Plywood, walls and ceiling

CSIRO Material 108
FR plywood (4 mm thick) on 16 mm gypsum plasterboard, ceiling only
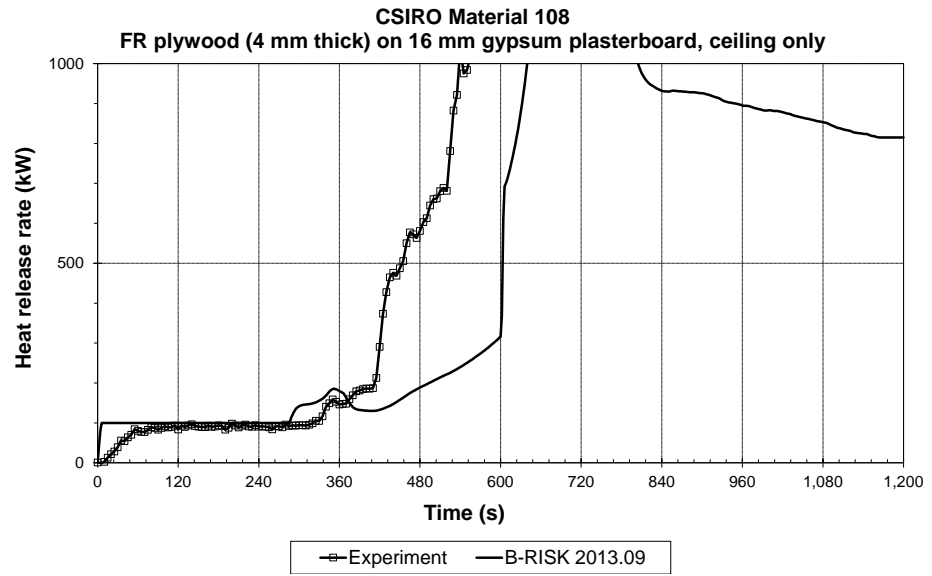
Figure 21. FR plywood, ceiling only

CSIRO Material 108
FR plywood (4 mm thick) on 16 mm gypsum plasterboard, walls only
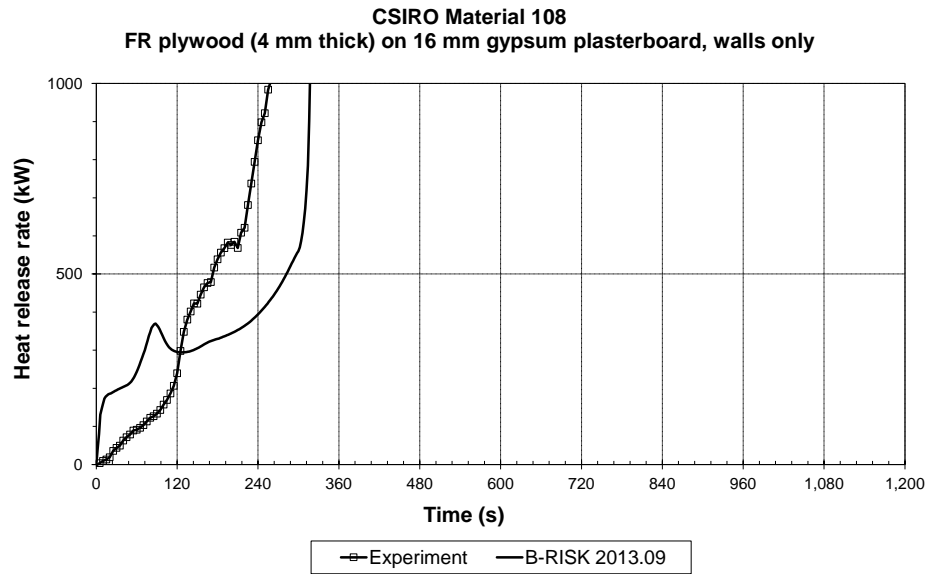
Figure 22. FR plywood, walls only

CSIRO Material 108
FR plywood (4 mm thick) on 16 mm gypsum plasterboard, walls and ceiling
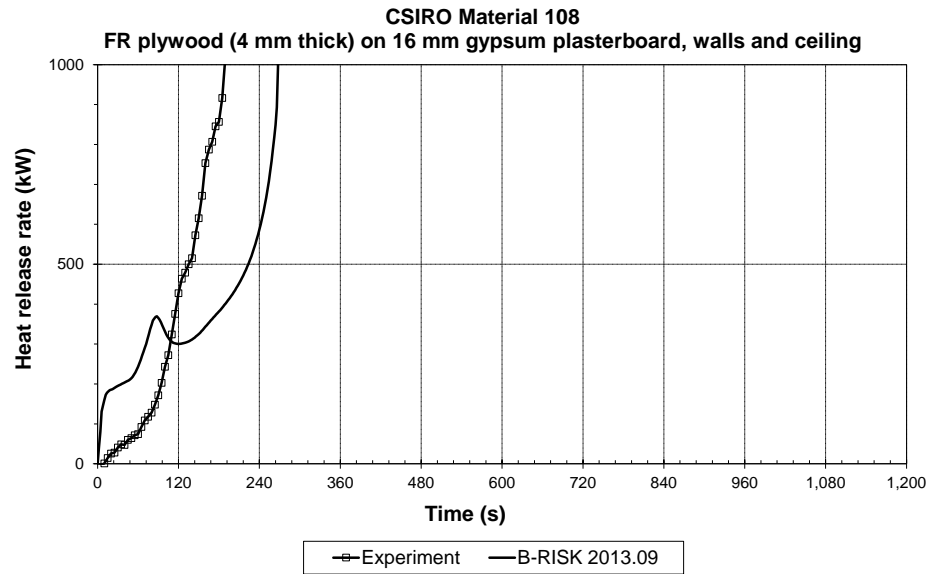
Figure 23. FR plywood, walls and ceiling

5. LARGE ROOM – FIRE GROWTH ON SURFACE LININGS

5.1 CASE 5-1

5.1.1 Reference

Mikkola, E. & Kokkala, M., 1991. *Experimental Programme of EUREFIC. In EUREIC Seminar Proceedings.* Copenhagen, Denmark, Interscience Communications Ltd.

5.1.2 Description

The test room was 9 x 6.75 x 4.9 m high with a single door opening of 2 x 2 m high in the wall opposite the gas burner (Mikkola & Kokkala, 1991). The walls and ceiling of the test room were made of 200 mm thick lightweight concrete of density 500 kg/m³. The burner was located in a corner and the heat output was 100 kW for ten minutes, 300 kW for the next ten minutes and 900 kW for the last ten minutes. Walls and ceiling were lined with surface lining products selected from the EUREFIC project.

5.1.3 Model Parameters

B-RISK 2013.09 is used.

Simulations use the "flame spread model" option.

B-RISK predictions use the nominal steady HRR from the experiments (100 kW for ten minutes followed by 300 kW for ten minutes and 900 kW for a further ten minutes) and assumes the gas fuel is propane. The radiant loss fraction is taken as 0.3, the net heat of combustion as 43.7 kJ/g, the HRRPUA as 3460 kW/m^2, the soot yield as 0.024 g/g and the CO_2 yield as 2.34 g/g. The burner is assumed to be in contact with two rear walls (in corner) and elevated 0.3 m above the floor.

5.1.4 Comparison

A comparison of the HRR measured in the large-scale tests with the B-RISK predicted values over the 20-minute period of the test is shown in Figure 24 to Figure 27.

Eurefic Material #2
Ordinary birch plywood (12 mm thick)
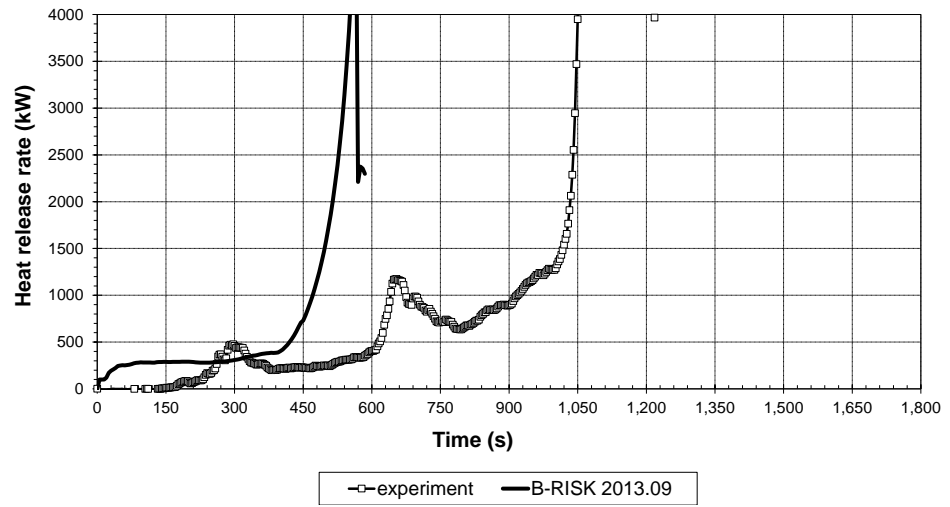
Figure 24. Ordinary birch plywood

Eurefic Material #3
Textile wallcovering on gypsum paper-faced plasterboard (12 mm thick)
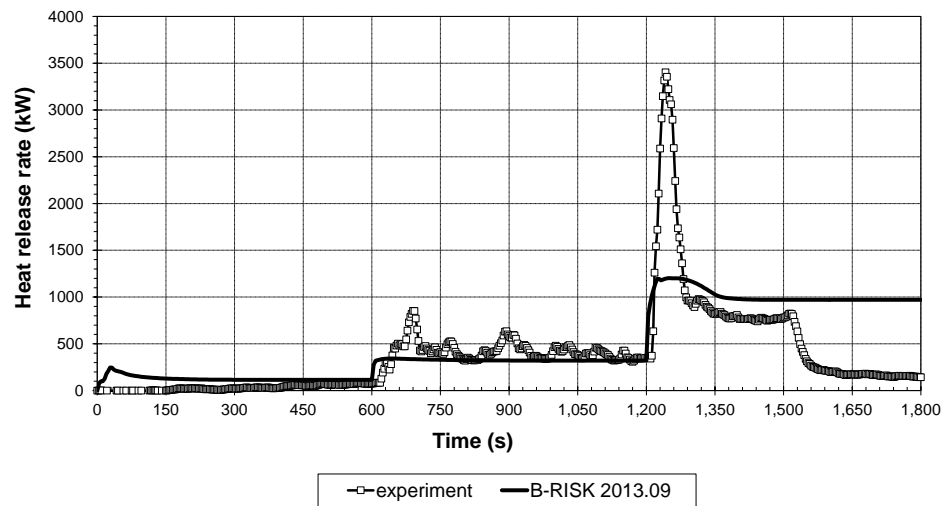
Figure 25. Textile wall covering on gypsum paper-faced plasterboard

Eurefic Material #6
FR particleboard type B1 (16 mm thick)
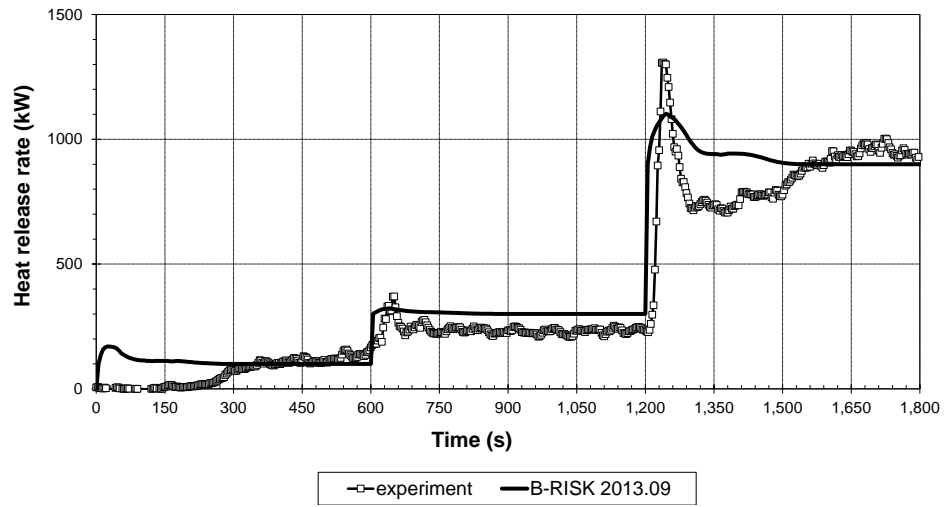
Figure 26. FR particleboard Type B1

Eurefic Material #10
PVC wallcarpet on gypsum paper-faced plasterboard (12 mm thick)
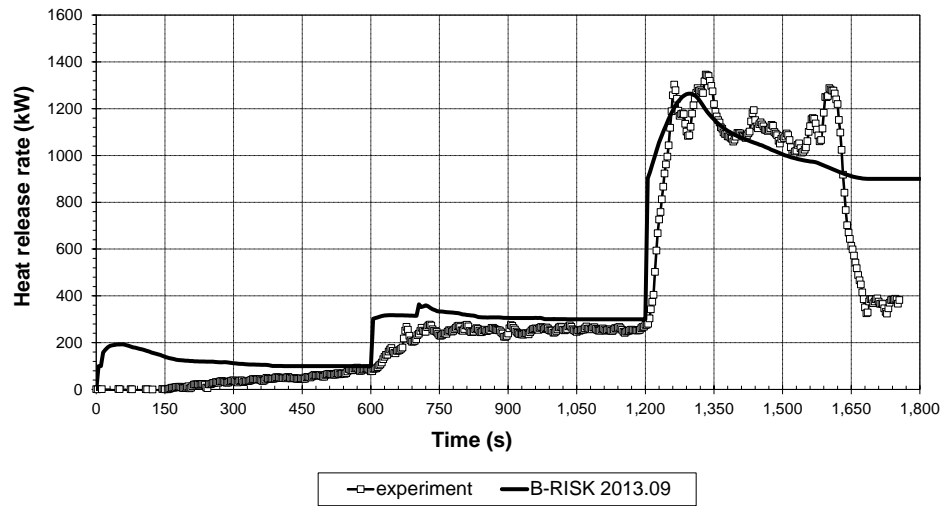
Figure 27. PVC wall carpet on gypsum paper-faced plasterboard

6. POST-FLASHOVER FIRE IN SINGLE COMPARTMENT

6.1 CASE 6-1

6.1.1 Reference

Nyman, J., 2002. *Equivalent Fire Resistance Ratings of Construction Elements Exposed to Realistic Fires, Fire Engineering Research Report 02/13*. University of Canterbury, Christchurch, New Zealand.University of Canterbury, Christchurch, New Zealand.

http://www.civil.canterbury.ac.nz/fire/pdfreports/JNyman02.pdf

Nyman, J., Gerlich, J. T., Wade, C. A. & Buchanan, A. H., 2008. Predicting Fire Resistance Performance of Drywall Construction Exposed to Parametric Design Fires – A Review. Journal of Fire Protection Engineering, 18(2).

6.1.2 Description

A set of three full-scale compartment tests were carried out using numerous light timber framed (LTF) and light steel framed non-loadbearing walls (mostly plasterboard lined) and LTF ceiling/floor assemblies (Nyman, 2002; Nyman, et al., 2008). The compartments had dimensions of 3.6 m long x 2.4 m wide x 2.4 m high. In each test, a polyurethane foam upholstered two-seater sofa was ignited with the fire spreading to a series of wood cribs also in the compartment. Wall integrity failures were observed in each of the three tests at 22, 37.5 and 23 minutes respectively. In the modelling, vents representing the section of collapsing wall were opened at these times.

6.1.3 Model Parameters

B-RISK 2013.09 is used.

Simulations use the "wood crib post-flashover model" option.

The wall and ceiling surfaces were taken as gypsum plasterboard with thermal conductivity 0.2 W/mK, density 720 kg/m^3 and specific heat 3402 J/kgK giving $\sqrt{(k\rho c)}$ = 700 Js$^{-1/2}$K^{-1}m^{-2}.

In Test A, a vent 2.4 m wide x 2.4 m high was opened at 22 minutes to represent the rear wall collapsing. In Test B, a vent 2.4 m wide x 2.4 m high was opened at 37.5 minutes to represent the rear wall collapsing. In Test C, a vent 1.8 m wide x 2.4 m high was opened at 22 minutes to represent 50% of side wall collapsing. The size of the door opening (0.8 or 1.2 m wide) and the fire load energy density (800 or 1200 MJ/m^2) are as noted in Figure 28 to Figure 30 for each of the tests.

6.1.4 Comparison

The HRR of an identical sofa was measured in a room of the same dimensions using oxygen consumption calorimetry and the data collected was used to describe the heat release of the initial burning item in the B-RISK simulation prior to flashover.

Figure 28 to Figure 30 show the measured and predicted rate of heat release for each test.

800 MJ/m², Vent 2 m high x 0.8 m wide
plasterboard lined, timber framed walls, ceiling
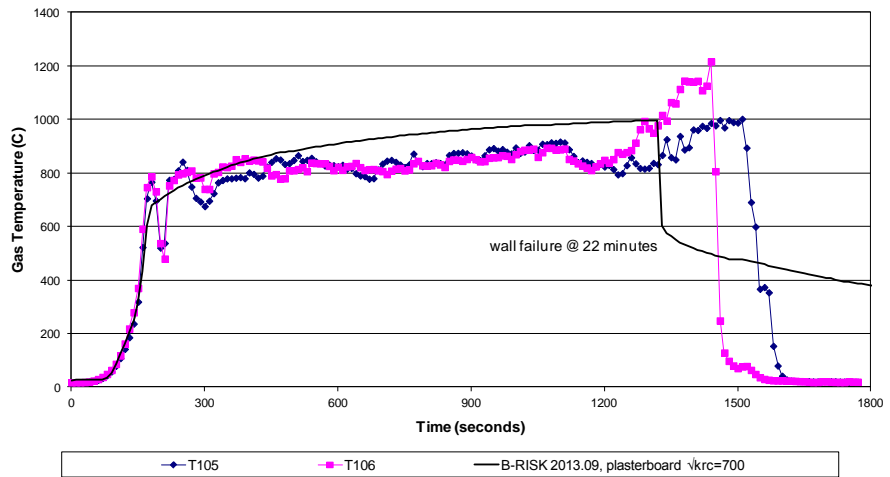
Figure 28. Gas temperatures 800 MJ/m², vent 2 x 0.8 m

1200 MJ/m², vent 2 m high x 0.8 m wide
plasterboard lined, timber framed walls, ceiling
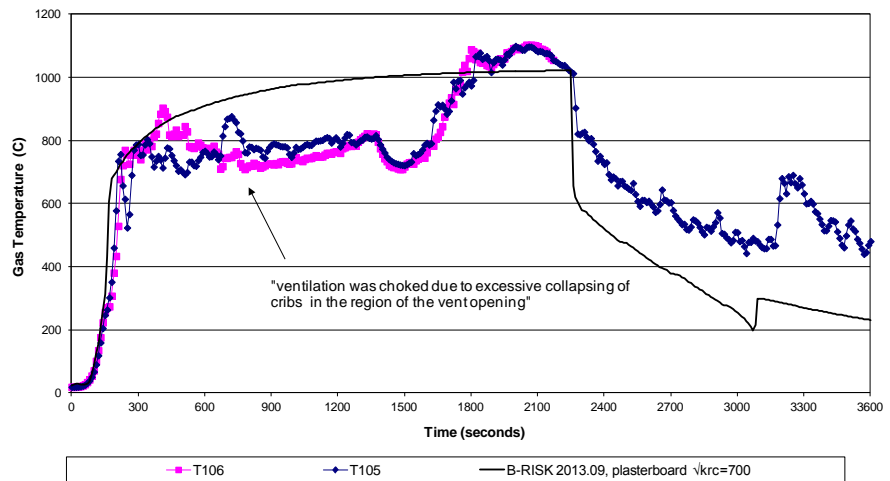
Figure 29. Gas temperatures 1200 MJ/m², vent 2 x 0.8 m

**800 MJ/m², Vent 2 m high x 1.2 m wide
plasterboard lined, timber framed walls, ceiling**

wall integrity failure @ 23 minutes

T105　　　T106　　　B-RISK 2013.09, plasterboard √krc=700
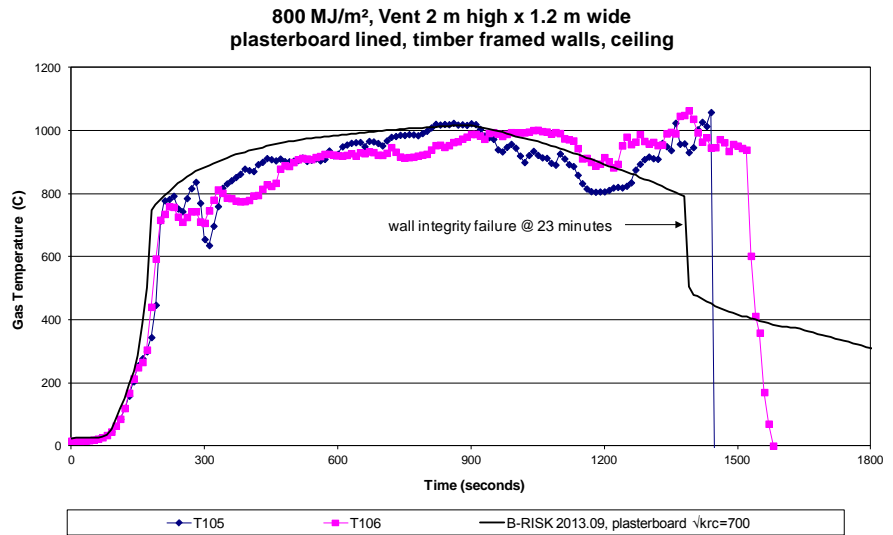
Figure 30. Gas temperatures 800 MJ/m², vent 2 x 1.2 m

7. GLASS FRACTURE

7.1 CASE 7-1

7.1.1 References

Parry, R., 2002. *Implementation of a glass fracture module for the BRANZfire compartment fire zone modelling software. Fire Engineering Research Report No. 2002-5.* University of Canterbury, Christchurch, New Zealand.

http://www.civil.canterbury.ac.nz/postgrads/rparry/Fire%20Project%20Report3.pdf

Parry, R., Wade, C. & Spearpoint, M., 2003. Implementing a glass fracture module in the BRANZfire zone model. *Journal of Fire Protection Engineering,* Volume 13, pp. 157-183.

Shields, T. J., Silcock, G. & Flood, M., 2002a. Performance of a Single Glazing Assembly Exposed to Enclosure Corner Fires of Increasing Severity. *Fire and Materials,* Volume 25, pp. 123-152.

Shields, T. J., Silcock, G. & Flood, M., 2002b. Performance of a Single Glazing Assembly Exposed to a Fire in the Centre of an Enclosure. *Fire and Materials,* Volume 26, pp. 51-75.

7.1.2 Description

Pan fires of varying size burning mineralised methylated spirits were located in the corner and in the centre of a vented compartment 3.6 x 2.4 x 2.4 m high. The pans were elevated 0.3 m above floor level. There was a doorway vent 0.4 x 2 m high and a glazed window assembly comprising three panes. Pane 1 measured 0.844 x 0.844 m with the sill at a height of 1.06 m. Pane 2 measured 0.844 x 0.844 m with the sill at floor level. Pane 3 measured 0.844 x 1.895 m with the sill at floor level. In all cases the glazing was 6 mm thick with a 20 mm shaded edge and with properties for soda-lime-silica float glass taken from the Pilkington technical literature (k = 0.937 $Wm^{-1}K^{-1}$, α = 4.2E-07 m^2s^{-1}, E = 72 GPa, β = 0.83E-05 K^{-1}). A glass breaking stress of $σ_f$ = 47 MPa is used (Shields et al 2002a, 2002b).

7.1.3 Model Parameters

B-RISK 2013.09 is used.

Simulations use the "glass fracture model" option (Parry, 2002; Parry, et al., 2003).

B-RISK is used to simulate the fire environment in the compartment and to predict the time of first fracture for each glazed pane. The HRR for each size of pan as published by Shields et al (2002a, 2002b) is input with fuel properties selected as for ethanol.

The model includes the option to include, or not, additional heat flux from the flame to the glass. Results of both these options are presented. It is assumed that no glass fallout occurred so that the first pane does not result in any change in vent area or influence the fracture times of any of the other windows.

7.1.4 Comparison

The predicted glass fracture times are compared with the measured time to first cracking and results are summarised in Table 5.

Best agreement was obtained for Pane 1 where the glass was entirely submerged in the hot layer. B-RISK was not able to adequately predict the fracture time for Pane 2 where the glass was expected to be located entirely within the lower gas layer in the room, unless radiant heating from the flame was included. The data presented in Table 5 applies to the specific experiments associated with the published HRR data. There were also duplicate experiments reported (typically three-five) for each pan size and location. The data is presented graphically in Figure 31 and Figure 32 with error bars indicating the uncertainty (two standard deviation) associated with the experimental data.

Table 5. Comparison with FireSERT Compartment Fire Tests (with flame flux heating not modelled but flame flux heating modelled in brackets)

| Pan fire size (m) | Pane 1 – sill 1.06 m (0.844 x 0.844 m) Vent 3 | | Pane 2 – sill 0 m (0.844 x 0.844 m) Vent 2 | | Pane 3 – sill 0 m (0.844 x 1.895 m) Vent 4 | |
	Time to first crack (sec)	Predicted time (sec)	Time to first crack (sec)	Predicted time (sec)	Time to first crack (sec)	Predicted time (sec)
0.5 x 0.5 corner	347	218 (200)	578	DNF (DNF)	326	212 (201)
0.7 x 0.7 corner	126	123 (115)	234	DNF (473)	136	121 (115)
0.8 x 0.8 corner	131	113 (102)	202	DNF (395)	121	111 (103)
0.9 x 0.9 corner	70	88 (77)	145	DNF (231)	82	86 (80)
0.6 x 0.6 centre	475	366 (206)	675	DNF (261)	857	358 (203)
0.7 x 0.7 centre	282	279 (157)	348	DNF (181)	315	274 (155)
0.8 x 0.8 centre	195	198 (99)	309	DNF (111)	111	194 (98)
0.9 x 0.9 centre	126	259 (187)	156	265 (189)	110	257 (186)

DNF = did not fracture

B-RISK 2013.09 (without flame flux option)

Squares =Pane 1
(0.844 w x 0.844 h sill 1.06 m)

Triangles = Pane 2
(0.844 w x 0.844 h sill 0 m)

Circles = Pane 3
(0.844 w x 1.895 h sill 0 m)
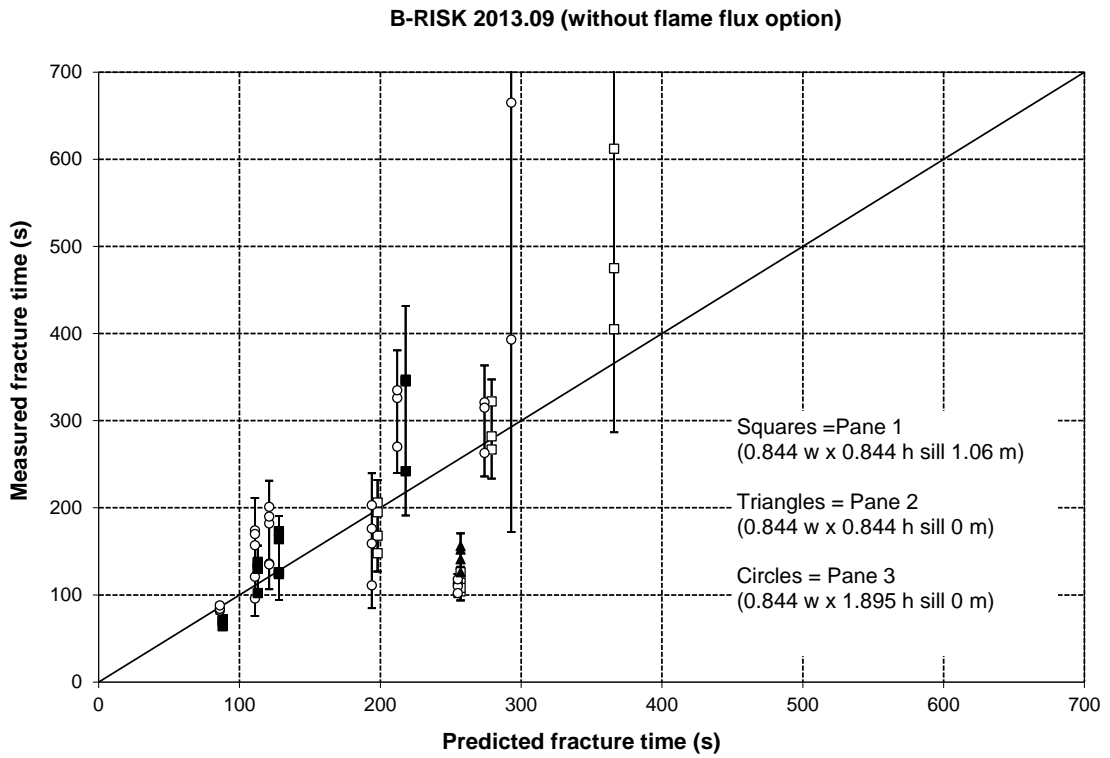
Figure 31. Comparison of predicted vs measured glass fracture times (error bars span two standard deviation)

B-RISK 2013.09 (with flame flux option)

Squares = Pane 1 (0.844 w x 0.844 h sill 1.06 m)

Triangles = Pane 2 (0.844 w x 0.844 h sill 0 m)

Circles = Pane 3 (0.844 w x 1.895 h sill 0 m)
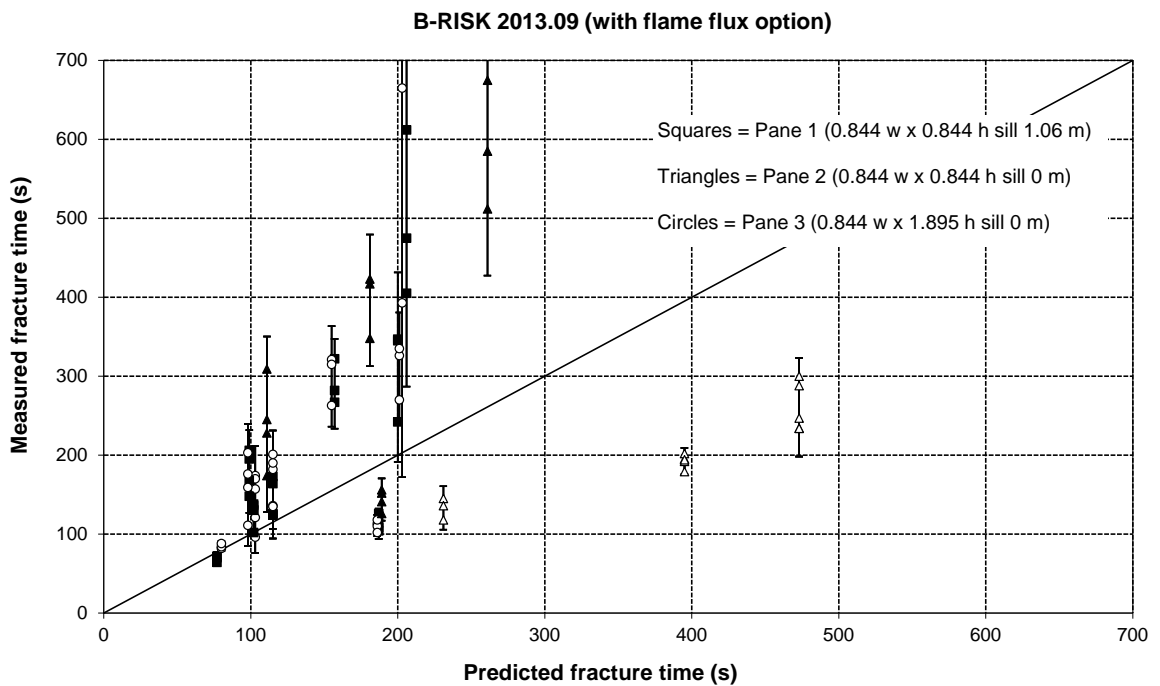
Figure 32. Comparison of predicted vs measured glass fracture times (error bars span two standard deviation)

8. SPRINKLER AND DETECTOR RESPONSE TIMES

8.1 CASE 8-1

8.1.1 References

Davis WD. 1999. 'Zone Fire Model JET: A Model for the Prediction of Detector Activation and Gas Temperature in the Presence of a Smoke Layer'. *NISTIR 6324*. National Institute of Codes and Standards, USA.

http://fire.nist.gov/bfrlpubs/fire99/PDF/f99033.pdf

Gott, J. E., Lowe, D. L., Notarianni, K. A. & Davis, W. D., 1997. Analysis of High Bay Hangar Facilities for Fire Detector Sensitivity and Placement. NIST TN 1423, USA: National Institute of Standards and Technology.

http://fire.nist.gov/bfrlpubs/fire97/PDF/f97019.pdf

8.1.2 Description

A series of JP-5 pool fires were conducted in a hangar of size 97.8 x 73.8 x 15.1 m high (Gott, et al., 1997). The fires were centred under a draft curtained area 18.3 x 24.4 m with a ceiling height of 14.9 m. The draft curtain was 3.7 m deep. The roof and draft curtains were assumed to be of sheet steel construction.

Ambient temperature = 25⁰C.

The fire was a 2.5 m diameter pan of JP-5 fuel, size 7.7 MW fire estimated to reach maximum steady-state value after 90 seconds.

Energy yield (kJ/g) = 42.0.

CO_2 yield (kg/kg fuel) = 2.850.

Soot yield (kg/kg fuel) = 0.037.

Radiant loss fraction = 0.31.

Sprinkler characteristics: Response Time Index (RTI) = 35 (ms) $^{1/2}$ actuation temperature 79⁰C; C-factor = 0.5 (m/s) $^{1/2}$; with the deflector positioned 0.3 m below the ceiling. There was no actual water flow in this experiment.

The thermal detector parameters used were: RTI = 50 (ms) $^{1/2}$ link actuation temperature 57.2⁰C, located 250 mm below the ceiling.

Smoke optical density for alarm (1/m) = 0.097.

Detector characteristic length number (m) = 15.0.

Distance below ceiling (m) = 0.025.

Detector response is based on OD inside the detector chamber.

8.1.3 Model Parameters

B-RISK 2013.09 is used. Simulations use the "NIST JET ceiling jet model" (Davis, 1999).

8.1.4 Comparison

Table 6 shows the results of the B-RISK prediction compared to the experimentally-measured response time of the sprinkler devices.

Table 6. Sprinkler response and ceiling jet temperatures

Radial distance (m)	Predicted sprinkler activation time (s)	Measured sprinkler activation time (s)
0	81	78
3.1	122	88, 104, 147, nr
6.1	187	140, 144, 207, 251
8.5	nr	247, 295
9.1	nr	439, nr
11.6	nr	nr, nr

Table 7 shows the results of the B-RISK prediction compared to the experimentally-measured response time of the heat detector.

Table 7. Heat detector response

Radial distance (m)	Predicted heat detector activation time (s)	Measured heat detector activation times (s)
3.0	65	19, 65, 69, 85
6.1	73	27, 65, 65, 69
8.5	80	65, 69
9.1	82	32, 69
11.6	89	73, 85

Table 8 shows the results of the B-RISK prediction compared to the experimentally-measured response time of the photoelectric smoke detector.

Table 8. Smoke detector response

Radial distance (m)	Predicted photoelectric smoke detector activation time (s)	Measured photoelectric smoke detector activation time (s)
3.1	30	18, 27, 27, 38
6.1	39	23, 27, 31, 42
8.5	44	27, 31
9.1	46	31, 46
11.6	50	51, nr

8.2 CASE 8-2

8.2.1 Reference

Davis, W. D., Notarianni, K. A. & McGrattan, K. B., 1996. *Comparison of Fire Model Predictions with Experiments Conducted in a Hangar with 15 m Ceiling. NISTIR 5927.* National Institute of Codes and Standards, USA.

http://fire.nist.gov/bfrlpubs/fire96/PDF/f96077.pdf

8.2.2 Description

A series of JP-5 pool fires were conducted in a hangar of size 97.8 x 73.8 m x 15.1 m high (Gott, et al., 1997). The fires were centred under a draft-curtained area 18.3 x 24.4 m with a ceiling height of 14.2-14.9m. The draft curtain was 3.7 m deep. The roof and draft curtains were assumed to be of sheet steel construction.

Two experiments burning pans of JP-5 fuel in the hangar are used is this report. Fuel properties were taken as:

- Energy yield (kJ/g) = 42
- CO_2 yield (kg/kg fuel) = 2.850
- Soot yield (kg/kg fuel) = 0.037
- Radiant loss fraction = 0.31

Data from two fires are used here:

1) Fire was a 0.6 x 0.6 m pan of JP-5 fuel, nominal size 500 kW fire, ambient temperature = 28ºC

2) Fire was a pan of 1.5 m diameter JP-5 fuel, nominal size 2700 kW fire, ambient temperature = 27ºC

The growth rate of each fire as given by Davis et al (1996) is shown in Table 9.

Table 9 Rate of Heat Release Fire Growth (Davis, 1999)

Time (s)	500 kW fire (kW)	2700 kW fire (kW)
0	0	0
1	99	803
10	-	965
20	174	1135
50	273	1582
100	388	2139
200	481	2693
300	478	2766

Smoke detector characteristics were reported as:

- Photoelectric, analogue-addressable
- Smoke optical density for alarm (1/m) = 0.097 (default)
- Distance below ceiling (m) = 0.250 (estimated)
- Detector response is based on OD outside the detector chamber

8.2.3 Model Parameters

B-RISK 2013.12 is used. Simulations use the "NIST JET ceiling jet model" option (Davis, 1999).

8.2.4 Comparison

Smoke detector response times from the experiments and from B-RISK predictions are shown in Figure 33.
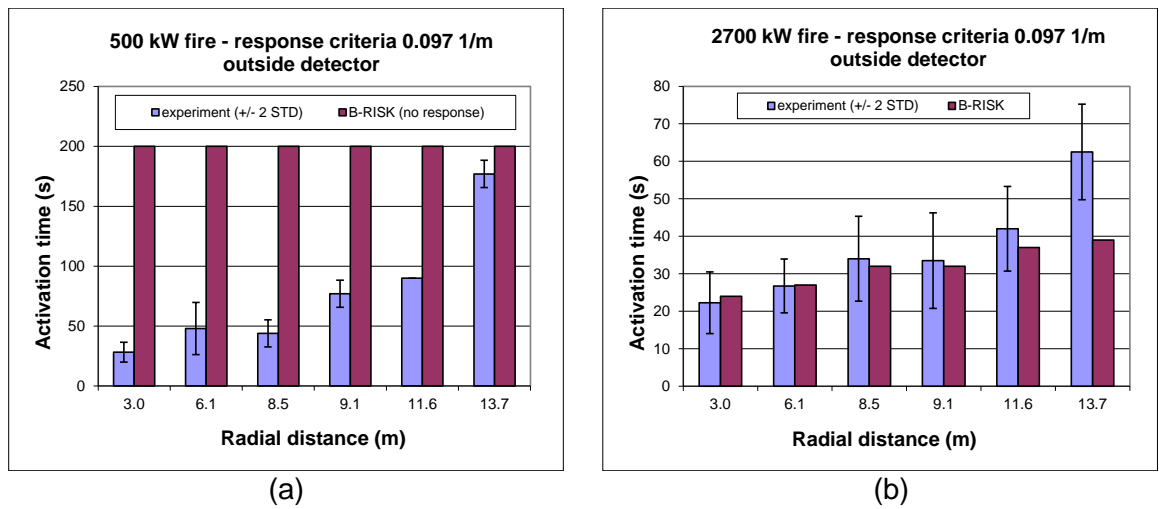
Figure 33. Smoke alarm response for fires of nominal HRR a) 500 kW and b) 2700 kW
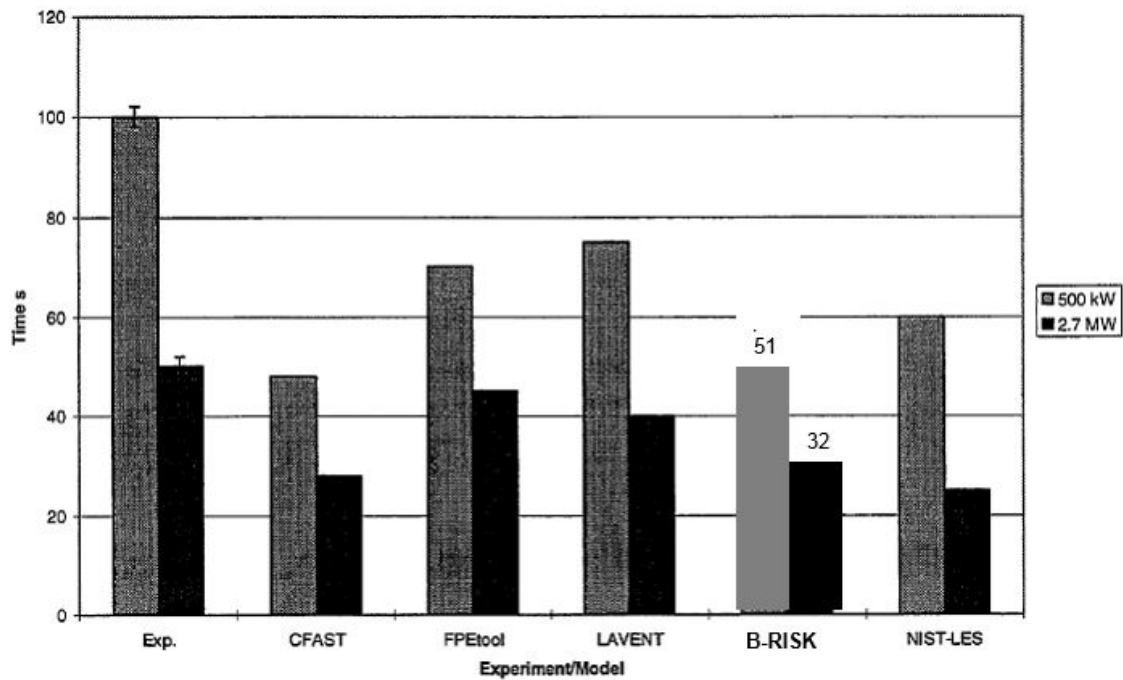
Figure 34. Draft curtain filling time – time for temp rise > 0.5 K at 11.9 m above floor (adapted from Davis et al, 1996)

Table 10 summary results for the 500 kW fire indicate a trend of over-predicting the gas temperatures in the ceiling jet. At a radial distance of 9.1 m, the predicted ceiling jet temperature is within 20% of the measured temperatures.

Table 11 shows for the 2.7 MW fire a trend of over-predicting the gas temperatures in the ceiling jet. At a radial distance of 9.1 m, the predicted ceiling jet temperature is within 24% of the measured temperatures.

Figure 35 to Figure 46 show the predicted and measured ceiling jet temperatures for each fire size at various radial distances from the plume.

Table 10. Ceiling jet temperature as a function of distance beneath the ceiling and radial distance for the 500 kW fire

Time (s)	Depth (m)	B-RISK r = 6.1 m	Experiment r = 6.1 m 4 TC	B-RISK r = 9.1 m	Experiment r = 9.1 m 1 TC
75	0.15	36	31-36	35	31
	0.30	36	33-36	36	32
	0.46	36	33-34	35	32
	0.61	35	33-34	35	32
	0.76	35	33-34	35	32
150	0.15	39	31-37	37	31
	0.30	39	33-37	38	32
	0.46	38	33-36	38	32
	0.61	38	33-36	38	32
	0.76	37	33-37	37	32
225	0.15	40	35-37	38	35
	0.30	40	37	39	34
	0.46	39	35-38	39	35
	0.61	39	37	39	36
	0.76	39	36-37	38	36

Table 11. Ceiling jet temperature as a function of distance beneath the ceiling and radial distance for the 2.7 MW fire

Time (s)	Depth (m)	B-RISK r = 6.1 m	Experiment r = 6.1 m 4 TC	B-RISK r = 9.1 m	Experiment r = 9.1 m 1 TC
75	0.15	54	43-52	50	41
	0.30	54	44-52	52	42
	0.46	53	44-52	52	43
	0.61	51	45-54	51	43
	0.76	50	46-54	50	42
150	0.15	61	47-61	56	52
	0.30	61	50-61	58	51
	0.46	60	50-60	58	52
	0.61	58	52-59	57	54
	0.76	57	54-57	57	54
225	0.15	65	50-63	59	55
	0.30	64	52-63	61	55
	0.46	63	52-63	61	57
	0.61	62	55-63	61	57
	0.76	61	58-62	60	55
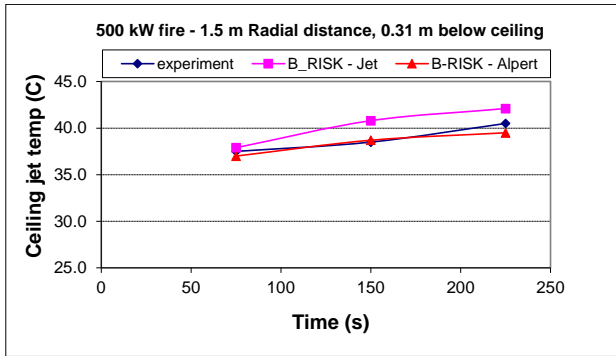
Figure 35. Ceiling jet temp 500 kW @ 1.5 m
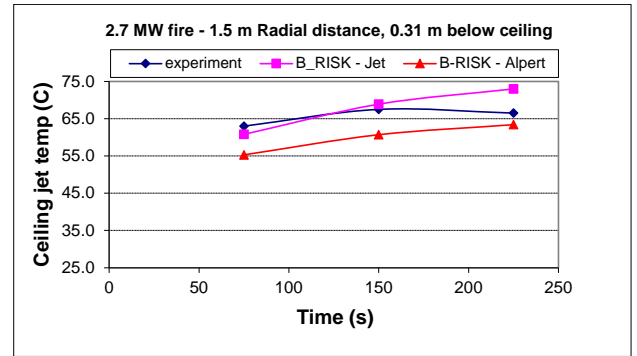
Figure 36. Ceiling jet temp 2700 kW @ 1.5 m
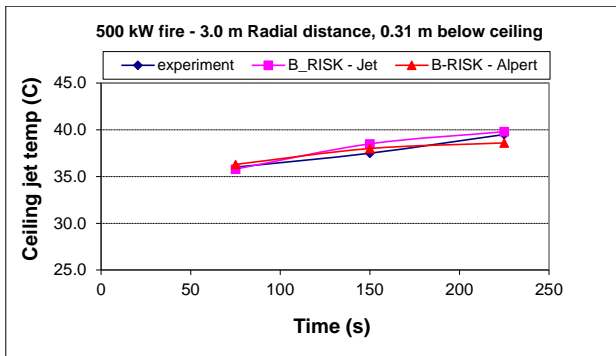
Figure 37. Ceiling jet temp 500 kW @ 3.0 m
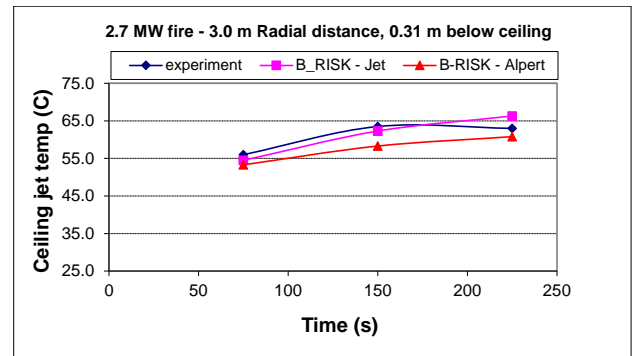
Figure 38. Ceiling jet temp 2700 kW @ 3.0 m
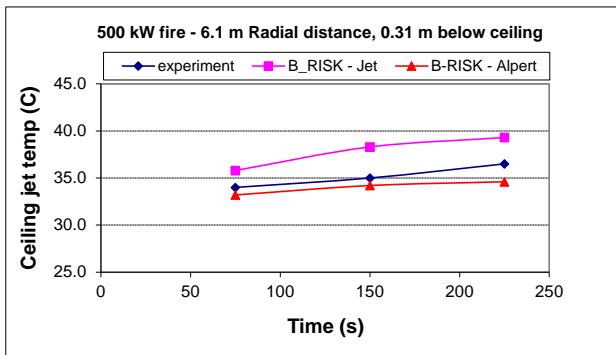
Figure 39. Ceiling jet temp 500 kW @ 6.1 m
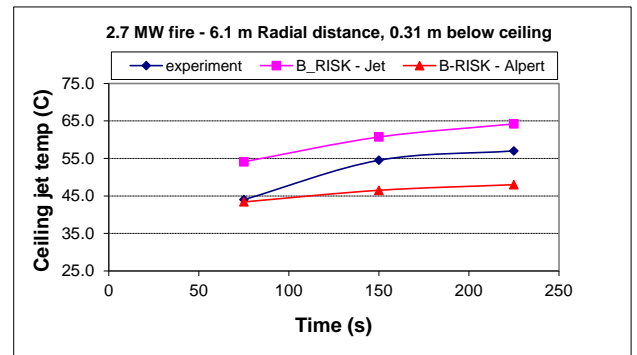
Figure 40. Ceiling jet temp 2700 kW @ 6.1 m
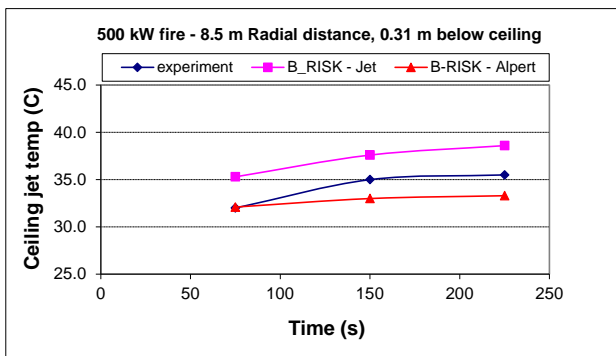
Figure 41. Ceiling jet temp 500 kW @ 8.5 m
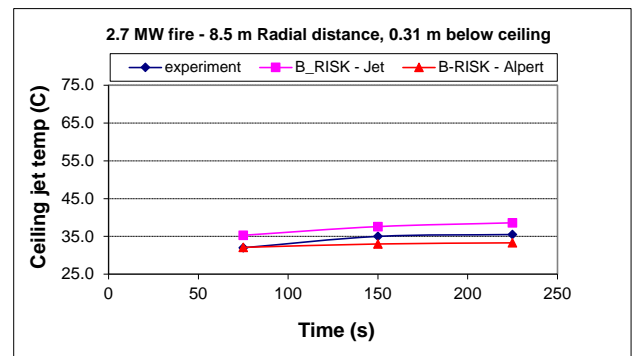
Figure 42. Ceiling jet temp 2700 kW @ 8.5 m

43
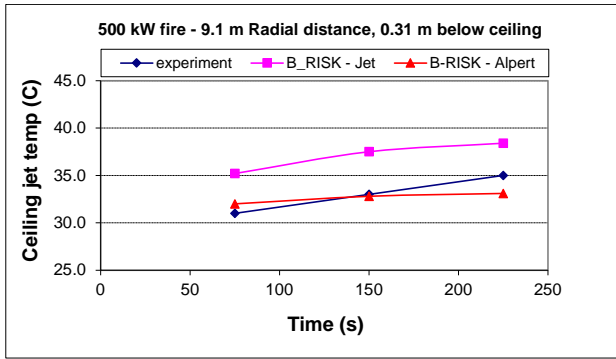
Figure 43. Ceiling jet temp 500 kW @ 9.1 m
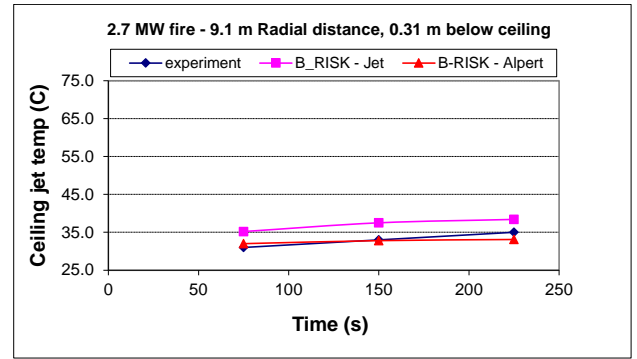
Figure 44. Ceiling jet temp 2700 kW @ 9.1 m
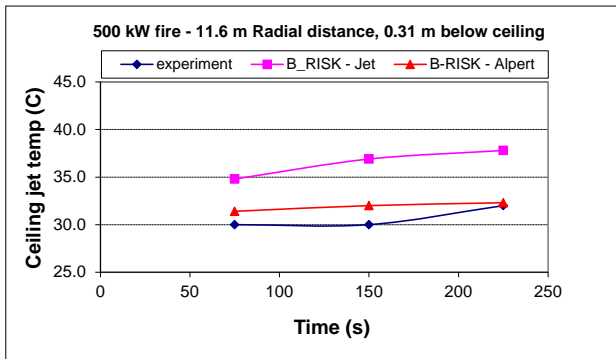
Figure 45. Ceiling jet temp 500 kW @ 11.6 m
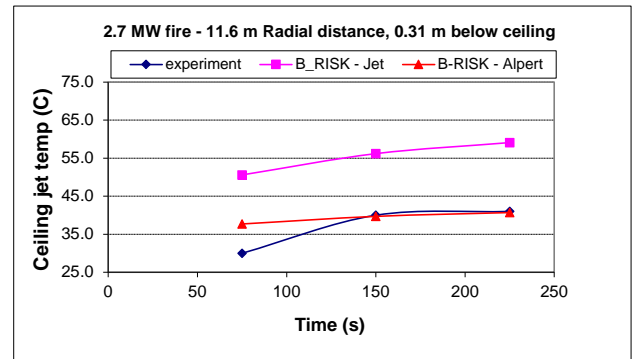
Figure 46. Ceiling jet temp 2700 kW @ 11.6 m

8.3 CASE 8-3

8.3.1 References

Bittern, A. 2004. *Analysis of FDS Predicted Sprinkler Activation Times with Experiments. Masters of Engineering in Fire Engineering Report.* University of Canterbury, Christchurch, New Zealand.

http://www.civil.canterbury.ac.nz/fire/pdfreports/Adam%20Bittern.pdf

Wade, C. A., Spearpoint, M. J., Bittern, A. & Tsai, K., 2007. Assessing the Sprinkler Activation Predictive Capability of the BRANZFIRE Fire Model. *Fire Technology,* Volume 43, pp. 175-193.

8.3.2 Description

A set of 22 fire experiments were conducted where a single chair was burned in an enclosure (Bittern, 2004). Two sprinkler heads were installed for each experiment and the sprinkler activation time, chair mass loss rate and gas temperature profile in the room were measured and reported by Bittern. A bare-wire Type K thermocouple was located adjacent to each sprinkler head and stainless steel-sheathed, mineral-insulated Type K thermocouples were used to measure the gas temperature, away from the sprinkler, at depths of 0.1 m, 0.3 m and 1.4 m below the ceiling.

Two different fire location positions (centre and corner of the enclosure) and two different door configurations (open and shut) were investigated. Table 12 summarises the position of the fire and door configuration for each experiment. Experiment 11 was excluded for this comparison as no mass loss data for the chair was collected.

The compartment was built from timber-framed walls and ceiling, and lined with painted 10 mm thick gypsum plasterboard. The compartment had internal dimensions of 8.0 x 4.0 x 2.4 m high. The compartment layout is shown in Figure 47. The door set was made of a wooden frame with a plywood door leaf with dimensions of 0.8 x 2.1 m high. The floor of the compartment was concrete.

Table 12. Fire position and door configuration

Experiment no.	Fire position	Door configuration
1-10	Centre	Open
12-15	Centre	Shut
16-22	Corner	Shut
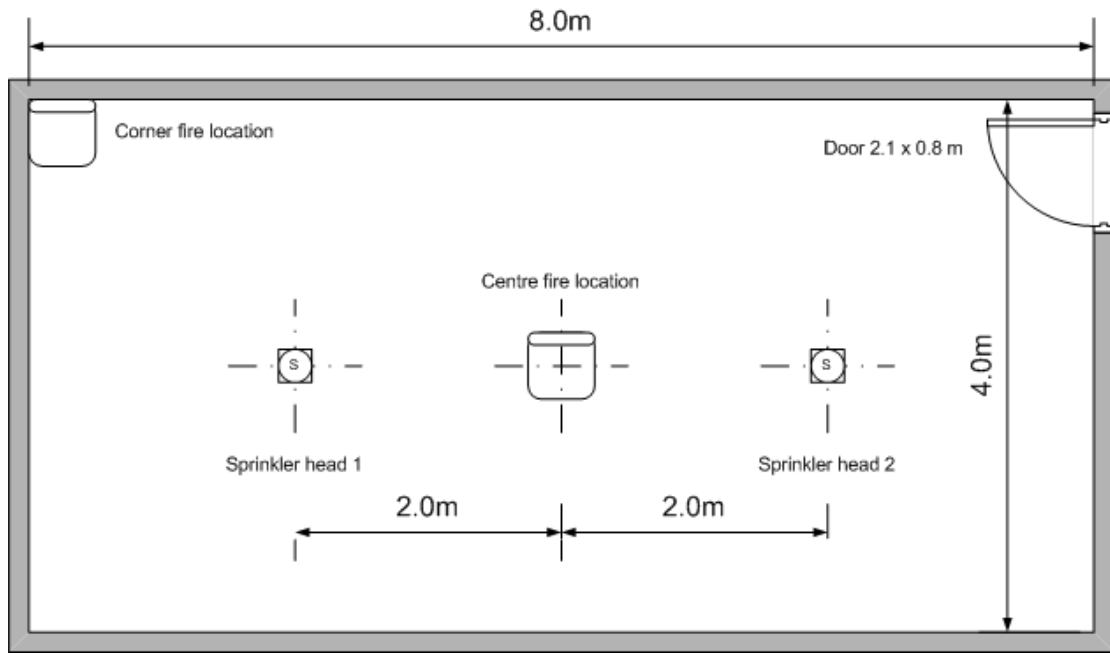
Figure 47. Compartment layout plan view (extracted from Bittern, 2004)

The fuel package used for each experiment was made from two flexible polyurethane foam slabs (to form the seat and back of the chair) and covered with fabric as shown in Figure 48. The foam was 28 kg/m³ cushion grade non-fire retardant and the fabric was 10 g/m² acrylic. The foam was typical of that used in domestic furniture in New Zealand. Each foam slab measured 500 x 400 x 100 mm thick in size, weighed approximately 0.56 kg and was arranged to form the seat as shown in Figure 48. Plasterboard (10 mm) was used to form a backing board for the seat assembly to prevent the foam from dropping to the floor when burning. The chair was placed on a load cell to record the mass loss during the experiment with the base of the seat approximately 0.65 m above the floor. The seat was ignited with a solid petroleum fire-lighter (20 x 20 x 10 mm) positioned at the interface between the back and the seat.

Figure 48. Upholstered chair in centre fire position (extracted from Bittern, 2004)

46

The average heat of combustion of the foam was measured in a cone calorimeter to be 21.0 MJ/kg (Tests 1-10) and 20.4 MJ/kg (Tests 11-22). This was used with the measured mass loss rate for each experiment to determine the HRR of the chair.

Two sprinkler heads spaced 4 m apart and generally complying with the New Zealand Standard NZS 4541:2003 were installed beneath the ceiling for each experiment. There were four different models of sprinkler head used for the experiments:

1. Residential Type A – pendent, nominal activation temperature 68°C (TYCO F680)

2. Residential Type B – pendent, nominal activation temperature 68°C (TYCO 2234)

3. Standard Response SS68 – pendent, standard coverage, nominal activation temperature 68°C (TYCO 3251)

4. Standard Response SS93 – pendent, standard coverage, nominal activation temperature 93°C (TYCO 3251)

The four sprinkler heads were supplied by the manufacturer TYCO and were selected based on availability. The selected sprinkler heads provided a variation in activation temperature and RTI.

The sprinkler heads were not charged with flowing water during the experiment, but the pipe sections connected to the head did contain water under pressure. This was achieved by holding the water back with a closing valve in the pipe network. Pressure gauges were also installed immediately upstream of each sprinkler head, but before the closing valve, to indicate sprinkler activation.

Technical data for each sprinkler head is shown in Table 13. The RTI was based on a manufacturer's estimate. A conduction factor of 0.4 $(m/s)^{1/2}$ was selected for the base case for all sprinklers in this study.

The glass bulbs were typically about 20 mm long, with the mid-point located approximately 15 mm below the ceiling. The heat-sensitive element therefore spanned a depth from 5-25 mm below the ceiling.

Table 13. Sprinkler head data (base case)

	Activation temperature (°C)	RTI ($m^{1/2}s^{1/2}$)	C-factor ($(m/s)^{1/2}$)
Residential Type A (3 mm glass bulb)	68	36	0.4
Residential Type B (3 mm glass bulb)	68	36	0.4
Standard Response SS68 (5 mm glass bulb)	68	95	0.4
Standard Response SS93 (5 mm glass bulb)	93	95	0.4

8.3.3 Model Parameters

Simulations use the "NIST JET ceiling jet model" option (Davis, 1999).

The radial distance from the centre of the fire plume to each sprinkler head was 2 m for Experiments 1-15. Regarding Experiments 16-22, with the corner fire location, the radial distances between the fire and the sprinkler heads were 2.8 m and 6.3 m for heads 1 and 2 respectively.

Since the primary fuel was flexible polyurethane foam, the radiant loss fraction assumed in the fire model was 0.46 based on the ratio of the radiative to chemical heat of combustion for GM23 foam from the literature. Other combustion parameter settings in the fire model were as for polyurethane foam.

A summary of the fire model input data is given in Table 14.

Table 14. Summary of fire model input data

Thermal properties – walls and ceiling 10 mm gypsum plasterboard	ρ = 731 kg/m³ k = 0.17 W/mK ε = 0.88
Thermal properties – floor 100 mm concrete	ρ = 2300 kg/m³ k = 1.2 W/mK ε = 0.50
Ambient conditions	RH = 65% ambient temperature as per the experiments
Fuel radiant loss fraction	0.46
Heat of combustion	21.0 MJ/kg (Tests 1-10) 20.4 MJ/kg (Tests 11-22)
Soot yield	0.227 g/g
Height of fire above floor	0.65 m

8.3.4 Comparison

The results presented here use the BRANZFIRE model and are taken from Wade, et al (2007). Sprinkler response times obtained using B-RISK were checked for the first ten experiments and only varied by a few seconds and therefore all simulations were not repeated.

Figure 49 shows a comparison of the measured and predicted sprinkler activation times for the base case with the JET ceiling jet option. Simulations were terminated at 600 seconds – when no activation was predicted during that time it appears as 600 seconds on the figure. For Experiments 1-15, with the fire located centrally between the sprinkler heads, on average the prediction was 21% longer than the measured activation times. In the case of the corner fire Experiments 16-22, agreement between the predictions and experiments was reasonable (37% longer) for the sprinkler head located nearest the fire (at 2.8 m), but agreement was poor (98% longer – for Experiments 16-19) for the sprinkler head located furthest from the fire (at 6.3 m). This suggests that the drop-off in ceiling jet temperature with radial distance in the model was too great compared to the actual case.
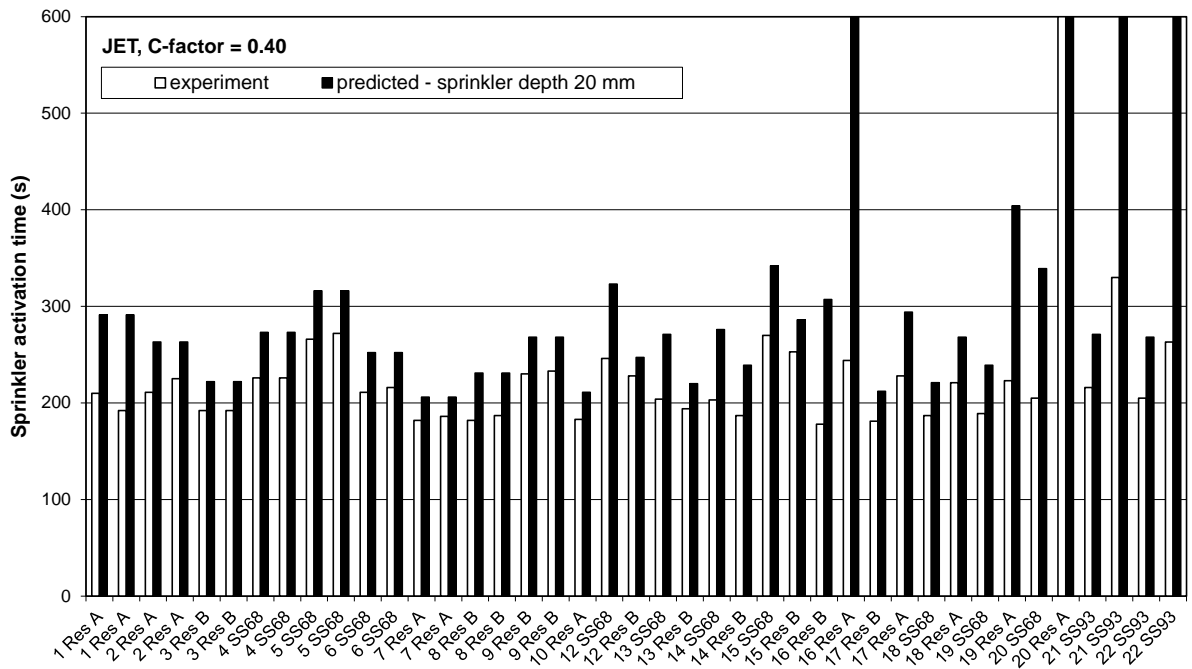
Figure 49. Comparison of measured and predicted activation time for base case – with BRANZFIRE/JET model

Gas temperatures at the sprinkler location

Figure 50 compares the measured and predicted gas temperatures (in the ceiling jet) at the location of the sprinkler at the measured time of sprinkler activation. The predicted gas temperatures (based on the JET ceiling jet option) are generally higher than the measured gas temperatures, with a few exceptions. Better agreement is achieved for the centre fires compared with the corner fires. Given that the predicted sprinkler response times are longer than the measured times, this result suggests that the assumed thermal response characteristics for the sprinklers are conservative.

Figure 50. Comparison of the measured and predicted gas temperatures at the location of the sprinkler at the measured sprinkler activation time

The response of sprinklers in small rooms is strongly influenced by the presence of a developing hot layer. If using the B-RISK model for predicting sprinkler response times, the use of the JET ceiling jet option is recommended, particularly for small rooms, as better agreement with experimental results is expected.

The JET ceiling jet option (for the base case) gave sprinkler activation times that were, on average, 21% longer than the measured response times for fires located in the centre of the room. Furthermore, the mismatch of the predictions (based on the JET ceiling jet model and the experimental results) increases with distance from the plume. The use of the Alpert ceiling jet option indicated much longer response times in small rooms compared to actual response times. However, this would usually be considered conservative for design purposes.

8.4 CASE 8-4

8.4.1 Reference

Mealy, C., Floyd, J. & Gottuk, D., 2008. Smoke Detector Spacing Requirements Complex Beamed and Sloped Ceilings Volume 1: Experimental Validation of Smoke Detector Spacing Requirements. Fire Protection Research Foundation.

https://www.nfpa.org/~/media/Files/Research/smokedetectorspacing_-_volume1.ashx

8.4.2 Description

The fire experiments described here were conducted as part of an investigation into the spacing of smoke detectors where a full-scale mock-up of a hallway was constructed and experiments carried out (Mealy, et al., 2008). The mock-up was constructed to allow for changes in ceiling height, hallway width, beam spacing, beam depth, and fire size and fuel type. It was instrumented with thermocouples, velocity probes, ionisation, photoelectric and aspiration smoke detectors, and optical density meters.

The experiments used here were conducted within a corridor with a smooth (gypsum plasterboard) ceiling. The corridor was 14.6 x 3.7 m with a variable height of 2.7, 3.6 or 5.5 m. Both ends of the corridor were fully vented. The fire source was a 0.3 x 0.3 m square gas burner centrally located in the corridor. The fuel was propylene gas with an output of 100 kW.

Multiple spot-type smoke detectors were located at radial distances of 0.9, 2.7, 4.5 and 6.3 m from the fire plume centreline.

8.4.3 Model Parameters

B-RISK 2013.12 is used. Simulations use the "NIST JET ceiling jet model" option (Davis, 1999).

The heat of combustion was taken as 40.5 MJ/kg, radiant loss fraction 0.37 and the soot yield was experimentally estimated to be 0.048 g/g.

Default values for optical density at activation were 0.097 m^{-1}), distance of detector below ceiling (0.025 m). The optical density was assessed at the location of and outside the detector.

8.4.4 Comparison

Table 15 shows the results of the B-RISK prediction compared to the experimentally-measured response time of the smoke detectors.

Table 15. Smoke detector response times and predictions compared to experiments for various radial distances (r) and ceiling heights

Ceiling height (m)		r = 0.9m (x 8 detectors)	r = 2.7m (x 8 detectors)	r = 4.5m (x 16 detectors)	r = 6.3m (x 16 detectors)
2.7	Measured	9-18	15-30	17-33	21-36
	B-RISK	7	10	13	15
3.6	Measured	10-18	18-36	18-42	19-42
	B-RISK	9	12	15	18
5.5	Measured	14-36	25-36	27-43	22-45
	B-RISK	15	17	21	25

9. SMOKE DENSITY

9.1 CASE 9-1

9.1.1 Reference

Davis, W. D., Cleary, T., Donnelly, M. & Hellerman, S., 2003. *Predicting Smoke and Carbon Monoxide Detector Response in the Ceiling Jet in the Presence of a Smoke Layer, NISTIR 6976*. National Institute of Standards and Technology, USA.

http://fire.nist.gov/bfrlpubs/fire03/PDF/f03003.pdf

9.1.2 Description

Three experiments using a small propene (C_3H_6) gas burner and conducted in an enclosure with floor dimensions 3.15 x 3.02 x 1.5 m high are presented (Davis, et al., 2003). A sand burner was centred in the room with the height between the top of the burner and the ceiling as shown below. The first burner was round with a diameter of 0.085 m while the second burner was square with an effective diameter of 0.194 m.

Experiment	Burner output (kW)	Burner to ceiling height (m)
A	2.5	1.50
B	2.5	2.19
C	7.6	1.50

The ceiling construction was described as acoustic ceiling tile and walls were glazed cinderblock. A helium-neon laser extinction smoke meter measured obscuration and this was located 1 m from the plume centreline and 63.5 mm beneath the ceiling. By measuring the reduction in the beam intensity, the smoke density was determined, assuming the extinction coefficient per unit mass was 8.71 m²/g.

9.1.3 Model Parameters

B-RISK 2013.09 is used. Simulations use the "NIST JET ceiling jet model" option (Davis, 1999).

Assumptions:

- Propene soot yield = 0.095 g/g
- Radiant fraction = 0.32
- Heat of combustion = 40.5 kJ/g

9.1.4 Comparison

Figure 51 to Figure 53 show a comparison between the smoke densities determined from the three experiments with the B-RISK predictions.
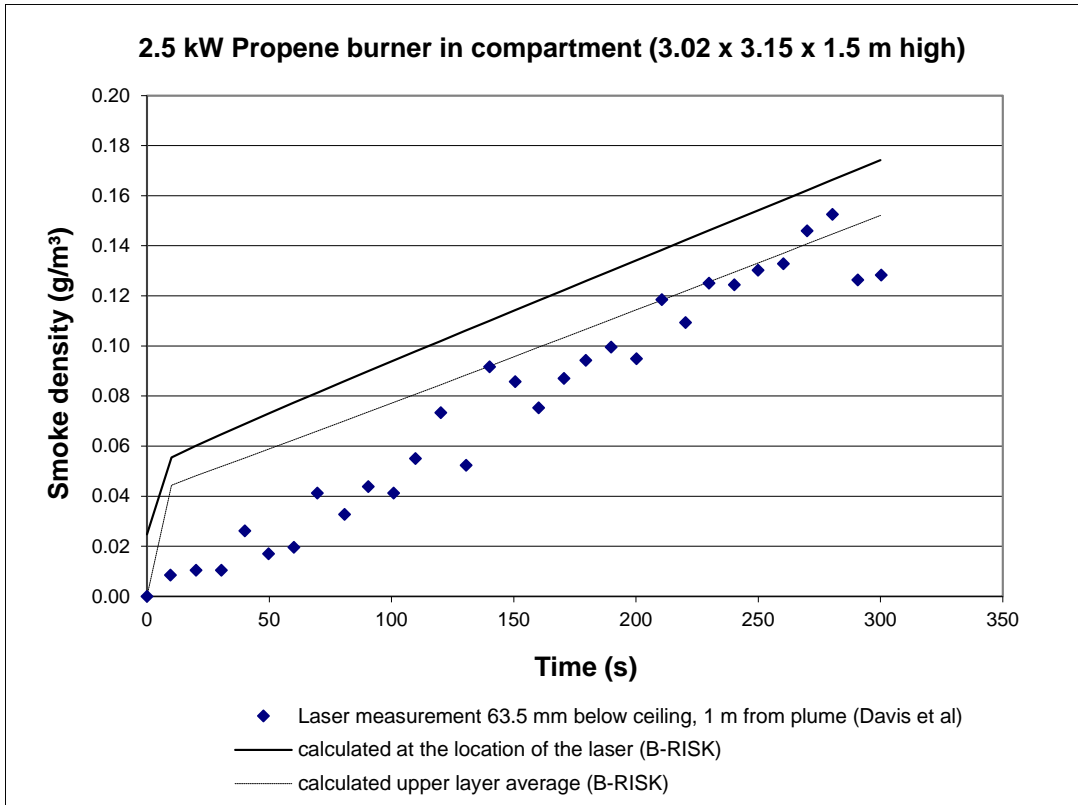
Figure 51. Experiment A – 2.5 kW propene burner, 1.5 m below ceiling
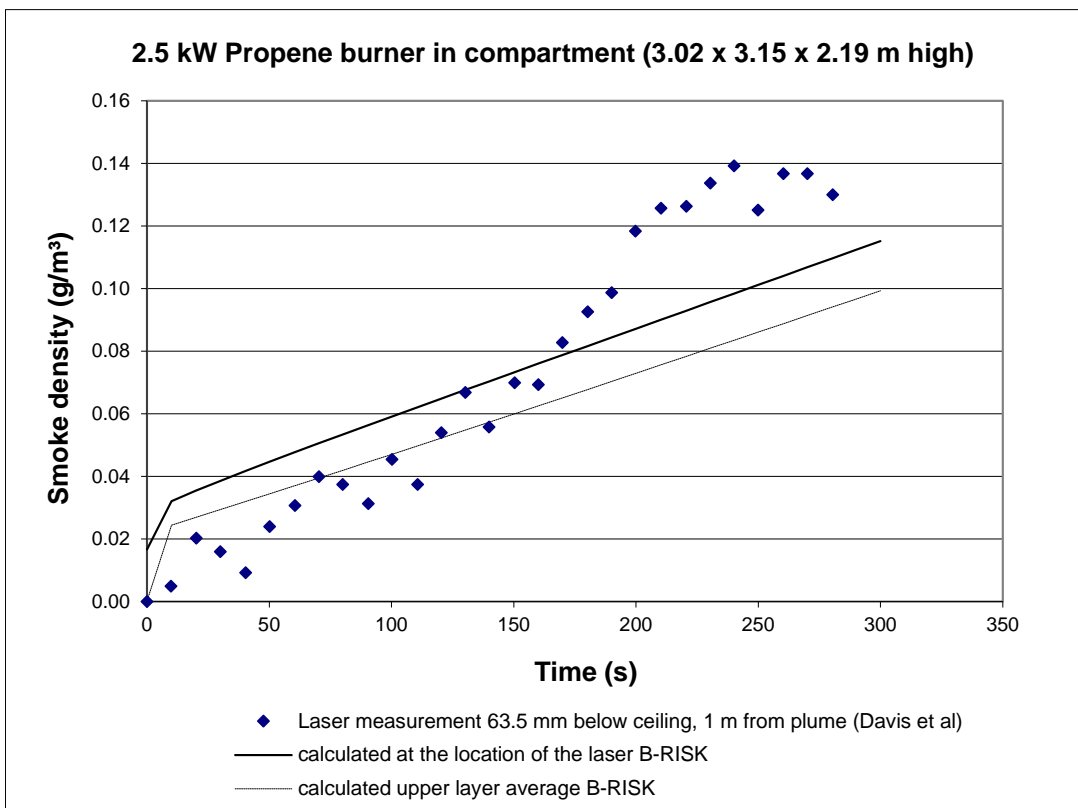
Figure 52. Experiment B – 2.5 kW propene burner, 2.19 m below ceiling

54
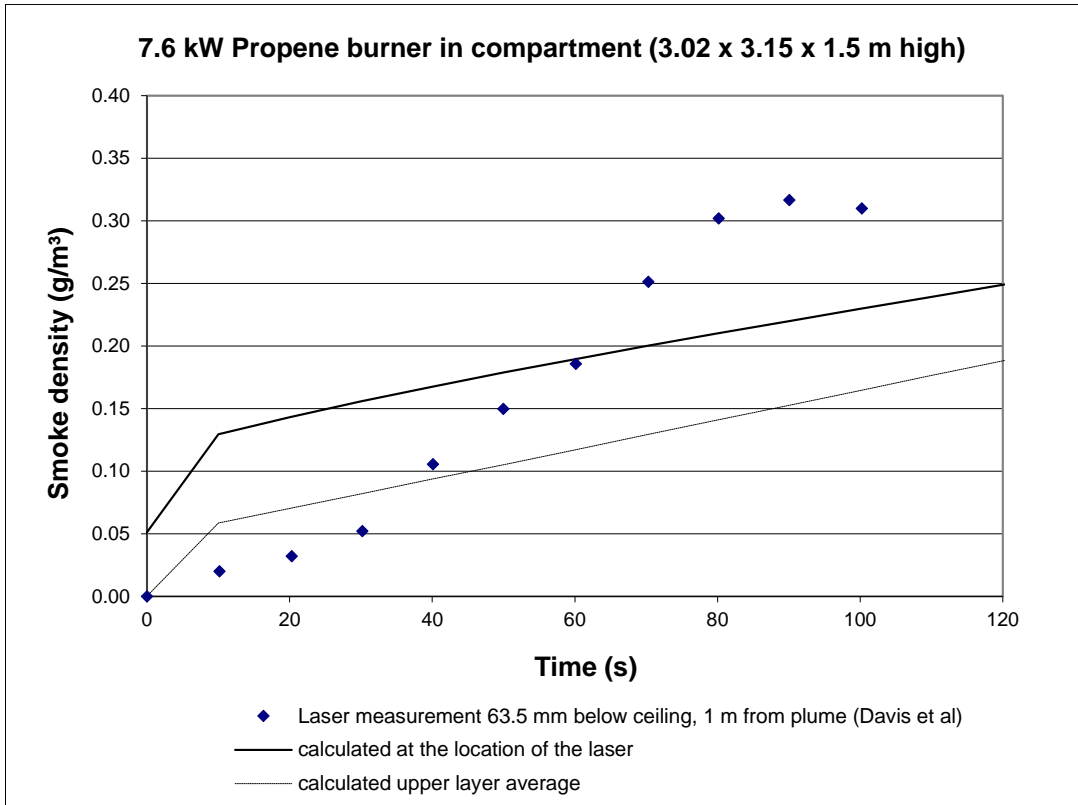
Figure 53. Experiment C – 7.6 kW propene burner, 1.5 m below ceiling

10. SPILL PLUMES

10.1 CASE 10-1

10.1.1 References

Harrison, R. & Spearpoint, M., 2008. *Characterisation of balcony spill plume entrainment using physical scale modelling.* Proceedings of the 9th Symposium of the International Association of Fire Safety Science, Karlsruhe, Germany, pp 727-738.

Harrison, R. & Spearpoint, M. J., 2010. Physical scale modelling of adhered spill plume entrainment. *Fire Safety Journal,* 45(3), pp. 149-158.

Harrison R. 2009. Entrainment of air into thermal spill plumes, Thesis for Doctor of Philosophy in Fire Engineering. Christchurch, New Zealand: University of Canterbury.

Harrison, R., Wade, C. & Spearpoint, M., 2013. Modeling Spill Plumes in the B-RISK Fire Model (accepted June 2013). *Journal of Fire Protection Engineering.*

10.1.2 Description

Reduced-scale experiments described by (Harrison & Spearpoint, 2008; Harrison & Spearpoint, 2010) utilised a one-tenth physical scale model that examined plume entrainment and behaviour for the five different types of spill plume considered. Figure 54 shows a cross section schematic through the rig used for the reduced-scale experiments.
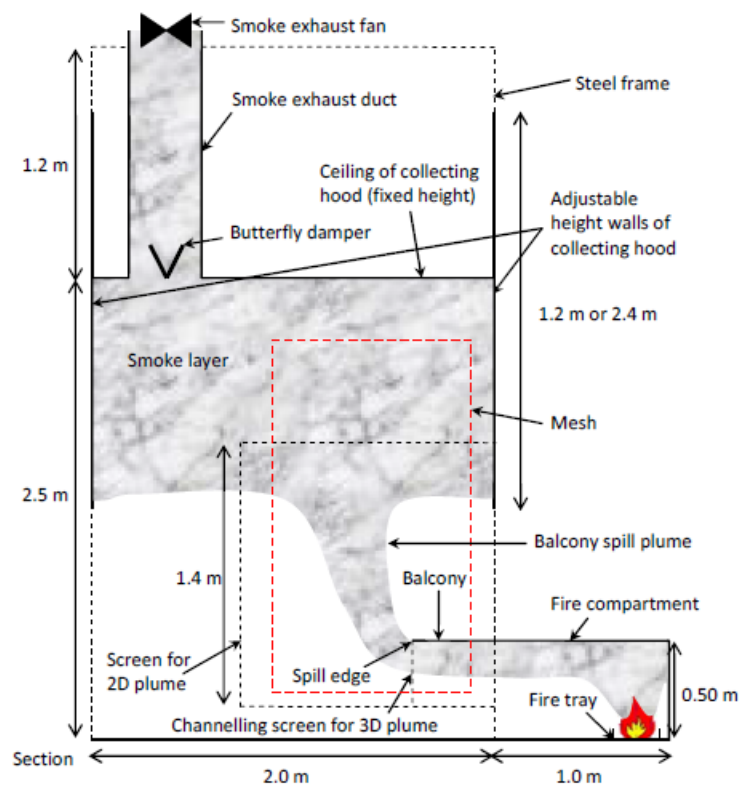
Figure 54. Cross section through experimental rig for reduced-scale experiments (extracted from Harrison, 2009)

In the experiments the fire compartment (1.0 x 1.0 m x 0.5 m high) was constructed from 25 mm thick ceramic fibre insulation (CFI) board with a 1 mm thick steel substrate and the adjacent compartment was constructed from 10 mm thick CFI board with a 1 mm thick steel substrate.

The fire source was generated by supplying Industrial Methylated Spirits (IMS) to a metal tray within the fire compartment at a controlled and measured rate to generate the required fire size.

10.1.3 Model Parameters

B-RISK 2013.08 is used. Later versions of B-RISK include a different near-vent mixing algorithm which may produce slightly different results.

The heat losses from the compartment boundaries are modelled assuming a thermal conductivity of 0.068 W/mK, specific heat 1090 J/kgK, density 336 kg/m^3 and emissivity 0.9. The walls of the compartment and hood are modelled assuming 25 mm thick CFI board with a 1 mm thick steel substrate.

The radiant loss fraction is taken as 0.2 and the heat of combustion as 30 kJ/g for the B-RISK simulations.

10.1.4 Comparison

The comparisons shown here are as reported by (Harrison, et al., 2013).

The 2-D Balcony Spill Plume

Table16 shows the series of eight B-RISK simulations carried out for heights of rise of plume above the spill edge of up to 0.79 m at model-scale for narrow (0.2 m) and wide (1.0 m) plume widths, and for a fire size of 10 kW on model-scale. Figure 55 shows a comparison between the predictions and the experimental results for the clear layer height above the floor of the collecting hood. Figure 55 shows that all but one of the eight simulations provide predictions of layer height that match the experiment, within experimental error.

Simulation	$\dot{Q}_t$	W_s	z_s	T_∞	V	Layer height in hood Expt	Layer height in hood B-RISK
	kW	m	m	C	m^3/s	m	m
1	10.0	1.0	0	16.1	12.94	0.50	0.48
2	10.0	1.0	0.31	11.5	9.25	0.81	0.85
3	10.0	1.0	0.55	16.8	13.53	1.05	1.02
4	10.0	1.0	0.79	14.5	11.68	1.29	1.29
5	10.0	0.2	0	14.6	11.73	0.50	0.49
6	10.0	0.2	0.31	12.5	10.06	0.81	0.78
7	10.0	0.2	0.55	16.6	13.37	1.05	0.98
8	10.0	0.2	0.79	14.3	11.52	1.29	1.21

Table 16. B-RISK simulations and experiments for the 2-D balcony spill plume (extracted from Harrison, et al., 2013)
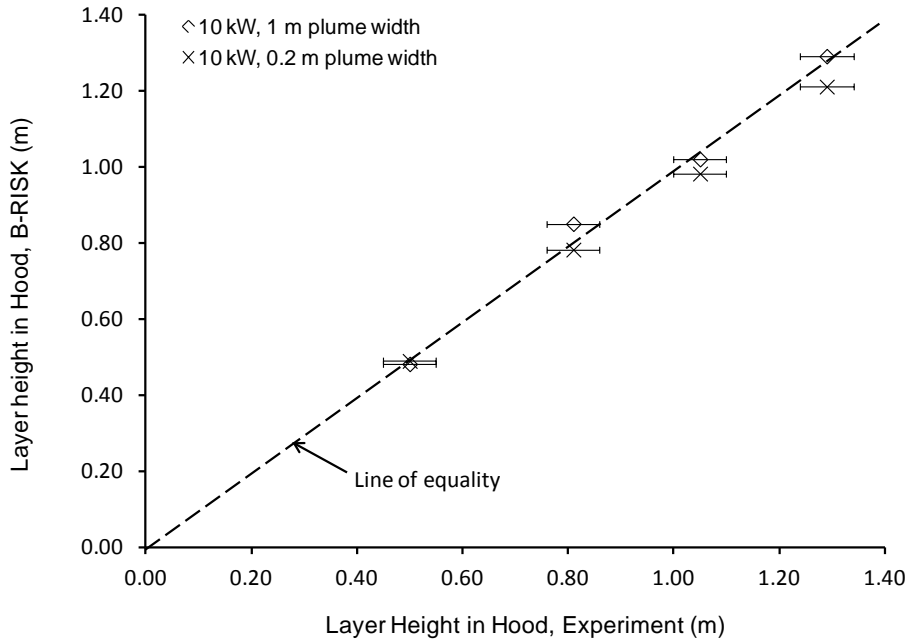
Figure 55. B-RISK prediction of layer height in hood versus the experiment for the 2-D balcony spill plume (extracted from Harrison, et al., 2013)

The Channelled 3-D Balcony Spill Plume

Table 17 shows the series of 24 B-RISK simulations carried out for heights of rise of plume above the spill edge of up to 0.73 m, for narrow (0.2 m) and wide (1.0 m) plume widths, and for fire sizes of 5, 10 and 15 kW on model-scale. Figure 56 shows a comparison between the predictions and the experimental results for the clear layer height above the floor of the collecting hood. Figure 56 shows that all of the 24 simulations provide predictions of layer height that are within experimental error.

Simulation	$\dot{Q}_t$	W_s	z_s	T_∞	V	Layer height in hood Expt	B-RISK
	kW	m	m	C	m³/s	m	m
9	5.0	1.0	0	16.8	0.07	0.50	0.49
10	5.0	1.0	0.3	14.9	0.14	0.80	0.77
11	5.0	1.0	0.5	16.6	0.20	1.00	0.97
12	5.0	1.0	0.73	13.8	0.27	1.23	1.21
13	10.0	1.0	0	18.6	0.09	0.50	0.48
14	10.0	1.0	0.3	15.5	0.19	0.80	0.78
15	10.0	1.0	0.5	17.6	0.27	1.00	0.96
16	10.0	1.0	0.73	15.0	0.35	1.23	1.19
17	15.0	1.0	0	19.5	0.12	0.50	0.48
18	15.0	1.0	0.3	16.0	0.24	0.80	0.77
19	15.0	1.0	0.5	18.0	0.33	1.00	0.97
20	15.0	1.0	0.73	14.5	0.43	1.23	1.19
21	5.0	0.2	0	16.5	0.03	0.50	0.49
22	5.0	0.2	0.3	16.0	0.07	0.80	0.76
23	5.0	0.2	0.5	16.2	0.09	1.00	0.94
24	5.0	0.2	0.73	14.1	0.13	1.23	1.16
25	10.0	0.2	0	18.0	0.05	0.50	0.49
26	10.0	0.2	0.3	16.4	0.11	0.80	0.77
27	10.0	0.2	0.5	17.0	0.15	1.00	0.96
28	10.0	0.2	0.73	14.5	0.19	1.23	1.17
29	15.0	0.2	0	19.4	0.06	0.50	0.50
30	15.0	0.2	0.3	17.6	0.13	0.80	0.77
31	15.0	0.2	0.5	17.5	0.18	1.00	0.96
32	15.0	0.2	0.73	14.8	0.24	1.23	1.17

Table 17. B-RISK simulations and experiments for the channelled 3-D balcony spill plume (extracted from Harrison, et al., 2013)
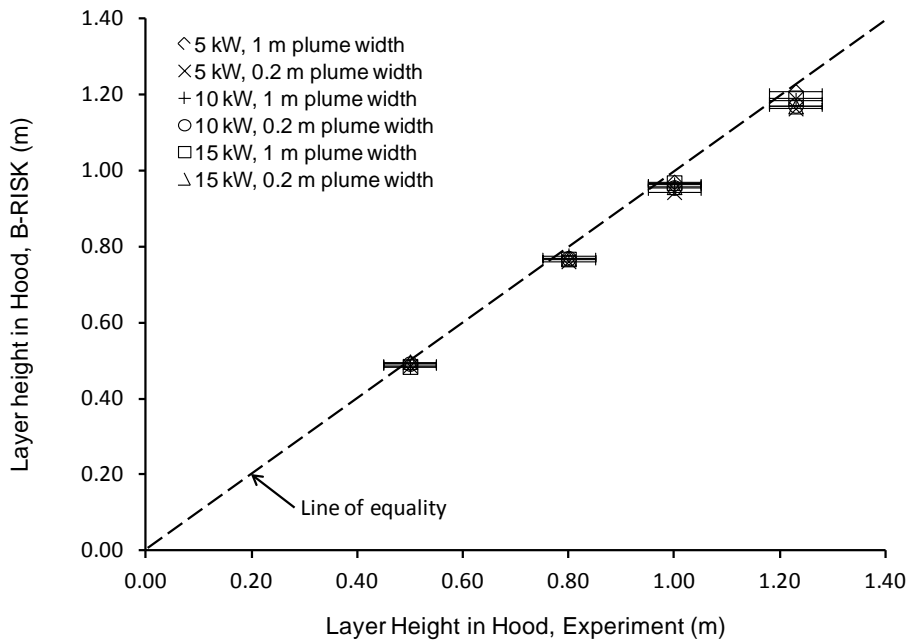
Figure 56. B-RISK prediction of layer height in hood versus the experiment for the channelled 3-D balcony spill plume (extracted from Harrison, et al., 2013)

The Unchannelled 3-D Balcony Spill Plume

Table 18 shows the series of 16 B-RISK simulations carried out for heights of rise of plume above the spill edge of up to 0.73 m, for intermediate (0.6 m) and wide (1.0 m) plume widths, and for fire sizes of 5 and 10 kW on model-scale. Figure 57 shows a comparison between the predictions and the experimental results for the layer height above the floor of the collecting hood. Figure 57 shows that all but one of the 16 B-RISK simulations provides a prediction of layer height that matches the experiment within experimental error.

Simulation	$\dot{Q}_t$	W_s	z_s	T_∞	V	Layer height in hood	
						Expt	B-RISK
	kW	m	m	C	m³/s	m	m
33	5.0	1.0	0	16.5	0.07	0.50	0.51
34	5.0	1.0	0.3	16.0	0.15	0.80	0.77
35	5.0	1.0	0.5	17.6	0.22	1.00	0.97
36	5.0	1.0	0.73	14.5	0.30	1.23	1.20
37	10.0	1.0	0	17.2	0.10	0.50	0.49
38	10.0	1.0	0.3	16.0	0.23	0.80	0.79
39	10.0	1.0	0.5	18.5	0.31	1.00	0.98
40	10.0	1.0	0.73	14.5	0.40	1.23	1.20
41	5.0	0.6	0	18.0	0.06	0.50	0.44
42	5.0	0.6	0.3	16.5	0.14	0.80	0.78
43	5.0	0.6	0.5	16.4	0.19	1.00	0.96
44	5.0	0.6	0.73	14.4	0.30	1.23	1.30
45	10.0	0.6	0	19.4	0.09	0.50	0.50
46	10.0	0.6	0.3	17.5	0.21	0.80	0.80
47	10.0	0.6	0.5	17.0	0.28	1.00	0.98
48	10.0	0.6	0.73	14.5	0.24	1.23	1.11

Table 18. The series of experiments for B-RISK simulations for the unchannelled 3-D balcony spill plume (extracted from Harrison, et al., 2013)
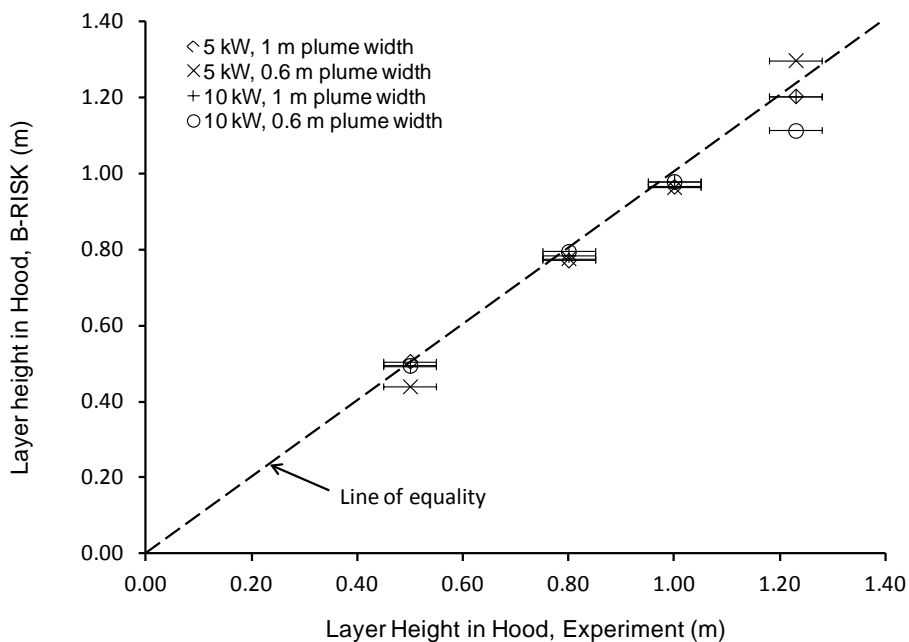
Figure 57. B-RISK prediction of layer height in hood versus the experiment for the unchannelled 3-D balcony spill plume (extracted from Harrison, et al., 2013)

The 2-D Adhered Spill Plume

Table 19 shows the series of eight B-RISK simulations carried out for heights of rise of plume above the spill edge up to 0.83 m, for narrow (0.2 m) and wide (1.0 m) plume widths, and for a fire size of 10 kW on model-scale. Figure 58 shows a comparison between the predictions and the experimental results for the clear layer height above the floor of the collecting hood. Figure 58 shows that the majority of the eight simulations provide predictions of layer height that agree with the experiment (predictions are within experimental error). There is a slight tendency for an over-prediction in entrainment at higher heights of rise of plume. However, all of the predictions are within 10% of the experiment.

Simulation	$\dot{Q}_t$	W_s	z_s	T_∞	V	Layer height in hood Expt	Layer height in hood B-RISK
	kW	m	m	C	m³/s	m	m
49	10.0	1.0	0	16.1	0.09	0.50	0.48
50	10.0	1.0	0.31	14.9	0.13	0.81	0.77
51	10.0	1.0	0.56	13.5	0.16	1.06	0.97
52	10.0	1.0	0.83	16.0	0.19	1.33	1.21
53	10.0	0.2	0	14.6	0.05	0.50	0.49
54	10.0	0.2	0.31	14.0	0.06	0.81	0.79
55	10.0	0.2	0.56	17.5	0.07	1.06	0.99
56	10.0	0.2	0.83	15.5	0.08	1.33	1.22

Table 19. B-RISK simulations and experiments for the 2-D adhered spill plume (extracted from Harrison, et al., 2013)
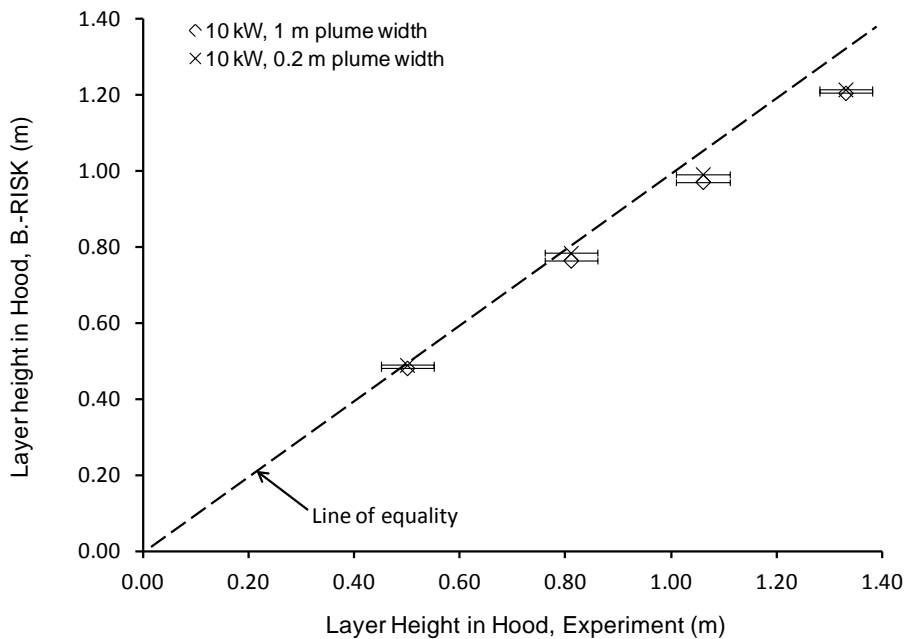
Figure 58. B-RISK prediction of layer height in hood versus the experiment for the 2-D adhered spill plume (extracted from Harrison, et al., 2013)

The 3-D Adhered Spill Plume

Table 20 shows the series of 24 B-RISK simulations carried out for heights of rise of plume above the spill edge of up to 0.73 m, for narrow (0.2 m) and wide (1.0 m) plume widths, and for fire sizes of 5, 10 and 15 kW on model-scale. Figure 59 shows a comparison between the predictions and the experimental results for the clear layer height above the floor of the collecting hood. Figure 59 shows that all of the 24 B-RISK simulations provide predictions of layer height that are within the experimental error.

Simulation	$\dot{Q}_t$	W_s	z_s	T_∞	V	Layer height in hood	
						Expt	B-RISK
	kW	m	m	C	m³/s	m	m
57	5.0	1.0	0	17.5	0.06	0.50	0.48
58	5.0	1.0	0.3	17.5	0.09	0.80	0.76
59	5.0	1.0	0.5	11.5	0.12	1.00	0.97
60	5.0	1.0	0.73	15.5	0.13	1.23	1.16
61	10.0	1.0	0	18.7	0.09	0.50	0.48
62	10.0	1.0	0.3	18.0	0.14	0.80	0.76
63	10.0	1.0	0.5	12.3	0.18	1.00	0.96
64	10.0	1.0	0.73	16.0	0.21	1.23	1.16
65	15.0	1.0	0	19.5	0.12	0.50	0.48
66	15.0	1.0	0.3	18.2	0.18	0.80	0.77
67	15.0	1.0	0.5	13.3	0.24	1.00	0.98
68	15.0	1.0	0.73	16.5	0.27	1.23	1.18
69	5.0	0.2	0	16.5	0.03	0.50	0.49
70	5.0	0.2	0.3	14.0	0.07	0.80	0.77
71	5.0	0.2	0.5	16.0	0.09	1.00	0.96
72	5.0	0.2	0.73	14.5	0.12	1.23	1.18
73	10.0	0.2	0	18.5	0.05	0.50	0.49
74	10.0	0.2	0.3	16.0	0.09	0.80	0.77
75	10.0	0.2	0.5	16.4	0.14	1.00	0.97
76	10.0	0.2	0.73	14.0	0.19	1.23	1.20
77	15.0	0.2	0	19.5	0.06	0.50	0.50
78	15.0	0.2	0.3	17.0	0.12	0.80	0.77
79	15.0	0.2	0.5	17.1	0.17	1.00	0.97
80	15.0	0.2	0.73	15.5	0.24	1.23	1.21

Table 20. B-RISK simulations and experiments for the 3-D adhered spill plume (extracted from Harrison, et al., 2013)
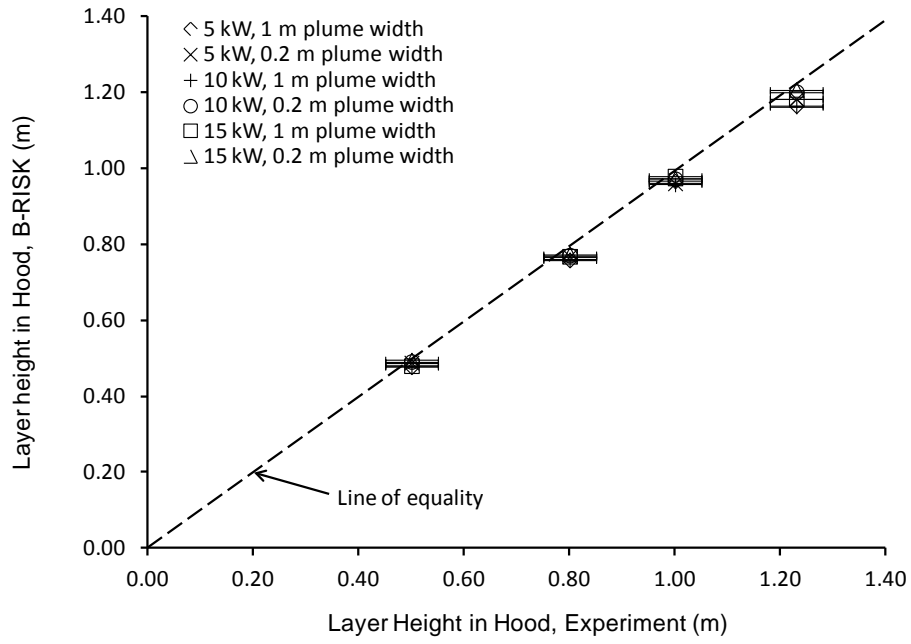
Figure 59: B-RISK prediction of layer height in hood versus the experiment for the 3-D adhered spill plume (extracted from Harrison, et al., 2013)

10.2 CASE 10-2

10.2.1 References

Morgan, H. P. et al., 1995. *BATC - ot smoke ventilation test at Brussels Airport.* Proceedings of the International Conference on Fire Research and Engineering, Orlando, Florida, 10-15 September 1995.

Harrison, R. & Spearpoint, M., 2012. Spill plume formulae. *Fire Risk Management*, June, pp. 50-54.

Harrison, R., Wade, C. & Spearpoint, M., 2013. Modeling Spill Plumes in the B-RISK Fire Model (accepted June 2013). *Journal of Fire Protection Engineering.*

10.2.2 Description

A hot smoke test carried out in the atrium space of the (then unfinished) terminal building at Brussels Airport (Morgan, et al., 1995).

Figure 60 shows a schematic drawing of a half-section of the atrium space at Brussels Airport. The atrium was approximately 85 x 12 m x 17 m high (to the top of a glazed barrel vault roof). There were two floors, the ground floor (the departure level) and the first mezzanine floor. A fire compartment made of 10 mm thick calcium silicate board attached to an angled iron structure was built on the departure level and fronted onto the atrium space. The compartment was 9.6 x 3.5 x 3.5 m high to represent a shop unit. The front of the compartment was open on the 9.6 m width face and there was a channelling screen at either side of the compartment projecting forward by a distance of 2.0 m. The compartment structure was continued upwards by 1.5 m to the level of the mezzanine floor.
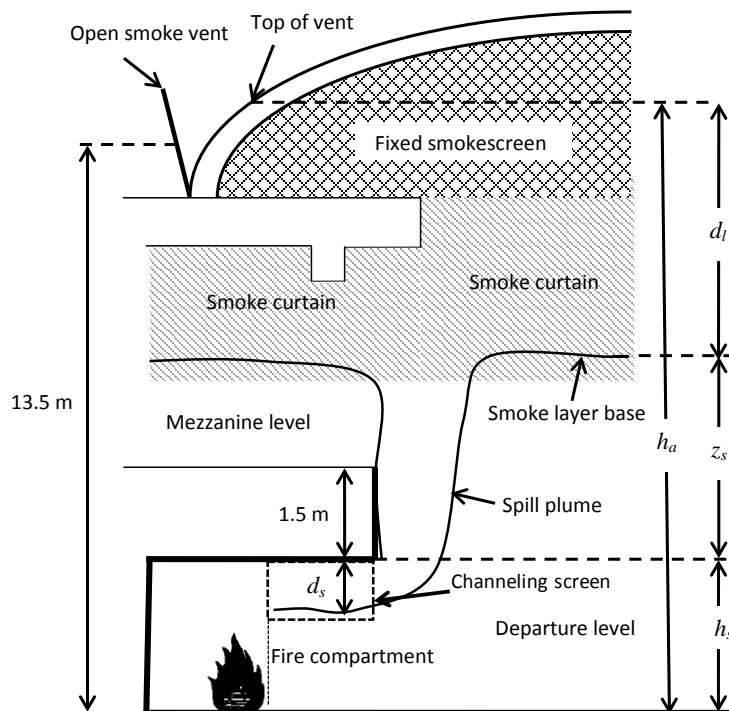
Figure 60. Schematic drawing of a half-section of the atrium space [adapted from (Harrison & Spearpoint, 2012)]

10.2.3 Model Parameters

B-RISK 2013.08 is used.

The channelling screen is not part of the B-RISK geometry but is accounted for by specifying a channelled 3-D balcony spill plume as a vent characteristic. The 1.5 m upstand is also not part of the B-RISK geometry and this is therefore expected to lead to an over-prediction of the entrainment when modelled as a balcony spill plume. The atrium is modelled with a sloping ceiling, an apex height of 17 m and an eaves height of 13.5 m, and therefore the predicted smoke-filling rate reflects the reduced volume beneath the roofline by approximating the barrel-vaulted ceiling with a gable.

Heat losses to the enclosure surfaces are modelled using thermal properties as shown in Table 21.

Table 21. Thermal properties of enclosure surfaces for airport building

Construction element	Material	Thermal conductivity (W/mK)	Density (kg/m^3)	Specific heat (J/kgK)	Emissivity	Thickness (mm)
Atrium walls, ceiling and all floors	Concrete	1.2	2300	880	0.5	100
Fire compartment walls and ceiling	Calcium silicate board	0.12	720	1250	0.83	10

The hot buoyant layer was produced using IMS pool fires in the compartment. The fuel was burnt in two 1.5 m square steel fire trays located at floor level. The total heat release rate from each tray was 1186 kW, to give a test fire with a total steady-state heat release rate of 2372 kW. The radiant loss fraction is taken as 0.2 and the heat of combustion as 30 kJ/g. The pans are located in the room as shown by the orange cones in Figure 61, they are considered to be in a centre location for entrainment purposes (i.e. away from any walls). Ambient temperatures are taken as 291 K and relative humidity as 50%.

The installed smoke management system was naturally driven with smoke vents located 13.5 m above the floor in the atrium. These are modelled as two natural vents 1 m high x 40 m long with the sill at 13.0 m above the floor. Inlet vents supplying make-up air are represented as a single 27 m long x 3 m wide vent positioned at floor level in the atrium enclosure. The discharge coefficient used in the mass flow calculations for the inlet and exhaust vents are taken as 0.6, while 1.0 is used for the compartment opening where the top of the opening was flush with the compartment ceiling. All vents are taken as open from the start of the simulation and connected to the "outside".

In the test, the fire compartment was representative of a shop unit, where the air induced into the fire plume caused it to be "disturbed" and to "lean" towards the rear wall of the compartment, therefore the B-RISK modelling assumes a "disturbed" fire plume.

10.2.4 Comparison

The comparisons shown here are as reported by (Harrison, et al., 2013).

During the test, the observed smoke layer was maintained at a height of 10.5 ± 0.5 m above the atrium floor. After 600 seconds (steady-state) B-RISK predicts a smoke layer height of 8.9 m above the atrium floor being in the range 11-19% lower than the experimental measurement including uncertainty. Part of the discrepancy can be explained by the upstand directly above the compartment opening. Figure 61 shows a visual image of the smoke layer in SmokeView after a simulated period of 600 seconds.

This comparison with the full-scale hot smoke test observations provides further confidence in the use of B-RISK to predict channelled 3-D balcony spill plume entrainment for full-scale flows.
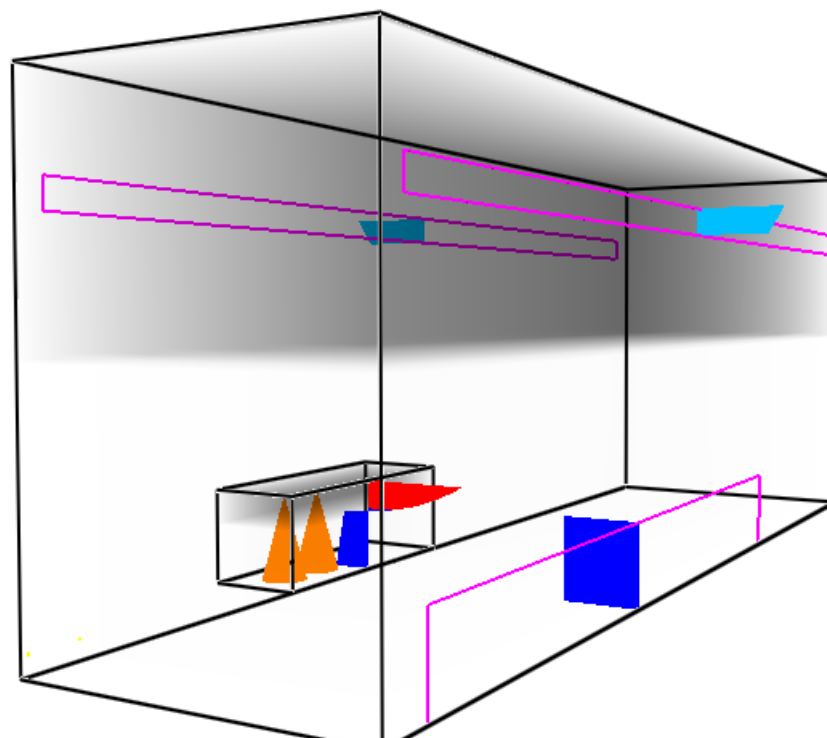
Figure 61. SmokeView visualisation of the model for part of the airport terminal building (extracted from Harrison, et al., 2013)

10.3 CASE 10-3

10.3.1 References

Harrison, R. et al, 1998. *A hot smoke ventilation test in an atrium in the new European Parliament Building.* Proceedings of the 2nd International Conference on Fires in Large Enclosed Spaces, Geneva, Switzerland, June 1998.

Harrison, R., Wade, C. & Spearpoint, M., 2013. Modeling Spill Plumes in the B-RISK Fire Model (accepted June 2013). *Journal of Fire Protection Engineering.*

10.3.2 Description

A hot smoke test was carried out in an atrium space of the (then unfinished) European Parliament Building in Brussels (Harrison, et al., 1998). The overall test area was approximately 74 x 12 x 27 m high and contained two reservoirs (or atrium spaces). The fire reservoir was designated as Reservoir 1 and the adjacent reservoir as Reservoir 2 (see Figure 62a). Directly above the fire compartment were six levels of offices, fully-glazed into the atrium, up to the glazed roof level, designated Levels 1 to 6. There were more office levels beyond the glazed roof. On the opposite side of the reservoir were three levels of foyers up to roof level designated Levels 1, 3 and 5 (see Figure 62b).

The smoke reservoir in the atrium was formed by full-height smoke curtains and the structure of the building. The foyer side of the reservoir contained smoke curtains intended to prevent smoke from entering these levels. There were full-height smoke curtains across the connecting bridges on either side of the fire reservoir which divided the length of the test area into two separate reservoirs. The building at the time of the test was not in its finished state with much of the cladding material not in place, leaving in some places, wider gaps between smoke curtains and walls or columns than would have been the case in the finished building.

The hot buoyant layer was produced by IMS pool fires in the compartment. The fuel was burnt in two 1 m square steel fire trays located at floor level.

The smoke management system was mechanically-driven using two fans located approximately 1 m below the roof of the reservoir. The actual fan capacities of each of the two fans was found from a fan test to be 22.2 m^3s^{-1} and 16.7 m^3s^{-1}, thus giving a total volumetric exhaust rate of 38.9 m^3s^{-1}.

During the test, smoke entered the Level 5 Foyer through curtain/curtain and curtain/structure gaps which caused the foyer and connecting lobby to fill with smoke. Smoke also passed through the gaps between the curtain and the structure on Level 5 (Bridge 2) due to deflection of the curtain. The total gap area on the Level 5 Foyer and the Level 5 Bridge was estimated to be 6.5 m^2 and 1.5 m^2 respectively. The amount of smoke leakage through the smoke curtain gaps are modelled in B-RISK as additional wall vents measuring 1.0 x 6.5 m high with the sill at 18.5 m above the atrium floor (Level 5 Foyer leakage), and 0.5 x 3.0 m high with the sill at 20 m above the atrium floor (Level 5 Bridge leakage) respectively.
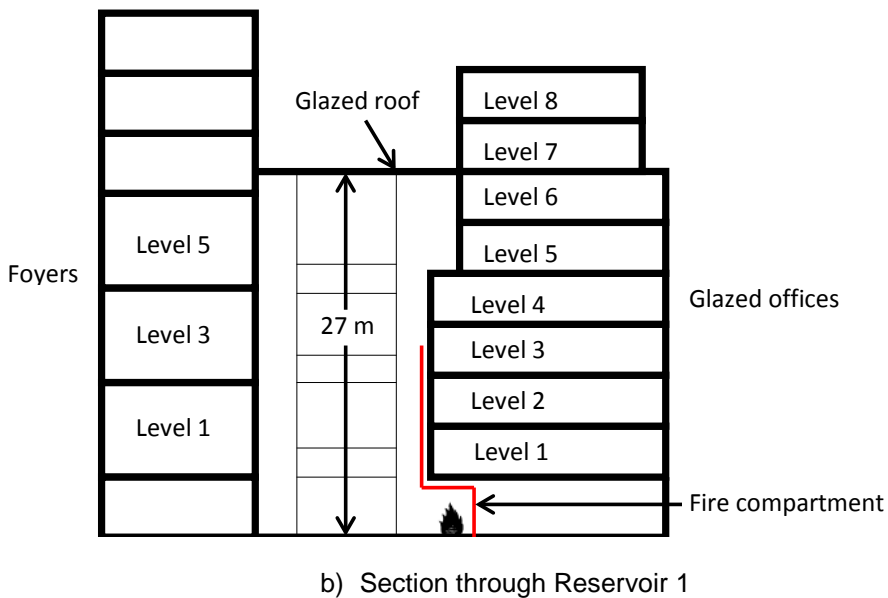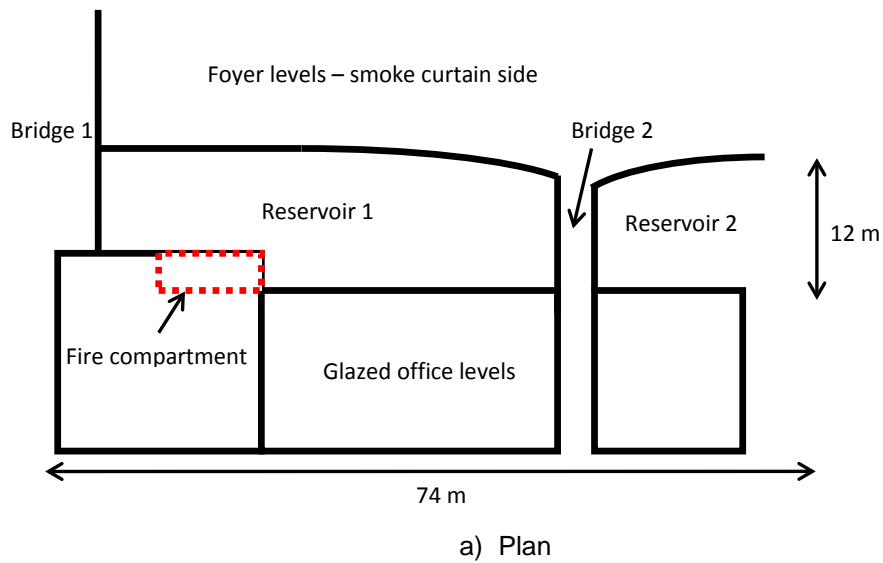
Figure 62. Schematic plan and section view of the atrium space (extracted from Harrison, et al., 1998)

10.3.3 Model Parameters

B-RISK 2013.08 is used.

The total heat release rate from each tray was 527 kW, to give a test fire with a total steady-state heat release rate of 1054 kW. The radiant loss fraction is taken as 0.2 and the heat of combustion as 30 kJ/g. The pans are located in the room as shown by the orange cones in Figure 63, they are considered to be in a centre location for entrainment purposes (i.e. away from any walls). Ambient temperatures are taken as 280 K and the relative humidity is 50%.

Both fans are included in the B-RISK simulations with the measured capacities and at an elevation of 26 m.

Inlet air was provided via low-level openings distributed around the atrium from spaces in the foyers and office levels which were open to other areas of the building. These

openings are represented in B-RISK as two vents from the atrium to the outside with dimensions 40 x 3 m high and 10 x 3 m high, both located with the sill at floor level. The discharge coefficient used in the mass flow calculations for the inlet and exhaust vents is taken as 0.6, while 1.0 is used for the compartment opening where the top of the opening was flush with the compartment ceiling.

In the test, the fire compartment was representative of a shop unit, where the air induced into the fire plume caused it to be "disturbed" and to "lean" towards the rear wall of the compartment, thus the "disturbed" plume option was used.

10.3.4 Comparison

The comparisons shown here are as reported by (Harrison, et al., 2013).

The clear layer height was observed to be maintained at 15.0 ± 1.0 m above the atrium floor during the test. B-RISK predicts a clear layer height of 15.2 m above the atrium floor being within the measured range (15.0 ± 1.0 m) including uncertainty.
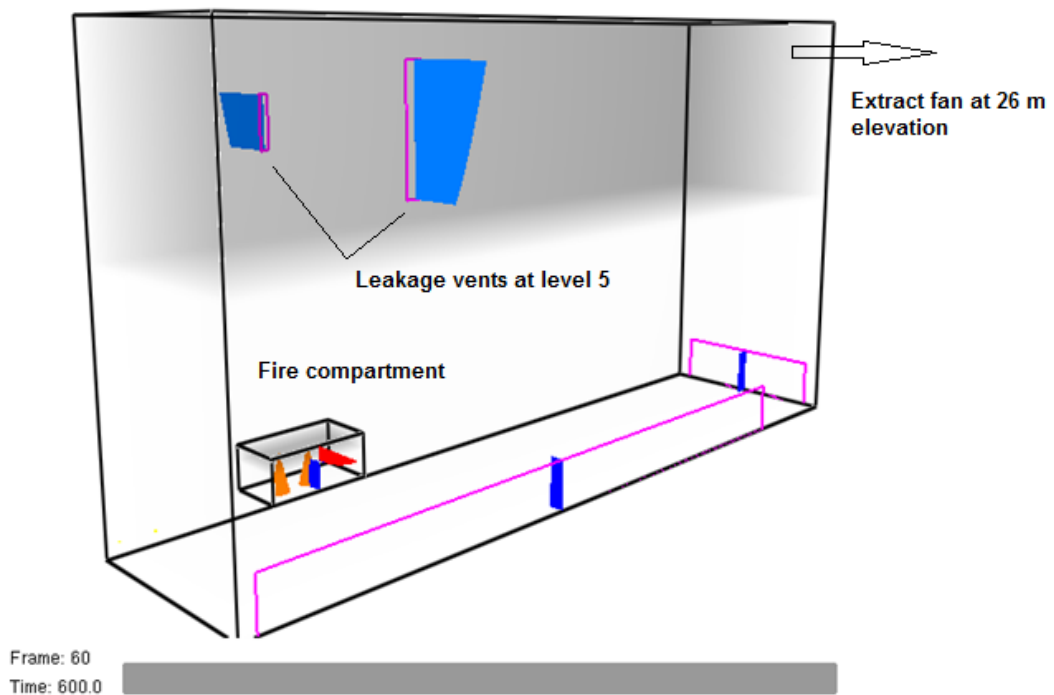
Figure 63. Annotated SmokeView visualisation of the model for part of the European Parliament Building (extracted from Harrison, et al., 2013)

11. REFERENCES

Bittern, A. 2004. *Analysis of FDS Predicted Sprinkler Activation Times with Experiments. Masters of Engineering in Fire Engineering Report.* University of Canterbury, Christchurch, New Zealand.

Davis, W. D., 1999. *Zone fire model JET: A model for the prediction of detector activation and gas temperatures in the presence of a smoke layer.* National Institute of Standards and Technology.

Davis, W. D., Cleary, T., Donnelly, M. & Hellerman, S., 2003. *Predicting Smoke and Carbon Monoxide Detector Response in the Ceiling Jet in the Presence of a Smoke Layer, NISTIR 6976.* National Institute of Standards and Technology, USA.

Davis, W. D., Notarianni, K. A. & McGrattan, K. B., 1996. *Comparison of Fire Model Predictions with Experiments Conducted in a Hangar with 15 m Ceiling. NISTIR 5927.* National Institute of Codes and Standards, USA.

Dowling, V. et al., 1999. *Large scale fire tests on three building materials.* Proceedings Third International Conference on Fire Research and Engineering, 4-8 October 1999, Chicago, USA. p217-227.

Gott, J. E., Lowe, D. L., Notarianni, K. A. & Davis, W. D., 1997. Analysis of High Bay Hangar Facilities for Fire Detector Sensitivity and Placement. NIST TN 1423, USA: National Institute of Standards and Technology.

Harrison R. 2009. Entrainment of air into thermal spill plumes, Thesis for Doctor of Philosophy in Fire Engineering. Christchurch, New Zealand: University of Canterbury. http://ir.canterbury.ac.nz/handle/10092/2865.

Harrison, R. & Spearpoint, M., 2008. *Characterisation of balcony spill plume entrainment using physical scale modelling.* Proceedings of the 9th Symposium of the International Association of Fire Safety Science, Karlsruhe, Germany, pp 727-738. doi:10.3801/IAFSS.FSS.9-727.

Harrison, R. & Spearpoint, M., 2012. Spill plume formulae. *Fire Risk Management*, June, pp. 50-54.

Harrison, R. & Spearpoint, M. J., 2010. Physical scale modelling of adhered spill plume entrainment. *Fire Safety Journal,* 45(3), pp. 149-158. doi:10.1016/jfiresaf.2010.02.005.

Harrison, R., Wade, C. & Spearpoint, M., 2013. Modeling Spill Plumes in the B-RISK Fire Model (in press, accepted June 2013). *Journal of Fire Protection Engineering.*

Harrison, R. et al, 1998. *A hot smoke ventilation test in an atrium in the new European Parliament Building.* Proceedings of the 2nd International Conference on Fires in Large Enclosed Spaces, Geneva, Switzerland, June 1998.

Interscience Communications Ltd (ICL), 1991. *EUREFIC European Reaction to Fire Classification.* Copenhagen, Denmark, Interscience Communications Ltd.

Mealy, C., Floyd, J. & Gottuk, D., 2008. *Smoke Detector Spacing Requirements Complex Beamed and Sloped Ceilings Volume 1: Experimental Validation of Smoke Detector Spacing Requirements.* Fire Protection Research Foundation.

Mikkola, E. & Kokkala, M., 1991. *Experimental Programme of EUREFIC. In EUREIC Seminar Proceedings.* Copenhagen, Denmark, Interscience Communications Ltd.

Morgan, H. P. et al., 1995. *BATC - ot smoke ventilation test at Brussels Airport.* Proceedings of the International Conference on Fire Research and Engineering, Orlando, Florida, 10-15 September 1995.

Nyman, J., 2002. Equivalent Fire Resistance Ratings of Construction Elements Exposed to Realistic Fires, Fire Engineering Research Report 02/13. University of Canterbury, Christchurch, New Zealand. University of Canterbury, Christchurch, New Zealand.

Nyman, J., Gerlich, J. T., Wade, C. A. & Buchanan, A. H., 2008. Predicting Fire Resistance Performance of Drywall Construction Exposed to Parametric Design Fires – A Review. Journal of Fire Protection Engineering, 18(2).

Parry, R., 2002. *Implementation of a glass fracture module for the BRANZfire compartment fire zone modelling software. Fire Engineering Research Report No. 2002-5.* University of Canterbury, Christchurch, New Zealand.

Parry, R., Wade, C. & Spearpoint, M., 2003. Implementing a glass fracture module in the BRANZfire zone model. *Journal of Fire Protection Engineering,* Volume 13, pp. 157-183.

Peacock, R. D., Davis, S. & Lee, B. T., 1988. An Experimental Data Set for the Accuracy Assessment of Room Fire Models. NBSIR-3752, Gaithersburg, USA: National Bureau of Standards.

Shields, T. J., Silcock, G. & Flood, M., 2002a. Performance of a Single Glazing Assembly Exposed to Enclosure Corner Fires of Increasing Severity. *Fire and Materials,* Volume 25, pp. 123-152.

Shields, T. J., Silcock, G. & Flood, M., 2002b. Performance of a Single Glazing Assembly Exposed to a Fire in the Centre of an Enclosure. *Fire and Materials,* Volume 26, pp. 51-75.

Steckler, K. D., Baum, H. & Quintiere, J. G., 1983. Fire Induced Flows Through Room Openings – Flow Coefficients. NBSIR 83-2801, Gaithersburg, USA: National Bureau of Standards.

Steckler, K. D., Quintiere, J. G. & Rinkinen, W. J., 1982. Flow induced by fire in a compartment. NBSIR 82-2520, Gaithersburg, USA: National Bureau of Standards.

Wade, C. A., Spearpoint, M. J., Bittern, A. & Tsai, K., 2007. Assessing the Sprinkler Activation Predictive Capability of the BRANZFIRE Fire Model. *Fire Technology,* Volume 43, pp. 175-193.

Wade, C. et al., 2013. *B-RISK User Guide and Technical Manual,* BRANZ, Porirua, New Zealand.